

# Stellar Structure and Evolution

## 1 Objectives of the course and links with other fields

In this course of stellar structure and evolution, we deeply study the internal physical characteristics of stars and their time evolution. In our exploration of this internal structure, we focus on the understanding of the underlying physical processes. As we will see stars are remarkable laboratories of fundamental physics :

– **Stars as laboratory of quantum physics :**

In stars, the microscopic and macroscopic world are put in close contact. First, the interaction between matter and radiation determines the efficiency of energy transport from their core to the surface. This interaction is explained and quantified in quantum physics by the perturbation of electronic states due to an electromagnetic wave.

– **Stars as laboratory of nuclear physics :**

Most of the time, the main source of energy in stars comes from nuclear reactions in their core. As the star evolves, these fusion reaction synthesize heavier nuclei. Stars are the great creators of the universe, all nuclei beyond hydrogen and helium (carbon, oxygen, nitrogen, iron, ...) were created in the core of stars one day.

– **Stars as laboratories of thermodynamics and statistical physics :**

As we will see, temperature and entropy conditions are extreme inside stars. Hence, a huge number of states is possible for the gas of free nuclei, electron and photons, a statistical equilibrium is established for the occupation of each state by each particle called thermodynamic equilibrium. The powerful tools of statistical physics can be used to describe this equilibrium and make the bridge between the microscopic and macroscopic worlds. As an example, purely quantum effects such as the Pauli exclusion principle can have a major impact on the structure, evolution and stability of stars.

– Finally, **macroscopic hydrodynamic processes** also play a key role in stars. The most significant of them is turbulent convection. It plays a key role in the transport of energy and chemical elements throughout the star.

## 2 Luminosity, effective temperature, magnitudes, Hertzsprung Russel diagram

We begin with basic definitions.

### 2.1 Luminosity - L

The **luminosity** of a star is the total power radiated by it.

As an example, the luminosity of the Sun can be determined as follows. The Sun-Earth distance  $d$  can be measured with a very high precision. The flux coming from the Sun reaching the top of the Earth's atmosphere can also be measured. The main difficulty is that photometers are sensitive to a restricted part of the electromagnetic spectrum. An extrapolation is thus required to estimate the flux integrated over all wavelengths, which is called the bolometric flux. The average bolometric flux of the Sun, called the **solar constant** is :  $C_{\odot} = \int_0^{\infty} C_{\lambda} d\lambda = 1367 \text{ W/m}^2$ .

The solar luminosity is obtained by multiplying it by the surface of a sphere of radius  $d$  :

$$L_{\odot} = 4\pi d^2 C_{\odot} = 3.828 \times 10^{26} \text{ W} = 3.828 \times 10^{33} \text{ erg/s} \quad (1)$$

Stars have a very wide range of possible luminosities, from less than  $10^{-3}L_{\odot}$  to more than  $10^6L_{\odot}$  !

### 2.2 Apparent magnitude - m

In astronomy, we use a logarithmic scale for the brightness of celestial objects. The apparent magnitude is defined as :

$$m = -2.5 \log(b) + C, \quad (2)$$

where  $b$  is the bolometric flux of the object as measured at the top of the Earth's atmosphere. The constant  $C$  appearing in this equation was originally chosen such that the apparent magnitude of the star Vega is zero.

The default of the apparent magnitude is that it depends on the distance of the object. It is not a function of the luminosity alone, it is not *absolute*. This leads us to another definition.

## 2.3 Absolute magnitude

The absolute magnitude  $M$  of a star is the apparent magnitude that it would have if were viewed from a reference distance of 10 parsecs. Noting  $B$  the bolometric flux that it would have at this reference distance, we have :

$$M = -2.5 \log(B) + C \quad (3)$$

We have :

$$L = 4\pi(10 * pc)^2 B = 4\pi(d_{pc} * pc)^2 b, \quad (4)$$

where  $pc$  is the length of a parsec, and  $d_{pc}$  is the distance in parsecs, and thus :

$$M - m = 5 - 5 \log(d_{pc}). \quad (5)$$

The determination of the absolute magnitude requires thus the measurement of the apparent magnitude and the distance. The latter is usually difficult to measure with precision. The absolute bolometric magnitude of the Sun is  $M_{bol,\odot} = 4.74$ .

$M_V = +17$  à  $M_V = -10$ .

## 2.4 Intensity of radiation

Photons propagate in different directions. The **intensity** (of radiation)  $I$  is a measure of the distribution of radiant heat flux per unit area and solid angle, in a particular direction. More precisely, consider an infinitesimal set of directions around  $\vec{n}$ , corresponding to the solid angle  $d\omega$ .  $I d\omega$  is then the heat flux of photons propagating in these directions (through a perpendicular surface). In general, the intensity depends on the considered direction  $\vec{n}$ , so it is a function  $I(\vec{r}, \vec{n}, t)$ . Consider the interior of a spherically symmetric star. I note  $\theta$  the angle to the radial direction and  $\mu = \cos \theta$ . The flux and intensities at a given point of the star are then related as follows :

$$F = 2\pi \int_{-1}^1 \mu I(\mu) d\mu. \quad (6)$$

Indeed,  $F$  is obtained by projecting the intensity on the radial direction (multiplication by  $\mu$ ) and integrating over all directions ( $2\pi d\mu$  is the solid angle of the directions between  $\theta$  and  $\theta + d\theta$ ). If the intensity does not depend on  $\vec{n}$ , the radiation field is said to be isotropic. From eq. 6, we see that the the flux is zero when the radiation field is purely isotropic. As we will see, the radiation field is quasi-isotropic in stellar interiors. However, the outside intensity is very slightly larger than the inside intensity and this is sufficient to create a significant flux. Near the surface, in the stellar atmosphere, the radiation field becomes more and more anisotropic, with inside intensity tending to zero.

## 2.5 Monochromatic flux and intensity

Radiation has a spectral nature. The monochromatic flux  $F_\lambda$  (resp. intensity) is a measure of the density of radiant heat flux (resp. intensity) per unit wavelength, at a given wavelength.  $\int_{\lambda_1}^{\lambda_2} F_\lambda d\lambda$  is thus the radiant heat flux in the interval of wavelengths  $[\lambda_1, \lambda_2]$ .

## 2.6 Black body radiation

Statistical physics tells us that in an opaque gas at local thermodynamic equilibrium, the occupation of the different states of energy by photons follows the Planck law of a black body. The monochromatic flux radiated by a black body of temperature  $T$  is :

$$F_\lambda = \frac{2\pi hc^2}{\lambda^5} \frac{1}{\exp(hc/(\lambda kT)) - 1}, \quad (7)$$

Integrating over all wavelengths gives the Stefan-Boltzmann law :

$$F = \int_0^\infty F_\lambda d\lambda = \sigma T^4. \quad (8)$$

Dividing equations 7 and 8 by  $\pi$  (resp. by  $c/4$ ) gives their analogs for the intensity (resp. the density of radiation energy per unit volume).

Finally, the Wien law relates the temperature and the wavelength at the maximum of the Planck spectrum :

$$\lambda_{\max} (\text{cm}) = 0.29/T(\text{K}) \quad (9)$$

## 2.7 Effective temperature

The radiation spectrum of stars is similar to black bodies. This leads us to the definition of the effective temperature.

*The effective temperature of a radiating body is the temperature that a black body radiating the same flux would have.*

From the Stefan-Boltzmann law, we have by definition of the effective temperature  $F = \sigma T_{eff}^4$  or equivalently  $T_{eff} \equiv (F/\sigma)^{1/4}$ . And for a spherical body like a star :

$$L = 4\pi R^2 F = 4\pi R^2 \sigma T_{eff}^4. \quad (10)$$

## 2.8 The Hertzsprung-Russell diagram

The Hertzsprung-Russel (HR) diagram is fundamental, allowing us to find our way in the world of stars. It remains the main tool to test the theory of stellar evolution through a comparison with observations.

We begin with the definition of the *theoretical Hertzsprung-Russell diagram* : its abscissa is the logarithm of the effective temperature  $\log T_{\text{eff}}$  (increasing from right to left !!) and its ordinate is the logarithm of its luminosity in solar units  $\log(L/L_{\odot})$ .

Determining these two quantities from photometry and/or spectroscopy requires the use of atmosphere models and bolometric corrections. *The observational Hertzsprung-Russell diagram* avoids these sources of uncertainty. Its ordinate is the absolute magnitude as measured in a given passband (usually corresponding to the visible V-filter around 540 nm) :  $M_V$ . Its abscissa is a color index, the difference of magnitude between two distinct passbands, for example  $m_B - m_V$  (Johnson filters) or better  $m_b - m_y$  (Strömgren filters).

The remarkable point is that stars with different masses and stages of evolution occupy different places in the HR diagram.

### 2.8.1 Radii of stars

Stars can have very different radii. The radius can directly be deduced from the location of a star in the HR diagram. Indeed, taking the logarithm of equation 10 gives :

$$\log(L/L_{\odot}) = 2 \log R + 4 \log T_{\text{eff}} + \log(4\pi\sigma/L_{\odot}) \quad (11)$$

Stars with same radius are thus located along a straight line in the HR diagram. The top right part corresponds to giants (around  $10 R_{\odot}$ ) and supergiants (up to hundreds  $R_{\odot}$ ). The bottom left corresponds to the very small stars : the white dwarfs with sizes similar to the Earth and densities around  $1 \text{ ton/cm}^3$  and the neutron stars with radii around 10 km and huge densities around...

### 2.8.2 The Main Sequence

Most of the stars ( $\approx 90\%$ ), including our Sun, occupy a strip going from the top left (high  $T_{\text{eff}}$  and  $L$ ) to the bottom right (low  $T_{\text{eff}}$  and  $L$ ) part of the HR diagram, this is the *main sequence*. These stars are at the same stage of their evolution : the phase of core hydrogen burning. More precisely, a chain of nuclear reactions leads to the

fusion of protons into helium nuclei in the core of these stars. The power produced by these nuclear reactions is equal to the radiated power (the luminosity). Because this phase is the longest during a stellar life, we understand why they are the most numerous. Stars of small masses occupy the bottom part of the main sequence and massive stars the upper part. This is a consequence of the mass-luminosity relation, which will be established later in the course.

### 2.8.3 Red giants

After the main sequence phase, we will see that the core of a star contracts and, simultaneously, its envelope expands and its effective temperature decreases. Once the increase of the radius is significant, the star becomes a *red giant*. Typical red giants in the phase of core helium burning have radii of about  $10 R_{\odot}$ . During this phase, helium nuclei merge into carbon nuclei. During other phases of evolution and/or for more massive stars, the radius can be even larger, reaching 100 to 1000  $R_{\odot}$ ! The star is then called a *supergiant*.

### 2.8.4 White dwarfs

At the end of its life, after having been a red supergiant, our Sun will expel its envelope and become a white dwarf. Nuclear reactions no longer occur and the star is slowly cooling. The mean density of a white dwarf is of the order of a ton per  $cm^3$ . Their radii are about hundred times smaller than the Sun (the earth's size). They are thus located in the bottom left part of the HR diagram.

## 2.9 Chemical composition of stars

Just after the Big Bang, no nuclei heavier than helium had time to be synthesized. As the consequence, hydrogen and helium remain by far the two most abundant nuclei of the universe. This is in particular the case of the initial composition of stars. In stellar physics, the hydrogen mass fraction is usually noted  $X$ , the helium mass fraction  $Y$  and the mass fraction of all other elements (improperly called metals by stellar physicists)  $Z$ . In the envelope of our Sun,  $X \simeq 0.72$  and  $Y \simeq 0.27$ . Similar values are found for most other stars. During the main sequence, hydrogen is progressively transformed into helium in the core. Later, during part of the red giant phase, this helium is transformed into carbon and oxygen. The most massive stars can synthesize heavier elements and finally explode as supernovae, enriching the interstellar medium with these new elements. New generations are formed from this modified medium, leading to a progressive enrichment of our galaxy. With a metal mass fraction  $Z \simeq 0.015$ , our Sun is a star of population I, typical of the

disk of our galaxy. The oldest stars of our galaxy, found in its halo and buldge were formed from a medium much poorer in heavy elements, they are population II stars with  $Z \simeq 0.0001$  typically.

## 3 Equations of stellar structure

### 3.1 Hypotheses

Stars rotate, hence the centrifugal force deforms them (the polar radius is smaller than the equatorial radius). Except when specified, we neglect in this course this effect and assume that stars have a spherical symmetry. We also neglect the impact of magnetic field on their internal structure. The different physical quantities : density, pressure, temperature, energy flux, chemical composition, . . . are assumed to depend on 2 variables only : the distance to the centre and the time. In the first part of these lecture notes, we mainly focus on the internal structure at a given time. In the second part, the evolution of stars is considered.

### 3.2 Mass and density

We consider a very thin spherical shell of radius  $r$ , thickness  $\delta r$  and volume  $\delta V$ . By definition of the density, the mass of the shell is  $\delta m = \rho \delta V$ . At first order in  $\delta r$ , we have  $\delta V = 4\pi r^2 \delta r$  and thus  $\delta m = 4\pi r^2 \rho \delta r$ . Dividing by  $\delta r$  and taking the limit for  $\delta r \rightarrow 0$ , we find the differential equation :

$$dm/dr = 4\pi r^2 \rho. \quad (12)$$

In this equation,  $m(r)$  is the mass of the sphere of radius  $r$  inside the star. This function increases from 0 at the centre to  $m(R) = M$  (the total mass) at the surface. Knowing the density profile inside the star, the integration of equation 12 gives  $m(r)$  :

$$m(r) = \int_0^r 4\pi r^2 \rho dr. \quad (13)$$

The average density is the ratio between the total mass and volume :

$$\langle \rho \rangle = M/(4/3\pi R^3) \quad (14)$$

For the Sun, we have :

$$\langle \rho \rangle_{\odot} = M_{\odot}/(4/3\pi R_{\odot}^3) \simeq 1.4 \times 10^3 \text{kg/m}^3, \quad (15)$$

slightly larger than water density.

Exercices :

Determine  $m(r)$  for a model of constant density  $\rho_0$  and for a model with density profile :  $\rho(r) = \rho_0(R^2 - r^2)$ .

### 3.3 Hydrostatic equilibrium

The Sun is not exploding or collapsing now. This implies that the resultant of the force on each mass element must be zero. The same is valid in stars, except during core collapses and explosions of Super-Novae. We isolate an infinitesimal mass element located at a distance  $r$  from the center. We assume that it has the form of a small cylinder, with height in the radial direction  $\delta r$  and horizontal surface  $\delta A$ . What are the forces exerted on this element ?

First, we have the contact forces exerted on its surface by the surrounding matter. Viscous stress never plays a role at equilibrium. Because of the spherical symmetry, the pressure is just a function of  $r$  and the resultant of the forces is zero in the horizontal plane. In the radial direction  $\vec{e}_r$ , it is simply given by :

$$(P(r) - P(r + \delta r))\delta A = -\delta P\delta A. \quad (16)$$

Second, the volume force due to gravity exerted by the sphere below is :

$$-g \delta m = -(Gm/r^2) \rho \delta A \delta r. \quad (17)$$

The sum of the contact forces and the volume force must be zero

$$-\delta P\delta A - (Gm/r^2) \rho \delta A \delta r = 0 \quad (18)$$

Dividing this expression by  $\delta A \delta r$  and taking the limit for  $\delta r \rightarrow 0$ , we find the differential equation :

$$dP/dr = -\rho Gm/r^2. \quad (19)$$

This is the differential form of the hydrostatic equilibrium equation. The mass  $m$  of each sphere is usually a better independent variable than their radius. Indeed, the mass can be assumed to be conserved (except in very massive stars and supergiants), but not the radius. Dividing equation 19 by equation 12 gives :

$$dP/dm = -Gm/(4\pi r^4) \quad (20)$$

We now integrate equation 19 from the distance  $r$  up to the stellar surface where the pressure is assumed to be zero, this gives :

$$P(r) = \int_r^R \rho (Gm/r^2) dr. \quad (21)$$

*The pressure at a given point of the star is thus equal to the weight of the gas column of unitary section above it.*

With a pressure lower than this weight, the star would be unable to support the weight of the upper layers and it would collapse. On the contrary, with a pressure

larger than the weight, these layers would be expelled. Equivalently, integrating the equation 20 over the mass gives :

$$P(m) = \int_m^M Gm/(4\pi r^4) dm. \quad (22)$$

This equation is very useful. It shows that when the star contracts, the pressure increases a lot and the contrary if it expands. From a simple dimensional analysis, we get an order of estimate of the pressure in the deep layers of a star with known mass and radius :

$$P \approx GM^2/R^4. \quad (23)$$

## Dynamic time

We now briefly consider the out of equilibrium case. Breaking the forces equilibrium leads to the explosion or collapse of the star, but over which time-scale ? We just want to have an order of magnitude, which allows us to make very crude simplifications. Let's assume that we suppress the pressure and only keep the gravity. The stellar surface would collapse with an acceleration  $GM/R^2$ . Since the radius decreases, this acceleration should increase, but we neglect that. The order of magnitude of the time  $t_{dyn}$  required to shrink into the center is then such that  $R/t_{dyn}^2 \approx GM/R^2$ . This gives the definition of the dynamic time :

$$t_{dyn} = \sqrt{R^3/GM} \propto \rho^{-1/2}. \quad (24)$$

We obtained it through crude simplifications but the order of magnitude is valid. If at a given time of the stellar life the hydrostatic equilibrium is broken, the time-scale of the explosion, collapse or pulsations is given by the dynamic time. The dynamic time of the Sun is :  $t_{dyn,\odot} = 26$  minutes.

Note that the dynamic time is also the appropriate time scale of dynamic phenomena at larger scales. It is then more appropriate to relate it

Exercices :

- Determine the pressure at the center of a star of constant density, as a function of its mass  $M$  and radius  $R$ .
- Search in the literature the dynamic time of a typical neutron star, white dwarf, red giant, red supergiant, blue supergiant.

## 3.4 Fast rotation and hydrostatic equilibrium

In fast rotating stars, the approximation of spherical symmetry is no longer valid. We briefly consider the centrifugal deformation of a star in this section. First, we must rewrite the equilibrium equation. The resultant of the forces per unit mass is now

equal to the centripetal acceleration. In the spherical symmetric case, the resultant of the surface forces per unit mass was  $-(1/\rho)dP/dr \vec{e}_r$ . Out of spherical symmetry, it is no longer in the radial direction and reads  $-\nabla P/\rho$ . In the spherical symmetric case, the gravitational force per unit mass was  $-Gm/r^2 \vec{e}_r$ . Out of spherical symmetry, it reads  $-\nabla\phi$ , where  $\phi$  is the gravitational potential. Finally, the centripetal acceleration reads  $-\Omega^2 s \vec{e}_s$  where  $\Omega$  is the angular rotation velocity ( $rad/s$ ),  $s$  is the distance from the rotation axis and  $\vec{e}_s = \nabla s$ . The Newton equation for a rotating body reads thus in each point :

$$\nabla P/\rho = -\nabla\phi + \Omega^2 s \vec{e}_s = \vec{g}_{eff}, \quad (25)$$

where we introduced the effective gravity : the static gravity + the centrifugal term. We clearly see in this equation that spherical symmetry is incompatible with rotation.

A rigorous modeling of rotating star is still very difficult (but some models begin to appear...). However, if the rotation is cylindrical ( $\Omega$  function of  $s$  only, that is constant on cylinders), the geometry can be simplified. Note that rigid rotation (constant  $\Omega$ ) is a particular case of cylindrical rotation. To show that, we take the rotational of eq. 25 :

$$\nabla \times (\Omega^2 s \vec{e}_s) = \nabla \times \left( \frac{\Omega^2 \nabla s^2}{2} \right) = \frac{\nabla \Omega^2 \times \nabla s^2}{2} = \nabla \times \left( \frac{\nabla P}{\rho} \right) = -\frac{\nabla \rho \times \nabla P}{\rho^2}, \quad (26)$$

where we used the properties  $\nabla \times (a \nabla b) = \nabla a \times \nabla b$  and  $\nabla \times (\nabla a) = 0$ . For cylindrical rotation,  $\nabla \Omega^2$  and  $\nabla s^2$  are coaligned along  $\vec{e}_s$ , their vectorial product is thus zero. The eq. 26 gives thus in this case :  $\nabla \rho \times \nabla P = 0$ . The gradients are thus aligned, the isobars and iso-density coincide. Moreover, as the fluid obeys an equation of state relating temperature, pressure, density (see Chapter 4), these surfaces are also isotherms (in chemically homogeneous regions). Finally, it should be noted that the centrifugal force is the gradient of a potential for cylindrical rotation. This allows us to define the total potential (gravitational + centrifugal) as :

$$\Psi = \phi - \int_0^s \Omega^2(s) s ds. \quad (27)$$

And the equilibrium equation reads simply :

$$\nabla P/\rho = -\nabla \Psi = \vec{g}_{eff} \quad (28)$$

The isobars are thus also equipotential (total). Taking the Laplacian of equation 27 gives from the Poisson equation :

$$\nabla^2 \Psi = 4\pi G \rho - 2\Omega^2. \quad (29)$$

Efficient numerical methods exist to solve equations 28 and 29 and thus determine the form of the equipotentials.

We can also associate to fast rotation the notion of critical velocity. Beyond this critical velocity, the centrifugal force overcomes the gravitational attraction and the star cannot maintain its cohesion. An order of magnitude of this critical velocity can be obtained by equalizing at the equatorial surface the centripetal and gravitational accelerations, in a spherical model :

$$\Omega^2 R = \frac{GM}{R^2}. \quad (30)$$

Isolating the equatorial velocity gives :

$$V_{crit} = \Omega R = \sqrt{\frac{GM}{R}}. \quad (31)$$

In the simplified model called Roche model, the gravitational potential is approximated by  $\phi = -Gm/r$ . This would be the real potential at the radius  $r$  if the whole mass  $m$  was concentrated in the center. For a star in rigid rotation, the total potential is then approximated by :

$$\Psi(r, \theta) = -\frac{Gm}{r} - \frac{1}{2}\Omega^2 r^2 \sin^2 \theta. \quad (32)$$

The stellar surface is an equipotential. We note  $R(\theta)$  the distance from the center to the surface as a function of the colatitude  $\theta$ . We deduce then from eq. 32 :

$$\frac{GM}{R(\theta)} + \frac{1}{2}\Omega^2 R(\theta)^2 \sin^2 \theta = \frac{GM}{R_p}, \quad (33)$$

where  $R_p$  is the polar radius. Isolating  $R(\theta)$  in this equation is straightforward and gives the form of the surface. In particular, we see that, at the critical velocity, the ratio between the polar and equatorial radius is 2/3.

### 3.5 Transport of energy by radiation

We saw that the pressure increases quickly with the depth inside stars, reaching values of the order of  $P \approx GM^2/R^4$ . On the opposite, in many stars such as main sequence stars (core hydrogen burning phase), the core density is not very high. As an example, the average density of the Sun is slightly larger than water. Assuming that the state of matter is reasonably well described by an ideal gas, we find for the Sun :

$$T_c \simeq \frac{P_c \mu m_u}{k \rho_c} \approx \frac{GM \mu m_u}{R k} \simeq 10^7 K. \quad (34)$$

Rigorous models give  $T_c \simeq 15 \times 10^6 K$  for the core temperature of the Sun. On the opposite, the Stefan-Boltzmann law shows that the surface temperature of the Sun is of the order of 5800 K. Such contrast of temperature necessarily leads to a significant

transport of energy from the core to the surface (2nd principle of thermodynamics). A common error is to think that transport and production of energy are related inside stars. This is completely wrong : the energy transport is due to the temperature gradient only. Moreover, the high temperatures in the stellar cores are NOT due to the production of energy by nuclear reactions !

In stellar interiors, the radiation spectrum is extremely close to a black body. In particular, the density of radiation energy per unit volume is given by :

$$E_{Rad} = aT^4, \quad (35)$$

where  $a = 4\sigma/c$ . Deep in the star, it is very high due to the very high temperatures. Hence, radiation is a very good candidate for the transport of energy. However, we will see in Chapter 5 that the interior of stars is very opaque. The photons strongly interact with matter through different kinds of electronic transitions (bound-bound, bound-free, free-free and scattering). As a consequence, photons are continuously absorbed and emitted in other directions. The mean free path of a photon is of the order of a centimeter or lower in stellar interiors. This is completely negligible compared to the scale heights of the different quantities :  $|dr/d\ln T|$ ,  $|dr/d\ln P|$ , ... (the scale height is the radial distance over which a given quantity varies by a factor  $e$ ). The photons received on earth are emitted from the surface of stars, the **photosphere**, and don't hold any direct information about their opaque interior. The continuous absorptions and reemissions over very small spatial scales quickly lead to the establishment of a statistical equilibrium for the occupation of the different states, which is called **local thermodynamic equilibrium**. For the photons, the function describing these different states is the Planck function. We gave its expression for the monochromatic flux in eq. 7. Dividing it by  $\pi$  (resp. by  $c/4$ ) gives its analogs for the intensity, which we note  $B_\nu(T)$ , and the density of radiation energy per unit volume.

The equation of radiative transfer in a plane parallel stratified medium reads :

$$\frac{\mu}{\kappa_\lambda \rho} \frac{dI_\lambda}{dr} = -\mu \frac{dI_\lambda}{d\tau} = B_\lambda - I_\lambda, \quad (36)$$

where  $I_\lambda$  is the monochromatic intensity,  $\mu = \cos \theta$  ( $\theta$  is the angle between the propagation direction and the radial direction),  $\kappa_\lambda$  is the opacity and  $\tau$  is the optical depth ( $d\tau = -\kappa_\lambda \rho dr$ ) at wavelength  $\lambda$ . The source function in the local thermodynamic equilibrium approximation is the Planck function  $B_\lambda$ . Integrating it gives the following formal solution :

$$I_\lambda(\tau) = \int_\tau^\infty B_\lambda(T(\tau')) e^{\tau-\tau'} d\tau' \simeq B_\lambda(T(\tau)).$$

When the mean free path of a photon is negligible compared to the temperature scale height, this integral solution can be strongly simplified. Indeed, in this case a

significant variation of  $\tau$  does not lead to a significant variation of the temperature ;  $B_\lambda(T(\tau))$  is thus a function of  $\tau$  varying much slowerly than the exponential in this integral. In very good approximation, it can thus be taken out of the integral and we get  $I_\lambda \simeq B_\lambda$ . Multiplying now equation 36 by  $2\pi\mu$  and integrating over  $\mu$  gives for the left hand side :

$$2\pi \int_{-1}^1 \frac{\mu^2}{\kappa_{\lambda\rho}} \frac{dI_\lambda}{dr} d\mu \simeq 2\pi \frac{1}{\kappa_{\lambda\rho}} \frac{dB_\lambda}{dr} \int_{-1}^1 \mu^2 d\mu = \frac{4\pi}{3\kappa_{\lambda\rho}} \frac{dB_\lambda}{dr}. \quad (37)$$

After integration, the first term of the right hand side is zero because  $B_\lambda$  does not depend on  $\mu$ . The second term becomes :  $-2\pi \int_{-1}^1 \mu I_\lambda d\mu = -F_\lambda$ . We have thus :

$$F_\lambda = -\frac{4\pi}{3\kappa_{\lambda\rho}} \frac{dB_\lambda}{dT} \frac{dT}{dr}.$$

We now integrate the flux over all wavelengths, which gives :

$$F = \int_0^\infty F_\lambda d\lambda = -\frac{4acT^3}{3\kappa\rho} \frac{dT}{dr}. \quad (38)$$

In this equation, we introduced the **Rosseland mean opacity** defined by :

$$\kappa = \left[ \frac{\pi}{acT^3} \int_0^\infty \frac{1}{\kappa_\lambda} \frac{dB_\lambda}{dT} d\lambda \right]^{-1}.$$

Multiplying equation 38 by  $4\pi r^2$  gives :

$$\begin{aligned} L_R &= 4\pi r^2 F \\ &= -\frac{16\pi r^2 acT^3}{3\kappa\rho} \frac{dT}{dr}, \end{aligned} \quad (39)$$

which is the equation used to model the transport of energy by radiation in stellar interiors.  $L_R$  is the power of radiation crossing the sphere of radius  $r$ . In view of the diffusive Brownian motion of photons throughout the star, this equation is often called the (radiative) diffusion equation. Equation 39 is very similar to the Fourier's law of thermal conduction, where the heat flux is also proportional to the temperature gradient. The factor  $4acT^3/(3\kappa\rho)$  is thus the radiative thermal conductivity. We will see later that  $dL/dr = 0$  in the envelope of stars where no energy is produced by nuclear reactions. In the uppermost layers, the opacity is the largest due to the numerous bound-bound and bound-free transitions. Since the luminosity is constant, the temperature gradient strongly increases in these opaque layers, in order to ensure the transport of energy. Similarly, a good isolation in a house allows to maintain a large temperature gradient between inside and outside.

In future derivations, when we will study convection, we will use the quantity  $\nabla$ , called the real gradient, defined by :

$$\nabla \equiv \frac{d \ln T}{d \ln P} = \frac{P}{T} \frac{dT/dr}{dP/dr} = -\frac{r^2 P}{\rho G m T} \frac{dT/dr}{dr}. \quad (40)$$

Substituting it in eq. 38 gives

$$L_R = \frac{16\pi acGmT^4}{3\kappa P} \nabla, \quad (41)$$

or equivalently :

$$\nabla = \frac{3\kappa PL_R}{16\pi acGmT^4}. \quad (42)$$

### 3.5.1 Radiative flux in rotating stars, the Von Zeipel theorem

As we have seen above, the spherical symmetry is broken by the centrifugal force in rotating stars. The (radiative) diffusion equation reads in this case :

$$\vec{F} = -\frac{4acT^3}{3\kappa\rho} \nabla T. \quad (43)$$

For a cylindrical rotation, we have seen that the pressure, density and temperature are constant on equipotential surfaces. We can thus write :

$$\vec{F} = -\chi(\Psi) \frac{dT}{d\Psi} \nabla \Psi = \chi \frac{dT}{d\Psi} \vec{g}_{eff}, \quad (44)$$

where  $\chi \equiv 4acT^3/(3\kappa\rho)$  is the radiative conductivity. Because of the centrifugal deformation,  $|\nabla\Psi| = g_{eff}$  and thus the temperature gradient and the radiative flux increase from the equator to the pole along any equipotential. This is in particular the case at the surface. By definition, the effective temperature is related to the surface flux by  $T_{eff} = (F/\sigma)^{1/4}$ . It increases thus also from the equator to the pole. In the scientific literature, this effect is called **gravity-darkening**. For rigid rotation, the expression for the flux can be simplified even more. In order to get it, we first determine the power  $L$  crossing an equipotential. It is obtained by integrating the flux over the whole surface :

$$L = \int_{\Sigma} \vec{F} \cdot \vec{n} d\sigma = -\chi \frac{dT}{d\Psi} \int_{\Sigma} \nabla \Psi \cdot \vec{n} d\sigma. \quad (45)$$

From the Gauss theorem and eq. 29, this gives :

$$L = -\chi \frac{dT}{d\Psi} \int_V \nabla^2 \Psi dV = -\chi \frac{dT}{d\Psi} \int_V (4\pi G\rho - 2\Omega^2) dV. \quad (46)$$

Noting  $m = \int_V \rho dV$  the mass of the volume  $V$  under the equipotential and  $\langle \rho \rangle = m/V$  the corresponding average density, we find :

$$L = -\chi \frac{dT}{d\Psi} 4\pi Gm \left( 1 - \frac{\Omega^2}{2\pi G \langle \rho \rangle} \right). \quad (47)$$

Finally, we substitute this result in eq. 44, which gives :

$$\vec{F} = -\frac{L}{4\pi G m^*} \vec{g}_{eff} \quad (48)$$

$$\text{with } m^* = m \left( 1 - \frac{\Omega^2}{2\pi G \langle \rho \rangle} \right). \quad (49)$$

This equation is valid for any equipotential. But in general, the Von Zeipel theorem is considered for the surface.

## 3.6 Transport of energy by convection

### 3.6.1 Convective instability

We have seen in the previous section that the high opacities in stellar envelopes lead to high temperature gradients. We will see in this section that they can lead to a new physical process : convection. The convective instability always occur in a fluid in hydrostatic equilibrium when a high enough temperature gradient is produced. This is for example the case if you heat a water pan : if the heat flux is high enough, convective motions occur in the water. We will see that these motions also ensure a bottom-up transport of energy, which must be added to the radiative transport.

To understand the origin of the convective instability, we consider a blob of matter displaced up. We assume that the speed of this element is much lower than the sound speed. As a consequence, pressure equilibrium between the blob and the surrounding can be assumed. I introduce the following notations :

- $\rho, T, P$  : initial density, temperature and pressure of the element and its surrounding,
- $\rho_e = \rho + \Delta\rho_e, T_e = T + \Delta T_e, P_e = P + \Delta P_e$  : final density, temperature and pressure of the element after its displacement,
- $\rho_m = \rho + \Delta\rho_m, T_m = T + \Delta T_m, P_m = P + \Delta P_m$  : final density, temperature and pressure of the surrounding medium where the element arrived.

As mentioned above, we assume pressure equilibrium between the element and the surrounding :  $P_e = P_m, \Delta P_e = \Delta P_m = \Delta P$ . We now compare the densities of the element and the surrounding medium.

**Case 1 :**

$$\rho_e > \rho_m \quad \Leftrightarrow \quad \Delta\rho_e > \Delta\rho_m \quad \Leftrightarrow \quad \frac{\Delta\rho_e}{\rho} > \frac{\Delta\rho_m}{\rho} \quad (50)$$

In this case, the resultant of the contact forces due to the pressure gradient exerted on the element by the surrounding medium is smaller than its weight. The Archimede

(buoyancy) force is thus oriented downwards and pushes back the element towards its initial position :

*The stratification of the medium is stable with respect to convection.*

**Case 2 :**

$$\rho_e < \rho_m \quad \Leftrightarrow \quad \Delta\rho_e < \Delta\rho_m \quad \Leftrightarrow \quad \frac{\Delta\rho_e}{\rho} < \frac{\Delta\rho_m}{\rho} \quad (51)$$

In this case, the resultant of the contact forces due to the pressure gradient exerted on the element by the surrounding medium is larger than its weight. The Archimede (buoyancy) force is thus oriented upwards and pushes even more the element upwards :

*The stratification of the medium is unstable with respect to convection.*

In this unstable case, large scale convective motions occur. The driver of these motions is the Archimede force. We come back now to the condition of convective instability. In order to simplify the derivations, we consider an ideal gas, where  $P \propto \rho T/\mu$ , where  $\mu$  is the mean molecular weight. Because of the pressure equilibrium, We can thus write :

$$\frac{\rho_e}{\rho_m} = \frac{T_m}{T_e} \frac{\mu_e}{\mu_m}. \quad (52)$$

In what follows, we assume that there is no chemical composition gradient in the considered region. The molecular weights are thus equal, which gives :

$$\frac{\rho_e}{\rho_m} = \frac{T_m}{T_e}. \quad (53)$$

From equations 51 and 53, we see that the medium is convectively unstable if and only if :

$$T_e > T_m \quad \Leftrightarrow \quad \frac{\Delta T_e}{T} > \frac{\Delta T_m}{T}. \quad (54)$$

This result is already important. It shows that in convectively unstable regions, the ascending elements are hotter than the surrounding medium. Therefore, they provide heat to it. On the contrary, the descending elements are heavier and colder than the surrounding medium. Therefore, they receive heat from it. The general picture is thus of convective elements pumping heat from below, raising and providing this heat to upper layers. Convection contributes thus to the outwards transport of energy. We will come back later to the quantification of this heat transport and continue now with the convective instability criterion. 54 We considered an ideal gas in the previous derivations. However, the inequality 54 is also valid for a non-ideal gas.

We divide now the inequality 54 by  $\Delta P/P$  and take the limit for infinitesimal variations. Since  $\Delta P < 0$ , the inequality is reversed and we get the instability condition :

$$\left(\frac{d\ln T}{d\ln P}\right)_e < \left(\frac{d\ln T}{d\ln P}\right)_m . \quad (55)$$

During its travel upwards, the element is expanding and providing heat to the surrounding medium. The temperature decrease of the element is thus larger than what it would have been without heat exchange (adiabatic expansion). We consider here reversible thermodynamic changes, in which adiabatic is equivalent to isentropic. We have thus :

$$\left.\frac{\partial \ln T}{\partial \ln P}\right|_S < \left(\frac{d\ln T}{d\ln P}\right)_e < \left(\frac{d\ln T}{d\ln P}\right)_m . \quad (56)$$

$\left.\frac{\partial \ln T}{\partial \ln P}\right|_S$  is usually noted  $\nabla_{ad}$  in stellar physics and it is called the « *adiabatic gradient* ». In an ideal fully ionized gas with negligible radiation pressure, we have  $\nabla_{ad} = 2/5$ . More generally,  $\nabla_{ad}$  is a state variable. As such, it only depends on the local temperature, density and chemical composition.  $\left(\frac{d\ln T}{d\ln P}\right)_m$ , the gradient corresponding to the stratification of the average medium is usually noted  $\nabla$  and it is called the « *real gradient* ». Finally, the gradient seen by the element  $\left(\frac{d\ln T}{d\ln P}\right)_e$  is usually noted  $\nabla_e$ . In convectively unstable regions, we have thus :

$$\nabla > \nabla_e > \nabla_{ad} . \quad (57)$$

In convectively stable regions, all the previous inequalities are reversed : a mass element displaced upwards becomes heavier and colder than the surrounding medium, it receives heat and its temperatures decreases less than for adiabatic expansion. The necessary and sufficient local condition of convective instability in a chemically homogeneous region is thus simply :

$$\nabla > \nabla_{ad} . \quad (58)$$

This criterion is however not adequate for practical use. Building a stellar model requires to solve differential equations, some of them (the energy transport equations) are not the same in radiative and convective zones. We need a criterion of convective instability expressed as a function of the dependent and independent variables of this differential problem :  $T, P, \rho, L, r, \kappa, m, \dots$ . This is not the case of the inequality 58.

As a preliminary, it should be noted that radiation transports energy in all parts of a star, in purely radiative zones as well as in convective ones, because a temperature gradient is always present. Eq. 42 is thus also valid in convective zones. Based on this, we introduce a new quantity called the « *radiative gradient* » and noted  $\nabla_{rad}$ . It is obtained by replacing the radiative luminosity in equation 42 by the total luminosity  $L = L_R + L_c$  ( $L_c$  is convective luminosity, the power of convection) :

$$\nabla_{rad} \equiv \frac{3\kappa PL}{16\pi acGmT^4} . \quad (59)$$

The radiative gradient is thus the (fictitious) gradient required to ensure the whole transport of energy  $L$  by radiation only.

It is larger than the real gradient since  $L \geq L_R$ .

### 3.6.2 The Schwarzschild criterion

From this definition, we obtain the Schwarzschild criterion of convective instability. A given layer is convectively unstable if :

$$\nabla_{rad} > \nabla_{ad}. \quad (60)$$

Proof of the Schwarzschild criterion :

– Convection  $\Rightarrow \nabla_{rad} > \nabla_{ad}$ .

From the criterion 58, convection  $\Rightarrow \nabla > \nabla_{ad}$ . Moreover, we have seen that convection ensures a transport of energy, so that  $L > L_R$ . Comparing equations 42 and 59 shows thus that :  $\nabla_{rad} > \nabla$ . Therefore  $\nabla_{rad} > \nabla_{ad}$ .

– No convection  $\Rightarrow \nabla_{rad} \leq \nabla_{ad}$ .

From the criterion 58, no convection  $\Rightarrow \nabla \leq \nabla_{ad}$ . Moreover, the whole energy is then transported by radiation,  $L = L_R$ , so that  $\nabla_{rad} = \nabla$ . We have thus  $\nabla_{rad} \leq \nabla_{ad}$ .

### 3.6.3 The Ledoux criterion

In the previous derivations (from eq. 53), we assumed that there is no chemical composition gradient in the considered region. However, numerous processes modify the chemical composition (nuclear reaction, microscopic diffusion, ...), leading to gradients in radiative zones. When we consider the motion of a mass element over a short time-scale it keeps its chemical composition but reaches regions where it is different. Its molecular weight is thus different from the surrounding medium. The famous Liège astrophysicist Paul Ledoux, considered as the father of the theory of stellar pulsations, proposed in the 40s the “Ledoux criterion” of convective instability taking this into account. Instead of an ideal gas, we consider now a fluid with a general equation of state  $\rho = \rho(T, P, \mu)$ . The differential of this equation reads :

$$\frac{d\rho}{\rho} = \alpha \frac{dP}{P} - \delta \frac{dT}{T} + \phi \frac{d\mu}{\mu}, \quad (61)$$

where  $\alpha \equiv \partial \ln \rho / \partial \ln P|_{T, \mu}$ ,  $\delta \equiv -\partial \ln \rho / \partial \ln T|_{P, \mu}$  and  $\phi \equiv \partial \ln \rho / \partial \ln \mu|_{P, T}$ . Note that in an ideal gas,  $\alpha = \delta = \phi = 1$ . Assuming pressure equilibrium and  $\Delta \mu_e = 0$

and using equation 61 for the element and the surrounding, a first order Taylor development of both sides of eq. 51 gives :

$$\frac{\Delta T_e}{T} > \frac{\Delta T_m}{T} - \frac{\phi}{\delta} \frac{\Delta \mu_m}{\mu}. \quad (62)$$

Dividing this equation by  $\Delta P/P$  and taking the limit for infinitesimal variations, we get the criterion of convective instability :

$$\nabla_e < \nabla - \frac{\phi}{\delta} \nabla_\mu, \quad (63)$$

and finally the **Ledoux criterion**, a given layer is convectively unstable if :

$$\nabla_{rad} - \frac{\phi}{\delta} \nabla_\mu > \nabla_{ad}. \quad (64)$$

In these inequalities, we used the notation  $\nabla_\mu = \left( \frac{d \ln \mu}{d \ln P} \right)_m$ . This criterion is easily understood. Consider a region of the star where the molecular weight decreases towards the surface. This is the most frequent case because nuclear reactions synthesize heavier nuclei in the core and heavier nuclei initially present in the envelope sink slowly towards the center (gravitational settling). We consider an element displaced upwards. It reaches thus layers where the molecular weight is lower. At fixed temperature and pressure, it is thus denser than the surrounding medium. The Archimede force is oriented downwards and pushes it back to its original place. We see thus that  $\nabla_\mu > 0$  has a stabilizing effect opposite to the occurrence of convection, in agreement with eq. 64.

### 3.6.4 Semi-convection

Imagine now that you are in a region of the star stable with respect to the Ledoux criterion but unstable with respect to the Schwarzschild criterion, what will occur? A mass element displaced upwards is denser (Ledoux) and hotter than the surrounding. It is thus pushed back by the Archimede force downwards until it becomes less dense than the surrounding. The result is an oscillation at a frequency called the Brunt-Väisälä frequency. However, the thermodynamic cycle corresponding to this oscillation is a motor thermodynamic cycle : heat is received by the element from the surrounding medium at the hot contraction phase when it is at the bottom and heat is released from the element to the surrounding at the cold expansion phase, when it is at the top. It is well known that such motor thermodynamic cycle produces a positive work, like in a car engine. In practice, this work is converted into mechanical energy, leading to a growth of the amplitude of the oscillation until non-linear effects break it and partial mixing occurs. The resulting profile of temperature and chemical composition is still a matter of debate between stellar physicists.

### 3.6.5 Thermohaline (fingering) convection

Imagine now that you are in a region convectively stable with respect to the previous criteria, but such that :

$$\nabla_{\mu} < 0. \quad (65)$$

Although this is rare, this can occur mainly by two channels. The first one is accretion, when the star accretes heavier nuclei from outside (for example planets or comets falling on the star!). The second one is radiative levitation, when radiative forces push upwards high cross section heavy nuclei. Consider a mass element displaced downwards. We assume that this motion is so slow that there is no difference of temperature and pressure between the element and the surrounding medium. As the element reaches regions of lower molecular weight, it becomes denser than the surrounding medium. Hence, the Archimed force pushes it even more downwards. This corresponds to a new kind of instability called thermohaline (or fingering or double-diffusive) convection. This instability is well known in oceanography : when water reaching the pole gets frozen, the remaining fluid gets more salty, with higher density than the deep water, so that it sinks.

### 3.6.6 Physical conditions leading to convection

Looking at the Schwarzschild criterion allows us to see what leads to convection : any physical situation leading to a large value of the radiative gradient (eq. 59).

#### Convective core

In the central part of a star, we will see that nuclear reactions typically occur. The large amount of heat provided by these reaction is evacuated towards the surface, so that  $L(r)$  is high there. Quite often, this energy production is concentrated into a small fraction of the mass near its center. This is a consequence of the very high sensitivity of nuclear reactions to temperature. The mass  $m$  of the sphere where nuclear reactions occur is thus small,  $L$  is high, thus  $L/m$  is very high, thus  $\nabla_{rad} \propto L/m$  is high and larger than the adiabatic gradient. Therefore, the star has a convective core in this situation.

#### Convective envelope

In superficial layers of a star, the opacity becomes much larger. We will analyse in detail the sources of opacity in Section 5. The larger superficial opacities are mainly due to the bound-bound and bound-free electronic transitions occurring there. The size of this superficial region of large opacity and relatively low temperature increases as the effective temperature decreases. Since  $\nabla_{rad} \propto \kappa/T^4$ , it becomes larger than the adiabatic gradient and a convective envelope is present. As an example, our Sun has a convective envelope with a size of about 1/3 of its radius. For even colder stars,

the convective l'enveloppe convective est de l'ordre d'un tiers du rayon total. Very cool stars, like M-dwarfs, are fully convective (from the center to the surface).

### 3.6.7 Physical characteristics of convective zones

The Reynolds number, a well-known dimensionless number, quantifies the degree of turbulence of hydrodynamic motions :

$$Re = \frac{VL}{\nu}, \quad (66)$$

where  $V$ ,  $L$  and  $\nu$  are typical velocity, size and kinematic viscosity of the medium. Motions are laminar for low  $Re$  and become turbulent above  $Re$  of several thousands. In stars, the convective velocities are very high in the outer part of the convective envelope, the size  $L$  is huge compared to phenomena on earth, and the viscosity is low, so that Reynolds numbers are huge, typically from  $10^{10}$  à  $10^{13}$  !!

*Convective motions are thus extremely turbulent in stars.*

Because of this extreme turbulence, modeling of convection in stellar envelopes is very difficult. The best models of these times are 3D Large Eddies Simulations requiring months of computation time (for the modelling of hours of real time) must be performed. And they still give an approximate view of reality because the Reynolds number of these simulations are drastically reduced (by increasing artificially the viscosity) to avoid major numerical problems. Modelling convection on stellar time-scales (billions of years for the sun) is thus totally impossible !

### 3.6.8 The Mixing-Length Theory

However, what we need to know from the transport of energy processes, allowing us to build a stellar model is the mean temperature gradient as a function of depth. Limiting oneself to this pragmatical goal, approximate analytical models of convection have been proposed. The simplest and by far most widely used is called the Mixing-Length Theory (MLT). The strong simplification behind this theory is to reduce the spectrum of turbulence to motions over a characteristic scale called the mixing-length. This mixing-length is usually parametrized as follows :

$$l = \alpha H_p = -\alpha \left( \frac{d \ln P}{dr} \right)^{-1}, \quad (67)$$

where  $H_p$  is the pressure scale-height and  $\alpha$  is called the mixing-length parameter. By calibrating appropriately this parameter, we can obtain stellar models in agreement with observations (good location in the HR diagram typically). It is assumed

in this theory that convective motions undergo a constant acceleration due to the Archimede force over a mixing-length and next transmit the difference of enthalpy  $\Delta h = h_e - h_m$  to the surrounding medium. This theory takes approximately into account the radiative loss of energy of convective elements during their motion, through a quantity  $\Gamma$  called the convective efficiency :

$$\Gamma \equiv \frac{\nabla - \nabla_e}{\nabla_e - \nabla_{\text{ad}}} = \frac{\tau_{\text{rad}}}{\tau_{\text{conv}}}, \quad (68)$$

where  $\tau_{\text{conv}}$  is the mean life time of a convective element and  $\tau_{\text{rad}}$  is the characteristic time of the radiative losses of a convective element. In the mixing-length theory,  $\Gamma$  is obtained by solving the following cubic equation :

$$\frac{9}{4} \Gamma^3 + \Gamma^2 + \Gamma = A (\nabla_{\text{rad}} - \nabla_{\text{ad}}), \quad (69)$$

where

$$A = \frac{\delta P}{2\rho} \left[ \frac{\kappa c_p \rho^3 g l^2}{12 a c T^3 P} \right]^2 \quad (70)$$

and  $\delta \equiv -\partial \ln \rho / \partial \ln T|_{P,\mu}$ . Once  $\Gamma$  is obtained by solving Eq. (69), the other gradients are easily determined from :

$$\frac{9}{4} \Gamma^3 = A (\nabla_{\text{rad}} - \nabla), \quad (71)$$

$$\Gamma^2 = A (\nabla - \nabla_e) \quad \text{and} \quad (72)$$

$$\Gamma = A (\nabla_e - \nabla_{\text{ad}}). \quad (73)$$

The convective flux is then given by :

$$F_C = (1/4) \alpha^2 c_p \rho T \sqrt{\frac{\delta P}{2\rho}} (\nabla - \nabla_e)^{3/2}. \quad (74)$$

The mean radial velocity of a convective element is :

$$V_{\text{conv}} = \frac{\alpha}{2} \sqrt{\frac{\delta P}{2\rho}} (\nabla - \nabla_e), \quad (75)$$

and the mean life time of a convective element is :

$$\tau_{\text{conv}} = \frac{l}{V_{\text{conv}}}. \quad (76)$$

I don't justify in these lecture notes the above equations. I just propose a simple interpretation of the most important factors appearing in eq. 74. By definition, the convective flux is the average flux of enthalpy due to convective motions. Assuming, as we did before, that equilibrium of pressure is maintained during the convective motions, we have :

$$F_c = \rho c_p \langle V_{\text{conv},r} (T_e - T_m) \rangle, \quad (77)$$

where the “ $\langle \rangle$ ” correspond to a statistical average over all convective motions (upwards and downwards). The factor  $\rho c_p T \alpha (\nabla - \nabla_e)$  in eq. 74 is associated to the quantity of enthalpy ( $\rho c_p (T_e - T_m)$ ) transmitted after a displacement over a distance  $l$ ; and the factor  $(P/\rho)^{1/2} \alpha (\nabla - \nabla_e)^{1/2}$  is associated to the mean velocity of a convective element accelerated over a distance  $l$  by the Archimede force.

We clearly see in equations 77 and 74 the factor  $\rho c_p T$ , which is the density of enthalpy (of an ideal gas). As we go down into a star,  $\rho$  and  $T$  increase quickly. The enthalpy density (the «heat capacity») becomes huge. A very small relative difference of temperature between the convective element and the medium ( $(T_e - T_m)/T$ ) is thus sufficient to lead to significant heat exchange. In other words, for a given convective flux, a value of  $\nabla - \nabla_{ad}$  very slightly above 0 is sufficient to ensure the energy transport. In the deep layers of a star, where the heat capacity is huge, convection is an extremely efficient energy transport process. As a consequence, the temperature gradient is nearly adiabatic in deep enough convective layers :

$$dT/dr \simeq -\nabla_{ad} \frac{Gm\rho T}{r^2 P} \quad \text{and} \quad ds/dr \simeq 0. \quad (78)$$

On the contrary,  $\rho$  and  $T$  are much lower near the stellar surface. In order to ensure the required transport of energy,  $\nabla - \nabla_{ad}$  must thus be significantly larger than 0 there. We see thus that the modelling of the near surface parts of convective envelopes, where convection is not very efficient is the difficult part. The mixing-length theory only gives a very approximate view of these layers.

### 3.6.9 Entropy profile in convective and radiative zones

To determine the entropy profile, we start from the general equation of state  $T = T(s, P, \mu)$  and differentiate it. This gives (without proof) :

$$\frac{dT}{T} = \frac{ds}{c_p} + \nabla_{ad} \frac{dP}{P} + \frac{\phi}{\delta} \frac{d\mu}{\mu}. \quad (79)$$

This directly gives :

$$\frac{ds}{dr} = c_p \frac{d \ln P}{dr} (\nabla - \nabla_{ad} - \frac{\phi}{\delta} \nabla_{\mu}) = -c_p \frac{\rho g}{P} (\nabla - \nabla_{ad} - \frac{\phi}{\delta} \nabla_{\mu}). \quad (80)$$

As we have just seen,  $\nabla \simeq \nabla_{ad}$  deep enough in convective zones and  $\nabla_{\mu} = 0$  since everything is mixed. The entropy profile is thus quasi-constant deep enough in convective zones and  $ds/dr < 0$  in the outermost layers of the convective envelope. On the opposite, in radiative zones we see from the Ledoux criterion that  $ds/dr > 0$ .

### 3.7 Conservation of energy

We have seen in the previous sections that the hydrostatic equilibrium of a star leads to huge pressures and thus huge temperatures in the core. The resulting temperature contrast between the core and the superficial layers leads to a transport of energy by radiation and, in some layers, by convection from the core to the surface, where this energy is radiated. As we will see in details in another section, the very high core temperatures ( $\approx 15 \times 10^6$  K for the Sun) can lead to thermonuclear fusion reactions. These reactions are exothermal and thus provide heat to the stellar plasma. In many cases, like during the phase of hydrogen core burning, the power produced in the core by nuclear reactions is equal to the power radiated by the star from its surface. This is a simple example of energy conservation, which we call **global thermal equilibrium**. However, we will see that stars can be out of thermal equilibrium during some phases of their evolution. It is important to understand that nuclear reactions are not the cause of the radiation of stars. Consider for example the Sun and imagine we turn suddenly off the nuclear reactions in its core. Would something happen instantaneously? No!... Why? Heat is no longer provided to the core, but the total internal energy of the Sun,  $\int_M u dm$ , constitutes a huge reservoir ( $u \approx c_v T$ , the internal energy per unit mass, is very large due to the large temperatures). By turning off the nuclear reactions, you put the Sun out of thermal equilibrium. But, with its current luminosity, you would have to wait for a time  $\tau_{th} \approx \int u dm / L \approx 10^7$  years before seeing a change due to this imbalance. Nuclear reactions are, as we will see, the key process for the understanding of nucleosynthesis and the long term evolution of stars. But they only have a secondary impact on the instantaneous stellar structure. It is now time to establish the equation of energy conservation in stellar interiors. For this purpose, we must quantify the local heat gain and loss throughout the star.

**$\epsilon_n$  is defined as the rate of heat production by nuclear reaction per unit time and mass at a given point of the star.**

Consider a spherical shell located at a distance  $r$  of the stellar center and of infinitesimal width  $\delta r$  and mass  $\delta m$ . As before, we assume spherical symmetry so that  $\epsilon_n$  is constant in the shell. The power provided to this shell by nuclear reaction is thus simply  $\epsilon_n \delta m$ .

Because of the energy transport processes, energy enters continuously from the bottom of the shell and goes out from its top. More quantitatively, the power entering in the shell from below is  $L(m)$  (or  $L(r)$  depending on your choice of independent variable), the power crossing the surface of the sphere of radius  $r$ . And the power going out of the shell from the top is  $L(m + \delta m)$  (or  $L(r + \delta r)$  depending on your choice of independent variable), the power crossing the surface of the sphere of radius  $r + \delta r$  and mass  $m + \delta m$ .

**Local thermal equilibrium** (which is not the same as local *thermodynamic* equi-

librium!) is defined as a physical situation where the heat gain and loss are exactly equilibrated everywhere in the star. For our shell, the provided heat,  $L(m) + \epsilon_n \delta m$  is then equal to the lost heat,  $L(m + \delta m)$ . We have thus :

$$\delta L = L(m + \delta m) - L(m) = \epsilon_n \delta m. \quad (81)$$

Dividing by  $\delta m$  and taking the limit for  $\delta m \rightarrow 0$  gives :

**The equation of energy conservation in thermal equilibrium is :**

$$\frac{dL}{dm} = \epsilon_n, \quad (82)$$

or by using eq. 12 :

$$\frac{dL}{dr} = 4\pi r^2 \rho \epsilon_n. \quad (83)$$

In thermal equilibrium, we see from this equation that  $L$  increases outwards in the nuclear reaction layers and is constant where there is no reaction. Eq. 82 is easily integrated. Since the luminosity is zero at the center (an infinitesimal point cannot produce a finite amount of energy),  $L(0) = 0$ , we find :

$$L(m) = \int_0^m \epsilon_n dm. \quad (84)$$

In particular, the luminosity of the star is equal to the total amount of energy produced by nuclear reactions in the whole star, local thermal equilibrium involves global thermal equilibrium.

We will see that, after a transient phase, thermal equilibrium is often established during the phases of nuclear burning, so that using eq. 82 is justified. However we will see also that, between each phase of nuclear burning, the star goes through a transient phase of thermal imbalance. Out of thermal equilibrium, the net heat provided to the gas is not zero. Let  $dq/dt$  be the heat provided per unit time and mass to the gas. The first law of thermodynamic gives, for reversible changes :

$$\frac{dq}{dt} = T \frac{ds}{dt} = \frac{du}{dt} + P \frac{dv}{dt}. \quad (85)$$

And from the above energetic balance sheet, the heat provided per unit time to the shell is :

$$\frac{dq}{dt} \delta m = \epsilon_n \delta m + L(m) - L(m + \delta m). \quad (86)$$

Dividing by  $\delta m$  and taking the limit finally gives :

$$T \frac{ds}{dt} = \frac{du}{dt} + P \frac{dv}{dt} = \epsilon_n - \frac{\partial L}{\partial m}. \quad (87)$$

A typical thermal imbalance situation is the phase of stellar evolution preceding the onset of nuclear reactions.  $\epsilon_n = 0$  during this phase. As  $L$  must necessarily be

positive at the surface,  $\partial L/\partial m > 0$ . Hence, eq. 87 shows that  $du/dt + Pdv/dt < 0$ . We will see later that the work term  $Pdv/dt$  usually dominates in stars. It is thus lower than zero and the star contracts due to this thermal imbalance.

It is usual to give to the conservation of energy equation a similar form whether or not thermal equilibrium. For this purpose, we define  $\epsilon_{grav} = -Tds/dt$ . Equation 87 reads then :

$$\frac{dL}{dm} = \epsilon_n + \epsilon_{grav}. \quad (88)$$

### 3.8 Synthesis of the equations of stellar structure

We synthesize in this section the differential equations to solve in order to describe the internal structure of a star. We consider the two possible choices of independent variables : the distance to the center  $r$  and the mass of each sphere  $m$ .

#### Mass of each sphere :

Independent variable = radius :

$$\frac{dm}{dr} = 4\pi r^2 \rho \quad (89)$$

Independent variable = mass :

$$\frac{dr}{dm} = \frac{1}{4\pi r^2 \rho} \quad (90)$$

#### Hydrostatic equilibrium :

Independent variable = radius :

$$\frac{dP}{dr} = -\frac{\rho Gm}{r^2} \quad (91)$$

Independent variable = mass :

$$\frac{dP}{dm} = -\frac{Gm}{4\pi r^4} \quad (92)$$

#### Transport of energy :

a) Radiative zone :

Independent variable = radius :

$$\frac{dT}{dr} = -\frac{3\kappa\rho L}{16\pi r^2 acT^3}. \quad (93)$$

Independent variable = mass :

$$\frac{dT}{dm} = -\frac{3\kappa L}{64\pi^2 r^4 a c T^3}. \quad (94)$$

b) Convective zone :

The modeling of convection is difficult and still uncertain. As mentioned above, the Mixing-Length Theory is a simple approximate theory relating the convective flux to the local temperature gradient (see equations 69 to 74).

Independent variable = radius :

$$\frac{dT}{dr} \simeq -\nabla \frac{Gm\rho T}{r^2 P}. \quad (95)$$

Independent variable = mass :

$$\frac{dT}{dm} \simeq -\nabla \frac{Gm T}{4\pi r^4 P}. \quad (96)$$

Note that deep enough in the star, convection is very efficient, so that the temperature gradient is nearly adiabatic :  $\nabla \simeq \nabla_{ad}$ .

### Conservation of energy :

Independent variable = radius :

$$\frac{dL}{dr} = 4\pi r^2 \rho (\epsilon_n + \epsilon_{grav}). \quad (97)$$

Independent variable = mass :

$$\frac{dL}{dm} = \epsilon_n + \epsilon_{grav}, \quad (98)$$

where  $\epsilon_{grav} = -T ds/dt$ .

We can now count the number of equations and unknowns. We have 4 differential equations. 4 dependent variables appear explicitly on the left hand sides of these equations :  $m$  (or  $r$ ),  $P$ ,  $T$  and  $L$ . However, in addition to these 4 variables, there are 4 others on the right hand side :  $\rho$ ,  $\kappa$ ,  $\epsilon_n$  and  $\epsilon_{grav}$ . We need thus additional equations.

These are first the equations of state of stellar matter. They express all thermodynamic quantities as a function of two independent ones ( $T$  and  $P$  in what follows) and the chemical composition :

$$\rho = \rho(T, P, X_i), \quad u = u(T, P, X_i), \quad s = s(T, P, X_i) \dots \quad (99)$$

where  $X_i$  is the vector of abundances. In chapter 4, we will analyse in detail the state of stellar matter.

Calculating stellar opacities is a very challenging task. The opacity  $\kappa$  is a state variable. As such, it is also a function of the local temperature, pressure and chemical composition :

$$\kappa = \kappa(T, P, X_i). \quad (100)$$

In chapter 5, we will analyse in detail opacities and more generally the interaction between radiation and stellar matter.

In stellar interiors, nuclear reactions are a consequence of the thermodynamic state, mainly the very high temperatures. The rate of energy production by nuclear reactions is thus also a state variable. As such, it is also a function of the local temperature, pressure and chemical composition :

$$\epsilon_n = \epsilon_n(T, P, X_i). \quad (101)$$

Substituting these equations in the system of 4 differential equations, we have as much equations as unknowns.

### 3.9 Boundary conditions

With 4 differential equations, we need 4 boundary conditions to close the problem. The 2 conditions to impose in the center are trivial, the mass of the central point and the power produced by it are zero :

$$m(0) = 0 \ ; \ L(0) = 0 . \quad (102)$$

On the opposite, obtaining accurate surface boundary conditions is not easy. The physical conditions in the atmosphere of a star are very different from the interior. There, the mean free path of a photon is of the order of the thickness of the atmosphere (contrary to the interior where it is negligible) and it depends on the wavelength. Eq. 93 is thus completely wrong in the atmosphere. The usual approach is thus to separate the problems of stellar interior and atmosphere modeling. In this approach, the previously computed atmosphere models provide the surface boundary conditions for the interior models. More precisely, a continuous match between the interior and atmosphere model is imposed at a given layer, which can typically be the photosphere. In stellar physics, the **photosphere** is defined as the layer where the local temperature is equal to the effective temperature, which means, by definition of the effective temperature, the layer where the energy flux  $F = \sigma T^4$  (below

the photosphere  $F < \sigma T^4$ , above it  $F > \sigma T^4$ ). At the photosphere, we have thus by definition :

$$T_{\text{phot}} = \left( L / (4\pi R^2 \sigma) \right)^{1/4} . \quad (103)$$

This is the first of the 2 surface boundary conditions. To obtain the second one, the computation of atmosphere models is required. The input parameters required to compute an atmosphere model are the effective temperature (or equivalently the flux), the gravity and the chemical composition. For given values of these parameters, we have one atmosphere model and thus one value of the pressure at the photosphere of this model :

$$P_{\text{phot}} = f(T_{\text{eff}}, g, X_i) \quad (104)$$

where  $X_i$  is the chemical abundance vector.

From eq. 103 and  $g = GM/R^2$ , for given  $M$ ,  $R$ ,  $L$  and  $X_i$ , the pressure at the photosphere is thus :

$$P_{\text{phot}} = f\left(\left(L / (4\pi R^2 \sigma)\right)^{1/4}, GM/R^2, X_i\right). \quad (105)$$

This is the second of the 2 surface boundary conditions.

The mathematical problem to solve in order to obtain a model describing the internal structure of a star is now well defined. It is useful to notice that it is more appropriate to choose the mass of each layer as independent variable. Indeed, one can often assume that the mass of a star is conserved during its evolution, it is an input of the problem to solve. On the contrary, the total radius is unknown and varies significantly as the star evolves, it is an output of the problem. We have thus to solve the 4 differential equations 90, 92, 94 (or 96) and 98 with the 4 boundary conditions 102, 103 and 105.

It is important to note that the chemical composition of the model from the center to the surface must be specified as input. Indeed, it significantly affects equations 99, 100, 101 and 105.

## 4 State of stellar matter

### 4.1 Ideal gas and mean molecular weight

Deep enough in the star, stellar matter is (nearly) fully ionized. This liberates a lot of space. The size of nuclei is much smaller than the distance between them. It is thus tempting to describe the state of matter as an ideal gas. However, the particles are charged and thus interact through coulombian forces, which contradicts the no interaction hypothesis of an ideal gas. To determine the significance of the

coulombian interaction, we compare the mean kinetic energy of particles to the electrostatic potential of an electron of charge  $e$  at a distance  $d$  of another one :

$$E_{cin} \simeq \frac{3}{2}kT \approx keV > e^2/d, \quad (106)$$

Because of the very high temperatures inside stars, the kinetic energy of particles is always significantly larger than the electrostatic potential. As a consequence, the coulombian forces are not able to significantly deviate the trajectories of particles over a distance  $d$  and the equation of state can be approximated by an ideal gas :

$$P_g = nkT = \frac{k\rho T}{\mu m_u}. \quad (107)$$

We see in this equation the total number of particles per unit volume  $n$  and the mean molecular weight  $\mu$  (dimensionless definition). For a fully ionized gas, it can be obtained as follows for a given chemical composition. The Dalton law says that the total pressure is the sum of the partial pressures of each constituent. We have thus :

$$P_g = P_e + \sum_i P_i, \quad (108)$$

where  $P_e$  is the electronic pressure and  $P_i$  is the partial pressure of the ions  $i$ . Similarly, we have :

$$n = n_e + \sum_i n_i, \quad (109)$$

where  $n_e$  is the number of free electrons and  $n_i$  is the number of ions  $i$  per unit volume. The neutrality of the gas imposes to have as much electrons as protons. We note  $Z_i$  the number of protons in the nucleus  $i$ . The number of free electrons,  $n_e$ , is thus equal to the sum of the number of protons associated to each nucleus :

$$n_e = \sum_i Z_i n_i. \quad (110)$$

Combining these 2 equations, we find thus :

$$n = \sum_i (Z_i + 1)n_i. \quad (111)$$

The number of ions  $i$  per unit volume is equal to the density of this ion  $\rho_i$  divided by its mass  $A_i m_u$ . By definition of the mass fraction, we have thus :

$$n_i = \frac{\rho_i}{A_i m_u} = \frac{\rho X_i}{A_i m_u}. \quad (112)$$

Combining equations 107, 111 and 112 we have thus :

$$P_g = nkT = kT \sum_i (Z_i + 1)n_i = \frac{k\rho T}{m_u} \sum_i (Z_i + 1)X_i/A_i = \frac{k\rho T}{\mu m_u}. \quad (113)$$

We have thus for the mean molecular weight :

$$\mu = \left( \sum_i X_i(1 + Z_i)/A_i \right)^{-1}. \quad (114)$$

It is important to note the difference between this relation and the corresponding one for a non-ionized gas. In such gas,  $Z_i$  should be replaced by 0 in eq. 114.

Exercice :

Calculate the mean molecular weights of the following fully ionized gases :

a) Pure hydrogen, b) pure helium, c) hydrogen ( $X=0.7$ ) + helium ( $Y=0.3$ ), d) helium ( $Y=0.4$ ) + carbon<sub>12</sub> ( $X_C = 0.4$ ) + oxygene<sub>16</sub> ( $X_O = 0.2$ ).

## 4.2 Partial ionization

However, the gas is not fully ionized everywhere in the star. As the temperature and pressure decrease from inside towards outside, the electrons recombine progressively in superficial layers called **partial ionization zones**. The partial ionizations of different elements correspond to regions with different ranges of temperature. For example the hydrogen partial ionization zone ( $H^+ + e^- \leftrightarrow H$ ) corresponds to temperatures between 10000 and 20000 K (it is just below the photosphere for an intermediate mass star). The first ionization zone of helium ( $He^+ + e^- \leftrightarrow He$ ) intersects it with temperatures between 15000 and 25000 K. The second partial ionization zone of helium ( $He^{++} + e^- \leftrightarrow He^+$ ) is slightly deeper, in the temperature range 35000-65000 K. The ionization potential increases of course with the charge of the nucleus ; the partial ionization zones of the heaviest elements (for example Iron) are thus deeper in the star.

The interior of stars is in local thermodynamic equilibrium. A statistical equilibrium is thus established between the continuous ionizations and recombinations of electrons in a partial ionization zone. The powerful tools of statistical physics allow us to determine the occupation of each ionization states corresponding to this equilibrium, this is the Saha equation (Meghnad Saha, 1920). Consider as a simple example a gas of pure hydrogen. I note  $n_0$  the number of neutral hydrogen atoms (proton with bound electron),  $n_+$  the number of free protons and  $n_e$  the number of free electrons per unit volume. The Saha equation reads then :

$$\frac{n_+ n_e}{n_0} = \frac{g}{h^3} (2\pi m_e kT)^{3/2} e^{-\chi/kT}, \quad (115)$$

where  $g$  is a constant and  $\chi$  is the ionization potential of hydrogen.

We note  $x_H$  the «degree of ionization» of hydrogen :

$$x_H = \frac{n_+}{n_0 + n_+}. \quad (116)$$

For a gas of pure hydrogen,  $n_+ = n_e$ . The equation of state reads thus :

$$P = (n_0 + 2n_+)kT = (1 + x_H)(n_0 + n_+)kT = (1 + x_H)\frac{k\rho T}{m_u}. \quad (117)$$

The mean molecular weight and the degree of ionization are thus related by  $\mu = (1 + x_H)^{-1}$ . As matter ionizes, the number of free electrons and thus the number of free particles increases and these free electrons become the main contributors to the pressure (the number of free electrons is larger than the number of ions in a fully ionized gas). Combining the previous equations, the degree of ionization is easily written as a simple function of the temperature and pressure :

$$\frac{x_H^2}{1 - x_H^2} = \frac{g}{h^3} \frac{(2\pi m_e)^{3/2} (kT)^{5/2}}{P} e^{-\chi/kT} \quad (118)$$

For  $kT \gg \chi$ , the right hand side of this equation is usually much larger than 1 and  $x_H \rightarrow 1$  (fully ionized hydrogen). For  $kT \ll \chi$ , the right hand side is negligible and  $x_H \rightarrow 0$  (atomic hydrogen).

Exercice : Plot the degree of ionization of hydrogen as a function of temperature for a pressure proportional to  $T^{5/2}$ .

### 4.3 The pressure integral

We establish now a result which will be very useful in the next sections. We consider a gas of particles with an isotropic distribution of velocities, we want to determine the pressure of the gas for a given distribution of momentum of the particles. We neglect the interactions between particles (ideal gas).

First note that :

**The pressure exerted by an ideal gas on a surface is the flux of perpendicular momentum through this surface due to the motions of the particles.**

As a preliminary step before considering the isotropic case, we consider particles moving at the same speed  $v$ , momentum  $p$ , all in the same direction having an angle  $\theta$  with respect to the perpendicular to the surface. We note  $n$  the number of particles

per unit volume. The perpendicular components of the momentum and velocity are then  $p \cos \theta$  and  $v \cos \theta$ , so that the pressure exerted on the surface is :

$$P = n p v \cos^2 \theta . \quad (119)$$

We can now consider the isotropic gas where particles propagate in all directions with the same probability and do not have the same speeds and momenta. I note  $n(p)$  the density of particles per unit volume and momentum. The pressure of this gas is given by the following integral :

$$P = \frac{1}{3} \int_0^\infty v p n(p) dp . \quad (120)$$

**Proof :**

$\sin \theta d\theta / 2$  is the fraction of particles propagating in a direction having an angle between  $\theta$  and  $\theta + d\theta$  with respect to the perpendicular to the surface.  $n(p) dp \sin \theta d\theta / 2$  is thus the number of particles per unit volume propagating in this direction and having a momentum between  $p$  and  $p + dp$ . Using eq. 119, the pressure exerted by these particles is :

$$dP = n(p) p v \cos^2 \theta (\sin \theta / 2) dp d\theta . \quad (121)$$

Integrating this expression over all possible  $\theta$  gives the total pressure :

$$P = \int_0^\infty n(p) p v dp \int_0^\pi \cos^2 \theta \sin \theta d\theta / 2 = \frac{1}{3} \int_0^\infty v p n(p) dp . \quad (122)$$

## 4.4 Radiation pressure

The gas of ions and electrons is not the only contributor to pressure in stellar interiors. Photons also have a momentum given by  $p = h\nu/c$ , where  $\nu$  is the frequency. A momentum flux is thus associated to radiation, it is called the radiation pressure. An absorbed or scattered photon transmits its momentum (or part of it) to the electron with which it interacts and push thus matter in its propagation direction. As an example, in the superficial layers of very massive stars, the momentum transmitted by photons to matter is very large, leading to expulsion of this matter through strong winds.

The interior of stars is very opaque, so that radiation is quasi-isotropic. We can thus apply the result obtained in Sect. 4.3 to an isotropic gas of photons in thermodynamic equilibrium (black body). It is more appropriate to use the frequency as integration

variable. We define  $n(\nu)$  as the number of photons per unit volume and frequency. The pressure integral (eq. 120) reads thus for the photons :

$$P_{rad} = \frac{1}{3} \int_0^\infty c (h\nu/c) n(\nu) d\nu = \frac{1}{3} \int_0^\infty E(\nu) d\nu, \quad (123)$$

where  $E(\nu)$  is the density of radiation energy per unit volume and frequency, it is given by the Planck law. Integrating it over all frequencies gives the Stefan-Boltzmann law for the radiation energy density :

$$\int_0^\infty E(\nu) d\nu = aT^4 \quad (124)$$

and we have the final result :

$$P_{rad} = \frac{1}{3} aT^4. \quad (125)$$

The equation of state of an ideal gas + radiation is thus given by :

$$P = P_g + P_{rad} = \frac{k\rho T}{\mu m_u} + \frac{1}{3} aT^4. \quad (126)$$

Since the dependence of the radiation pressure with respect to temperature is much higher than that of matter, radiation pressure dominates compared to matter (electrons and ions) at high temperatures and/or low density. This is so in very massive stars.

## 4.5 Quantum degeneracy of the electron gas

In the previous sections, we have neglected an aspect that can have sometimes significant consequences. Electrons and nucleons are fermions. As a consequence, they must obey to the

**Pauli exclusion principle** : 2 fermions may not be in the same quantum state.

At moderate or low density, this principle is not affecting significantly the occupation statistics of the gas particles. The fermions and in particular the electrons have enough free space around them, the number of easily accessible states is much higher than the number of occupied states. In this case, the equation of state can be approximated by eq. 126.

On the opposite, at very high density, the number of “easily” accessible electron states is lower than the number of electrons. In this case, the Pauli exclusion principle is very constraining, the gas is said to be “degenerated”.

We consider a gas of free particles without interaction between them (ideal gas). The phase space is appropriate to describe the state of a free particle, it is the 6 dimensions space providing the possible positions and momenta of a particle. We focus here on the electron gas. Indeed, we will see that degeneracy can mainly occur for the electrons. Electrons are spin 1/2 particles, which means that 2 values of the spin are possible. In the phase space, the Pauli principle reads :

**A volume of the phase space  $dx dy dz dp_x dp_y dp_z = h^3$  can be occupied by maximum 2 electrons (the two possible spins).**

Before showing the consequences of degeneracy, a reminder of the classical non-degenerate case is useful. In a classical gas in thermodynamic equilibrium, the distribution of free electrons momenta is given by the **Maxwell-Boltzmann** equation :

$$n(p) = n_e \frac{4\pi p^2}{(2\pi m_e kT)^{3/2}} \exp\left(-\frac{p^2}{2m_e kT}\right). \quad (127)$$

In this equation,  $n_e$  is the number of free electrons per unit volume,  $n(p)$  is the number of free electrons per unit volume and momentum (already encountered in Sect. 4.3) and  $m_e$  is the mass of one electron.

The problem is that this equation is not necessarily in agreement with the Pauli exclusion principle. When it is not, it is wrong and it must be replaced by the accurate **Fermi-Dirac** distribution, which will be presented later. To determine the limit imposed by the Pauli exclusion principle, we consider the infinitesimal volume of the 6 dimensions phase space corresponding to a spatial volume  $dV$  and all momenta between  $p$  and  $p + dp$ . Its volume in the phase space is :  $4\pi p^2 dp dV$  (volume of the spherical shell of radii between  $p$  and  $p + dp$  times  $dV$ ).

In the phase volume  $h^3$ , we have seen that the maximum number of electrons is 2. In the phase volume  $4\pi p^2 dp dV$ , the maximum number of electrons is thus :  $8\pi p^2 / h^3 dp dV$ . By definition,  $n(p) dp dV$  is the number of electrons in this volume. The Pauli exclusion principle imposes thus :

$$n(p) \leq 8\pi p^2 / h^3. \quad (128)$$

The Maxwell-Boltzmann distribution can sometimes violate this inequality, when ? The criterion of degeneracy answers to this question.

## Degeneracy criterion

We first replace  $n(p)$  by the Maxwell-Boltzmann expression (equation 127) in the inequality 128. As the exponential tends to 1 as the momentum tends to 0, this inequality is equivalent to :

$$\begin{aligned} n_e \frac{4\pi p^2}{(2\pi m_e kT)^{3/2}} &< 8\pi p^2/h^3 \\ \Leftrightarrow \frac{n_e}{(2\pi m_e kT)^{3/2}} &< \frac{2}{h^3} \end{aligned} \quad (129)$$

We wish to reexpress this criterion with the density  $\rho$  instead of  $n_e$ . It is clear that they are proportional. This leads me to introduce the **mean molecular weight per electron** defined by :

$$\mu_e \equiv \frac{\rho}{m_u n_e}. \quad (130)$$

Using this relation, the inequality 129 becomes :

$$\frac{\rho T^{-3/2}}{\mu_e} < \frac{2m_u(2\pi m_e k)^{3/2}}{h^3}. \quad (131)$$

Finally, replacing the constants by their values in MKSA units, the degeneracy criterion (violation of the Pauli exclusion principle by the Maxwell-Boltzmann distribution) is :

$$\frac{\rho T^{-3/2}}{\mu_e/2} > 1.6 \times 10^{-5} \text{ kg m}^{-3} \text{ K}^{-3/2}. \quad (132)$$

In the right member of inequality 131, you can see the mass of the considered particles (here the electron mass  $m_e$ ). The smaller this mass, the easier is this inequality violated. From that, we see that degeneracy appears first for the gas of electrons. Much larger  $\rho T^{-3/2}$  would be needed to enter in the degeneracy regime of nuclei. The unique extreme case where nuclei degeneracy is reached is in neutron stars. On the contrary, electron degeneracy is frequent in usual stars and, as we will see, it has a strong impact on stellar evolution when it is present.

## Completely degenerated gas

In order to describe the state of degenerated gas, the Fermi-Dirac distribution must be used. It asymptotically tends to the Maxwell-Boltzmann distribution when  $\rho T^{-3/2} \rightarrow 0$ . It is interesting to study the other extreme case where  $\rho T^{-3/2} \rightarrow \infty$ . More precisely, we consider the limit case where  $T \rightarrow 0$  and  $\rho$  is fixed. The gas is

said to be completely degenerated in this case. The Fermi-Dirac distribution tends asymptotically towards the following function when  $T \rightarrow 0$  :

$$\begin{aligned} n(p) &= \frac{8\pi p^2}{h^3} & \text{if } p \leq p_F \\ n(p) &= 0 & \text{if } p > p_F \end{aligned}$$

$p_F$  is called the **Fermi momentum**, it can be directly related to the density and pressure, as will be shown in what follows. We see that, in complete degeneracy, all cases of the phase space are occupied by electrons up to the Fermi momentum.

It is possible to analytically determine the equation of state in this extreme case. I begin by computing the number of electrons per unit volume. It is simply obtained by integrating  $n(p)$  over all possible momenta :

$$n_e = \frac{\rho}{\mu_e m_u} = \int_0^\infty n(p) dp = \int_0^{p_F} \frac{8\pi p^2}{h^3} dp = \frac{8\pi p_F^3}{3h^3} \quad (133)$$

From the definition of the mean molecular weight per electron (eq. 130), we have thus

$$\rho = \mu_e m_u \frac{8\pi p_F^3}{3h^3} \quad (134)$$

We compute now the electron pressure, using the pressure integral (equation 120) established in Sect. 4.3.

### Non-relativistic completely degenerated gas :

We begin with the case of a non-relativistic gas, in which  $v \ll c$  for most of the particles. We can then assume that  $v = p/m_e$ , where  $m_e$  is the electron rest mass. The pressure integral gives thus :

$$P_e = \frac{1}{3} \int_0^\infty \frac{p^2 f(p)}{m_e} dp = \frac{1}{3} \int_0^{p_F} \frac{8\pi p^4}{m_e h^3} dp = \frac{8\pi}{15h^3} \frac{p_F^5}{m_e}. \quad (135)$$

The Fermi momentum is easily eliminated by combining equations 134 et 135. This gives :

$$P_e = \frac{8\pi}{15h^3 m_e} \left( \frac{3h^3}{8\pi m_u} \right)^{5/3} \left( \frac{\rho}{\mu_e} \right)^{5/3} = K_1 \rho^{5/3}, \quad (136)$$

the pressure is thus proportional to the power 5/3 of the density in a non-relativistic completely degenerated gas and is independent of the temperature.

### Highly relativistic completely degenerated gas :

We consider now the extreme density case where  $p_F \gg m_e c$ . In this case, most of the electrons have relativistic speeds.  $v = p/m_e$  is wrong and we can assume instead that  $v \simeq c$  for most of the electrons. The pressure integral gives then :

$$P_e = \frac{1}{3} \int_0^\infty p c n(p) dp = \frac{1}{3} \int_0^{p_F} \frac{8\pi c p^3}{h^3} dp = \frac{2\pi c}{3h^3} p_F^4. \quad (137)$$

Again, the Fermi momentum is easily eliminated by combining now equations 134 et 137. This gives :

$$P_e = \frac{2\pi c}{3h^3} \left( \frac{3h^3}{8\pi m_u} \right)^{4/3} \left( \frac{\rho}{\mu_e} \right)^{4/3} = K_2 \rho^{4/3}, \quad (138)$$

the pressure is thus proportional to the power 4/3 of the density in a relativistic completely degenerated gas and it is independent of the temperature.

### Partially relativistic completely degenerated gas :

In the intermediate case, where  $p_F \approx m_e c$ , we must use the following relation provided by the theory of special relativity :

$$p = \frac{m_e v}{\sqrt{1 - v^2/c^2}} \Leftrightarrow v = \frac{p/m_e}{\sqrt{1 + (p/(m_e c))^2}}. \quad (139)$$

The pressure integral reads then :

$$P_e = \frac{1}{3} \int_0^{p_F} \frac{8\pi p^4 dp}{m_e h^3 \sqrt{1 + (p/(m_e c))^2}}. \quad (140)$$

Note finally that, in all completely degenerated cases, the pressure exerted by the ions appears to be negligible compared to the electron pressure. In the above equations, the electron pressure can thus be replaced by the total pressure.

### Partially degenerated gas :

Between the extreme cases of non-degenerated and completely degenerated gases, we have partially degenerated gases. In this case, the Fermi-Dirac distribution must be used :

$$n(p) = \frac{8\pi p^2}{h^3} \frac{1}{1 + \exp(E/kT - \psi)}, \quad (141)$$

where  $\psi$  is the degeneracy parameter ( $> 0$  for a degenerated gas). For significant degeneracy ( $\psi \gg 1$ ), the Fermi Dirac distribution can be separated in three part : at small momenta and energies,  $n(p) \simeq 8\pi p^2/h^3$  like in a completely degenerated gas ; at very high momenta and energies, the decreasing exponential dominates and, between, we have a continuous transition. The size of this transition region is of the order of  $kT$  if energy is the independent variable. For significant electron degeneracy, it is important to notice that most electrons have energies much larger than  $kT$ , which is completely different from usual non-degenerated gases (remind that the mean energy of a particle is  $(3/2)kT$  in a non-degenerated monoatomic gas). You must thus disregard this relation when you deal with a degenerated gas. Decreasing the temperature does not necessarily leads to a decrease of the electron energies. In a degenerated gas, this just leads to a decrease of the size of the transition region. Imagine that you maintain constant the density, changing the temperature will not significant modify the pressure integral. Hence,

$$\partial \ln P / \partial \ln T|_{\rho} \simeq 0, \quad \partial \ln \rho / \partial \ln T|_P \simeq 0, \quad (142)$$

in a degenerated gas. This has strong consequences on stellar evolution. One example is the onset of helium burning in the core of a low mass ( $< 2 M_{\odot}$ ) red giant. Due to the significant core contraction preceding this phase, the core density is huge. The temperature has also significantly increased, up to  $\approx 10^8$  K, but not as much as the density, so that the electron gas has become degenerated. When helium burning starts, the produced energy increases the kinetic energy of the nuclei and thus the temperature. But this has no impact on the pressure (exerted by the degenerated electrons) and the density (equations 142), which remain constant and are not able to control the temperature, a thermal runaway starts, the **Helium flash**.

### Electron density and mean molecular weight per electron

In the previous derivations, we introduced the electron number density  $n_e$  and the mean molecular weight per electron  $\mu_e$ , related by  $\mu_e = \rho / (m_u n_e)$ . It is useful to determine their values for a completely ionized gas. From equations 110 and 112, we have

$$n_e = \frac{\rho}{m_u} \sum_i (Z_i / A_i) X_i \quad (143)$$

The hydrogen mass fraction is usually noted  $X$ , the helium mass fraction  $Y$  and the one of all other elements (the “metals”)  $Z = 1 - X - Y$ . Supposing as a simplification that the numbers of protons and neutrons are equal in average in the heavy elements, equation 110 simplifies as :

$$n_e = \frac{\rho}{m_u} (X + Y/2 + (1 - X - Y)/2) = \frac{\rho}{m_u} \frac{1 + X}{2}$$

We have thus for the mean molecular weight per electron  $\mu_e$  :

$$\mu_e = \frac{\rho}{n_e m_u} \simeq \frac{2}{1 + X}. \quad (144)$$

The factor  $1 + X$  appearing in this equation will always be present when we consider physical quantities depending on the number of free electrons. An important example is the opacity, which will be considered in the next chapter.

## 4.6 State of matter as a function of $\rho$ and $T$

### Radiation pressure

We have seen (equation 126) that the radiation pressure is  $P_R = (1/3)aT^4$  and the gas pressure of an ideal non-degenerated gas :  $P_g = k\rho T/\mu m_u$ . The radiation pressure dominates when :

$$\frac{1}{3}aT^4 > \frac{k\rho T}{\mu m_u}$$

Taking the logarithm, this gives :

$$\log T > \frac{1}{3} \log \rho + cst.$$

In other words, radiation pressure dominates above a straight line of steepness  $1/3$  in the upper-left part of a  $\log \rho - \log T$  diagram.

### Electron degeneracy

Where is now the region where the electron gas becomes degenerated? Taking the logarithm of inequality 132, we see that this occurs when :

$$\log T < \frac{2}{3} \log \rho + cst.$$

In other words, the electron gas is degenerated below a straight line of steepness  $2/3$  in a  $\log \rho - \log T$  diagram. White dwarfs are typical stars where the electron gas is degenerated.

### Usual ideal gas

Significantly above this line and below the line associated to radiation pressure, the equation of state can be approximated by the ideal gas law. In particular, it is worth to notice that the different layers of the Sun, from its surface to its center lay in this latter region.

### Relativistic degeneracy

We have seen that it is important to distinguish relativistic and non-relativistic degeneracy. Indeed, this significantly affects the equation of state (compare equations 136 and 138). The degenerated electron gas becomes relativistic when the Fermi momentum  $p_F$  is larger than  $m_e c$ .  $p_F$  is related to the density through equation 134. Hence, the electron gas becomes relativistic when :

$$\rho > \mu_e m_u \frac{8\pi}{3} \left( \frac{m_e c}{h} \right)^3 \simeq 1.95 \times 10^6 (\mu_e/2) \text{ g/cm}^3. \quad (145)$$

This region is on the right of a vertical line in the  $\log \rho - \log T$  diagram.

Finally, it is worth to mention that at very high density and very low temperatures (compared to typical stellar values) the ions cristalize, changing of phase from gaseous to solid. This occurs in cold white dwarfs. Since they are mainly composed of carbon and oxygen, some refer to them as stellar diamonds !

## 5 Interaction between matter and radiation : the opacity

An accurate knowledge of the interaction between matter and radiation is essential for modeling the transport of energy by radiation inside stars. Concretely, the opacity  $\kappa$  explicitley appears in the radiative diffusion equation :

$$\frac{dT}{dr} = - \frac{3\kappa\rho L_R}{16\pi r^2 acT^3}.$$

We have demonstrated (see Sect. 3.5 for detail) that the opacity appearing in this equation is the **Rosseland mean opacity** defined by :

$$\kappa = \left[ \frac{\pi}{acT^3} \int_0^\infty \frac{1}{\kappa_\nu} \frac{dB_\nu}{dT} d\nu \right]^{-1}, \quad (146)$$

where  $B_\nu$  is the Planck function. This mean opacity came from the integration of the monochromatic flux over all frequencies, under the hypothesis of very small mean free path of photons :

$$F = \int_0^\infty F_\nu d\nu = - \frac{4\pi}{3\rho} \frac{dT}{dr} \int_0^\infty \frac{1}{\kappa_\nu} \frac{dB_\nu}{dT} d\nu.$$

The interpretation of this equation is important. 2 factors appear in it. First, there is the mean free path of a photon  $(\kappa_\nu \rho)^{-1}$ , the larger it is at a given frequency, the more efficient is the transport of energy at this frequency. Second, I remind that the radiation field is quasi-isotropic in stellar interiors. Due to the temperature gradient,

the number of photons going up is very slightly larger than the number of photons going down. This explains the factor  $dB_\nu/dr = (dB_\nu/dT)(dT/dr)$ . The larger it is, the larger the difference between the upwards and downwards radiative flux. This factor is the largest around the peak of the Planck function at  $\lambda \approx 0.29/T$  cm ( $\nu \approx kT$ ).

As a summary, **what matters for the modeling of radiation transport in stellar interiors is to know the transparency (photons mean free path) of the medium in the part of the spectrum where the photons are the most numerous.**

We consider now in more detail the different sources of opacity. For the typical values of the temperatures in stellar interiors,  $kT \approx 1 - 1000$  eV. Indeed, expressing the relation  $E = kT$  in eV gives  $E_{eV} = 8.62 \times 10^{-5} T(K)$ . The changes of state of electrons are the only transitions with such energies. We must thus focus on them for opacity computation. On the opposite, the nuclear energy levels are of the order of MeV. This is far too high for a star like our Sun, the interaction between nuclei and radiation is usually not significant. The only exception is the ultimate phase of evolution of very massive stars. Just before and during the collapse of the iron core initiating a type II Supernova explosion, the temperatures in the core are of the order of  $10^{10}$  K. Many photons have then enough energy to break nuclei. We are not there and we can restrict to electronic transitions here. The different possible electronic transitions can be subdivided in 4 families : the bound-bound, bound-free, free-free transitions and electron scattering.

### Cross-sections

It is usual to deal with cross-sections instead of opacities. Both are related through the definition of the mean free path  $l_\nu$  of a photon with frequency  $\nu$  :

$$l_\nu^{-1} = \kappa_\nu \rho = \sum_i \sigma_{\nu,i} n_i, \quad (147)$$

where  $i$  corresponds to a given electronic state,  $n_i$  is the number of electrons per unit volume in this state and  $\sigma_{\nu,i}$  is the cross section associated to electronic transitions from this state with a photon of frequency  $\nu$ .

## 5.1 Bound-bound transitions

In bound-bound transitions, an electron goes from a bound state to another bound state of higher energy. The required energy  $\Delta E = h\nu$  is provided by a photon of frequency  $\nu$ , which is absorbed. One could think that the cross-section associated to such transition is a Dirac peak at a frequency  $\nu_0 = \delta E_0/h$ . However, there are different sources of broadening producing instead a cross-section with finite  $>0$  linewidth.

### Natural broadening :

The natural broadening is associated to the time-energy uncertainty principle. As all states have a finite lifetime, their energy is uncertain. This energy uncertainty is inversely proportional to the lifetime. More precisely, the “natural” cross-section  $\sigma(\nu)$  is the following Lorentzian profile centered on  $\nu_0$  :

$$\sigma(\nu) \propto \frac{1}{1/(2\pi\tau)^2 + (\nu - \nu_0)^2}. \quad (148)$$

This natural broadening is always very small compared to the other contributions.

### Thermal broadening :

The particles of a gas have a distribution of energy typically given by the Maxwell-Boltzmann probability density function in non-degenerated case. From the point of view of the moving particle, the absorbed photon is blue-shifted or red-shifted by the Doppler effect depending on the velocity of the atom relative to the observer. For non-relativistic velocities, this shift is  $\delta\nu/\nu_0 = V/c$  where  $V$  is the relative velocity and  $c$  the speed of light. Noting  $\nu_0 = \delta E/h$  the frequency from the point of view of the absorbing particle and  $V_z$  the velocity projected on the observer direction, the frequency from the point of view of the observer is  $\nu = \nu_0 (1 + V_z/c)$ . Out of degeneracy, the density probability  $f(V_z)$  is a normal distribution :

$$f(V_z) = \sqrt{\frac{kT}{2\pi}} \exp(-mV_z^2/(2kT)), \quad (149)$$

where  $m$  is the absorbing particle’s mass. Thermal broadening produces thus a Gaussian cross-section centered on  $\nu_0$ , with a standard deviation  $\sqrt{kT/m}\nu_0/c$ . It is called thermal broadening.

### Pressure broadening and Stark effect :

When a free charged particle goes very close to an ion, it perturbs its potential and thus the energy levels of its bound electrons. The average effect of all these collisions is a broadening (and slight shifts) of the cross-sections called pressure broadening. The corresponding profile is more or less Lorentzian, like natural broadening, but with larger linewidth.

The final cross-section  $\sigma(\nu)$  associated to a given transition is obtained through a convolution product of these different profiles.

The high complexity of the problems now appears in the huge number of bound-bound transitions and the coupling between bound states. Each possible ion ( $k$ ), degree of ionization ( $i$ ), initial ( $j_1$ ) and final ( $j_2$ ) excited level of the electron must be considered. Noting  $n_{k,i,j}$  the number of elements per units volume in the state

$(k, i, j)$  and  $\sigma_{k,i,j_1,j_2}(\nu)$  the cross-section of the bound-bound transition from  $(k, i, j_1)$  to  $(k, i, j_2)$ , the opacity  $\kappa(\nu)$  resulting from all possible transitions is :

$$\kappa(\nu) = \rho^{-1} \sum_{k,i,j_1,j_2} n_{k,i,j_1} \sigma_{k,i,j_1,j_2}(\nu). \quad (150)$$

For given abundances of each element and under the hypothesis of thermodynamic equilibrium, the different number densities  $n_i$  can be obtained from simple relations. First, the Saha equation gives the fractional population of ionization degrees :

$$\frac{n_{I+1} n_e}{n_I} = \frac{g_{I+1}}{g_I} 2(2\pi m_e kT)^{3/2} e^{-\chi_I/kT}, \quad (151)$$

where  $n_I$  and  $n_{I+1}$  are the number densities of a given element in the ionization states  $I$  and  $I+1$ . I remind that the Roman numeral indexing ions is the number of its lost electrons minus 1 (e.g  $H_I$  is neutral hydrogen,  $H^+ = H_{II}$  is ionized hydrogen,  $He^{++} = He_{III}$  is fully ionized helium, ...).  $n_e$  is the electron number density and  $\chi_I$  is the ionization potential (see next section about bound-free transitions).

Second, the Boltzmann distribution gives the fractional population of excited states of bound electrons :

$$\frac{n_i}{n_j} = \frac{G_i}{G_j} e^{-\Delta E_{ij}/kT}, \quad (152)$$

where  $n_i$  and  $n_j$  are the number densities at excited states  $i$  and  $j$  and  $\Delta E_{ij} = E_i - E_j$  is the difference of energy between the two levels. Finally, the cross-sections must be determined for all possible transitions. You can imagine that computing all of them this is a huge work, particularly if you want to take the coupling between states into account !

However, at a given temperature, all transitions don't have an equal importance. **Only the transitions for which you have enough photons matter, in other words those such that  $\Delta E \approx kT$ .** An important example in stellar interiors is associated to elements of the iron group : iron, nickel, cobalt and manganese. All bound-bound (and bound-free) transitions from the third electronic level  $M$  to a higher level have similar  $\Delta E$  in these elements. The corresponding temperatures are  $T \approx \Delta E/k \approx 200\,000$  K. At these temperatures, a lot of photons are able to produce these transitions. This produces a peak of opacity around this temperature. This peak is very significant in B stars ; it plays a key role in the excitation of pulsation modes of  $\beta$  Cep and Slowly Pulsating B stars.

Finally, it is easy to understand that bound-bound transitions only play a role in regions where there are bound electrons. At temperatures below  $10^6$  K, they are numerous and the bound-bound transitions contribute up to 50 % of the total opacity. On the opposite, at  $T \approx 10^7$  K, most elements are fully ionized and the bound-bound transitions contribute to less than 10 % of the total opacity.

## 5.2 Bound-free transitions

In a bound-free transition, an absorbed photon provides enough energy to a bound electron to liberate it from the attraction of the nucleus. More precisely, the energy of the photon is larger than the ionization potential of the electron :  $E = h\nu \geq \chi$ . The electron arrives thus in the continuum of free electrons, its kinetic energy is the additional energy  $h\nu - \chi$ . The required frequency is thus  $\nu \geq \chi/h$ . Above this critical frequency, quantum mechanics shows that the cross-section follows a decreasing law  $\sigma(\nu) \propto \nu^{-3}$  until a new bound-free transition from a lower level becomes possible. At each frequency  $\nu_i = \chi_i/h$ , there is a discontinuous increase of the cross-section. This produces a saw-tooth  $\sigma(\nu)$  curve, each discontinuity being related to a given bound-free transition. As for the bound-bound transitions, all elements, degrees of ionization and electron levels must be considered to determine the contribution of bound-free transitions to the opacity.

Here also however, all transitions don't have an equal importance. Only the transitions for which you have enough photons matter, in other words those such that  $\nu \approx kT/h$ , this is the first condition. The second condition is to have enough electrons in the initial state. What are the ionization potentials fulfilling these two conditions ? The bound-free transitions such that  $\chi \ll kT$  don't fulfill the second condition ; the number of electrons in the corresponding initial state is too low, as can be seen from the Saha equation (151). On the other side, if  $\chi \gg kT$ , the number of photons able to produce the transition ( $\nu \geq \chi/h$ ) is too low. Hence, only the transitions such that  $\chi \approx kT$  play a significant role at a given temperature.

An important question is of course how the contribution of bound-free transitions to the Rosseland mean opacity varies with the temperature. What matters in this mean is the spectral domain  $\nu_0 \approx kT/h$  where most photons are. Forgetting the discontinuities,  $\kappa(\nu)$  follows grosso-modo a  $\nu^{-3}$  curve. Focusing on the most numerous photons, we have thus  $\kappa_{bf} \approx \kappa(\nu_0) \propto \nu_0^{-3} \propto T^{-3}$ . This justification of the  $T^{-3}$  dependence is very approximate. The dependence of the bound-free opacity with respect to the temperature, density and chemical composition is often approximated by the following law :

$$\kappa_{bf} \simeq 4.34 \times 10^{25} Z(1 + X)\rho T^{-3.5} \text{ cm}^2/\text{g} . \quad (153)$$

This law is too approximate and is never used for the computation of realistic stellar models, but it can be used to interpret tendencies. First you can note the  $T^{-3.5}$  dependence (a little better approximation than  $T^{-3}$ ). Except near the surface, the opacity decreases as the temperature increases. Therefore, the core of a star is always less opaque than its envelope. You can also note the presence of the factor  $Z$  (mass fraction of heavy elements). The heavy elements are indeed the only ones having bound electrons at temperatures larger than  $10^5$  K. The opacity due to bound-free transitions is thus proportional to their abundance.

As for the bound-bound transitions, the bound-free transitions significantly contribute to the opacity in the superficial layers of a star ( $T < 10^6$  K). In deeper layers, most elements are already ionized and the number of bound electrons is reduced. Without electrons in the good initial state, bound-free transitions no longer play a significant role there.

### 5.3 Free-free transitions

In a free-free transition, also called “inverse Bremsstrahlung”, a free electron absorbs a photon and goes in another direction with a surplus of kinetic energy  $h\nu$  provided by the photon. The inverse reaction is the well known Bremsstrahlung (from bremsen "to brake" and Strahlung "radiation"; i.e., "braking radiation" or "deceleration radiation"), where a charged particle deflected by another charged particle loses kinetic energy, which is converted into a photon. This clearly shows that this process (in one direction or the opposite) always requires the presence of a second charged particle (here an ion). Without it, conservation of both momentum and energy cannot be ensured. Unlike the previous processes, there is no constraint on the frequency of the absorbed photon. Quantum mechanics shows that the cross-section of this transition follows approximately this law :  $\sigma(\nu) \propto v^{-1}\nu^{-3}$  ( $v$  is the initial speed of the electron, the larger it is, the more difficult to deflect it). From this, it is easy to estimate the contribution of free-free transitions to the Rosseland mean opacity and its dependence with respect to temperature and chemical composition. Out of degeneracy, the mean speed of electrons is proportional to  $\sqrt{T}$ . The domain of the spectrum which matters corresponds to  $\nu_0 \approx kT/h$ . We have thus  $\kappa_{ff} \approx \kappa(\nu_0) \propto T^{-3.5}$ . The dependence of the free-free opacity with respect to the temperature, density and chemical composition is often approximated by the following law (it is called the Kramers law) :

$$\kappa_{ff} \simeq 3.68 \times 10^{22} (X + Y)(1 + X)\rho T^{-3.5} \text{ cm}^2/\text{g}. \quad (154)$$

This analytical law is less approximate than equation 153, but more accurate free-free opacities are used in modern stellar structure models. In addition to the  $T^{-3.5}$  dependence, you can note the presence of the factor  $(X + 1)$  ( $X$  is the hydrogen mass fraction). We come back to this in the next subsection. Note also that the Kramers law does not apply at all in a degenerated electron gas. Indeed, degeneracy limits the number of possible electron states and thus the number of possible free-free transitions. Matter is thus more transparent in a degenerated electron gas.

Free-free transitions significantly contribute to the opacity in the deep layers of a star ( $T > 10^6$  K). Indeed, most elements are ionized there, leading to numerous free electrons.

## 5.4 Electron scattering

At a microscopic scale, electron scattering can be seen as an elastic collision between a free electron and a photon. The photon and electron trajectories are deflected during the collision, but they keep their energy. No ion is required for this transition. The photon is not absorbed ; however, because its trajectory is deflected, this process also contributes to the opacity. The classical macroscopic view of this phenomenon is the following. An electro-magnetic wave produces a periodic variation of the electro-magnetic field in the plasma of free electrons. Therefore, the electrons oscillate at the same frequency. This oscillation of charges produces an electro-magnetic wave propagating in another direction (like in an antenna), and the wave is partly or totally reflected.

When the electron speeds are non-relativistic, this process is called **Thomson scattering**.

When the electron speeds are relativistic, this process is called **Compton scattering**.

In the non-relativistic limit, the cross-section associated to this process is a constant independent from the temperature and density, it is given by :

$$\sigma_{es} = 0.655 \times 10^{-24} \text{ cm}^2. \quad (155)$$

The contribution to the opacity is thus (using equation 144) :

$$\kappa_{es} = \frac{n_e}{\rho} \sigma_{es} = \frac{0.4}{\mu_e} \simeq 0.2 (1 + X) \text{ cm}^2/\text{g}. \quad (156)$$

Again, we see the  $X + 1$  dependence associated to the number of free electrons. It comes from equation 144 for the electron density. The evolution of the core of main sequence massive stars illustrates the importance of this factor. Due to hydrogen burning in the core,  $X$  decreases and electrons annihilate with the produced positrons (see next chapter). Therefore, fewer electrons can have free-free transitions and produce scattering in the core, so that core opacity decreases as the star evolves. This leads to a decrease of the mass of the convective core as the star evolves.

## 5.5 Conduction

Although this is not a process of interaction between matter and radiation, it is useful to finally mention the transport of energy by free electrons. At very high densities and relatively low temperatures, we have seen that the electron gas is degenerated. All cases of low energy being occupied, numerous electrons have very high energies. Through the motion of these electrons and their collisions, this kinetic energy can be transmitted to other layers by a diffusive process. This is the conduction by free electrons. In the non-degenerate case, the mean free path of electrons is negligible compared to the mean free path of photons, so that transport by conduction is negligible compared to transport by radiation. On the opposite, in the case of degeneracy all quantum cells in phase space below  $p_F$  are filled up, and electrons, when approaching other electrons have difficulties to change of momentum. “Encounters” are rare and the mean free path of electrons is much larger. Conduction by degenerated electrons becomes thus an efficient transport process. Like radiative transport, the conductive energy flux is proportional to  $-\nabla T$ . This effect is usually mimicked by an additional contribution to the transparency (inverse of the opacity) of the medium. Hence, conduction acts exactly like a decrease of the opacity.

## 6 Nuclear reactions

Nuclear reactions play a key role in stellar evolution. First, during the longest phases of stellar evolution, they are the main source of energy production in the core of star. More quantitatively we have seen that the modeling of the internal structure of a star is possible by solving a set of differential equations (see Sect. 3.8). In one of them, the equation of energy conservation (equation 98), the rate of energy production by nuclear reactions appears explicitly :  $\epsilon_n$ . We must know how it depends on the temperature, density and chemical composition to build a stellar model.

Second, we will see later that the main driver of stellar evolution is the modification of their chemical composition. It mainly comes from nuclear burning in the core. The knowledge of nuclear reactions is thus essential to understand the evolution of stars as a function of time. We will see that different phases of nuclear fusion reactions follow on from each other during a stellar life : fusion of hydrogen into helium, fusion of helium into carbon, carbon into oxygen, ... Stars are the great factories creating all chemical elements (beyond helium) in the universe. At the end of their life, the most massive ones explode as supernova and enrich the interstellar medium with these new elements. New generations of stars form from this enriched medium. This enables to understand how our solar system reached its present chemical composition. Different generations of stars followed on from each other, progressively enriching the stellar medium. Our Sun formed from a molecular cloud already significantly enriched in heavy elements (the mass fraction of heavy elements in the Sun is  $Z \simeq 0.015$ ), including the key elements for the emergence of life (carbon, oxygen, ...). The field of astrophysics studying the synthesis of new nuclei in the universe is called **nucleosynthesis**.

In this chapter, we will examine in detail the microscopic world of nuclear reactions, forgetting temporarily the global description of stars. I first remind the general form of a nuclear reactions between 2 nuclei :



## 6.1 Conservation laws

I first remind that nuclear reactions obey to conservation laws.

### Conservation of the total number of nucleons

The nucleons are here the protons and neutrons. We note  $A_X$  the number of nucleons of the nucleus  $X$ . For the above reaction, we have thus :

$$A_B + A_C = A_D + A_E + \dots$$

### Conservation of the total charge

The charged particles in nuclear reactions are the protons, electrons and the positrons. We note  $Z_X$  the number of protons in the nucleus  $X$ ,  $e_i^-$  the number of electron captures,  $e_f^-$  and  $e_f^+$  the numbers of emitted electrons and positrons, we have thus :

$$Z_B + Z_C - e_i^- = Z_D + Z_E + e_f^+ - e_f^- + \dots$$

### Conservation of momentum

The total momentum is a constant of motion. In a classical view, we can say that the sum of the initial momenta of the incident particles and nuclei is equal to the sum of the final momenta of the produced particles and nuclei. This naturally leads to choose the center of mass of the system as origin of the coordinate system. We will do that in all this chapter. In a classical view, we can consider 2 nuclei approaching from each other, with velocities  $\vec{v}_1$  and  $\vec{v}_2$  in this referential. We keep during the approach phase :

$$m_1 \vec{v}_1 = -m_2 \vec{v}_2 = \frac{m_1 m_2}{m_1 + m_2} (\vec{v}_1 - \vec{v}_2) = m_\mu \vec{v},$$

where  $m_\mu$  is the reduced mass and  $\vec{v} = \vec{v}_1 - \vec{v}_2$  is the relative velocity. In the classical non-relativistic cas, the Newton equation reads :

$$m_\mu \frac{d\vec{v}}{dt} = -\nabla V(r) \quad (\vec{r} = \vec{r}_1 - \vec{r}_2),$$

where  $V$  is the (coulombian) interaction potential of the 2 nuclei.

In quantum physics, the relative position of the nuclei is described by a wave function called the *wave function of the relative particle*.  $|\psi(\vec{r})|^2$  gives the probability density of having a relative position  $\vec{r}_1 - \vec{r}_2 = \vec{r}$ . It is obtained in the non-relativistic limit by solving the Schrödinger equation :

$$i\hbar \frac{\partial \psi}{\partial t} = -\frac{\hbar^2}{2m_\mu} \nabla^2 \psi + V \psi. \quad (157)$$

The center of mass of the system is described by another wave function, which is a plane wave when the (conserved) total momentum with respect to the observer is perfectly known (this is usually not the case because of the Heisenberg uncertainty principle).

### Conservation of angular momentum

The angular momentum is also a constant of motion. In simple terms, the sum of the initial angular momenta (orbital + spins) of the nuclei and electrons is equal to the sum of the final angular momenta. In many nuclear reactions, the initial angular momentum is 0, which corresponds to a frontal collision. An important exception is resonant reactions.

### Conservation of the lepton number

This conservation law matters for beta decays and electrons captures. The emission of an electron is always accompanied by the emission of an anti-neutrino. The emission of a positron is accompanied by the emission of a neutrino. The capture of an electron leads to the emission of a neutrino.

## 6.2 Energy of reactions

As we already said, energetical aspects are an essential aspect of nuclear reactions. In quasi all what follows, we will consider the general case of a nuclear fusion reaction :



The Einstein relation  $E = Mc^2$  establishes an essential correspondence between mass and energy. In nuclear reactions, the sum of the initial masses of all particles is not equal to the sum of the final ones. If the total initial mass is larger than the final one, the reaction is exothermic and the released energy is the mass difference times  $c^2$ . If it is smaller, the reaction is endothermic. As we will see, fusion reactions of light nuclei are exothermic. The energy of the above reaction is :

$$Q = (M_B + M_C - M_D)c^2. \quad (158)$$

It is useful to introduce now the mass excess (we should say “the energy excess”) of a given nucleus of mass  $M$  with  $A$  nucleons :

$$\Delta\mathcal{M} \equiv (M - Am_u)c^2 = 931.478 (M/m_u - A) \text{ MeV}. \quad (159)$$

It is the opposite of the binding energy of this nucleus : the work to be done to separate each nucleon at an infinite distance from each other. This naturally leads to the definition of the binding energy per nucleon :

$$f \equiv -\Delta\mathcal{M} / A. \quad (160)$$

One can easily get the energy of reaction from these quantities. From the nucleons conservation, we find directly :

$$Q = \Delta\mathcal{M}_B + \Delta\mathcal{M}_C - \Delta\mathcal{M}_D = A_D \left[ f_D - \left( \frac{A_B}{A_D} f_B + \frac{A_C}{A_D} f_C \right) \right]. \quad (161)$$

The curve  $f(A)$  giving the binding energy per nucleon as a function of the nucleons number  $A$  summarizes energetical aspects of nuclear reactions. It strongly increases for light nuclei up to a global maximum at the level of  $\text{Fe}^{56}$ , and next slowly decreases beyond it. Local maxima can also be seen at  $\text{He}^4$ ,  $\text{Be}^8$ ,  $\text{C}^{12}$ ,  $\text{O}^{16}$  (multiples of  $\alpha$  particles). In eq. 161, one can see that  $(A_B/A_D)f_B + (A_C/A_D)f_C$  is a weighted average of the binding energies of the initial nuclei.

Consider the fusion of 2 nuclei lighter than Iron. Since  $f(A)$  increases, we have :  $(A_B/A_D)f_B + (A_C/A_D)f_C < f_D$ . Equation 161 tells us that  $Q > 0$ , the reaction is thus exothermic. **The fusion reactions are exothermic for nuclei lighter than Iron.**

On the contrary, consider now the fusion of 2 nuclei heavier than Iron. Since  $f(A)$  decreases, we have :  $(A_B/A_D)f_B + (A_C/A_D)f_C > f_D$ . Equation 161 tells us that  $Q < 0$ , the reaction is thus endothermic. **The fusion reactions are endothermic for nuclei heavier than Iron.**

### 6.3 Cross sections and nuclear reaction rates

We introduce now the concept of nuclear reaction rate. Consider an experience where target nuclei  $C$  (number per unit volume  $N_C$ ) are bombarded by incident nuclei  $B$  (number per unit volume  $N_B$ ) arriving with a fixed speed  $v$ , producing some nuclear fusion reactions. The reaction rate  $r_v$  is the number of nuclear reactions occurring per unit time and volume. It is expressed as :

$$r_v = \sigma(v) v N_B N_C, \quad (162)$$

where appears a fundamental quantity, the **cross-section**  $\sigma(v)$ . This equation is easily understood. The larger the relative speed  $v$  and the larger the number of particle pairs per unit volume<sup>2</sup>  $N_B N_C$ , the more numerous are the collisions per unit time that could eventually produce nuclear reactions. Note that, if the 2 nuclei are identical,  $N_B N_C$  must be replaced by  $N_B^2/2$  in equation 162. Concerning the cross-section, you can visualize it as follows. Imagine a shield of surface  $\sigma(v)$  attached to each target nucleus and perpendicular to the relative velocity. A reaction occurs whenever an incident nucleus crosses a shield. The whole problem is of course the determination of this cross-section and how it depends on  $v$ .

Before doing that, I remind that the relative speed between two nuclei is not fixed in the stellar plasma. On the contrary, it follows a distribution because of the thermal

agitation. In order to get the mean reaction rate in the plasma, one must multiply  $r_v$  by the probability density  $f(v)$  and integrate. More precisely, since  $N_B N_C$  do not depend on  $v$ , we have to determine the average of  $\sigma(v)v$ , which we note  $\langle \sigma(v)v \rangle$ . We have thus for the reaction rate :

$$r = \langle \sigma(v)v \rangle N_B N_C . \quad (163)$$

We will see that only very high speeds have a significant weight in this integral and only very high temperatures can lead to high enough speeds. In this case where thermo-nuclear reactions result from the thermal agitation, we talk about **thermo-nuclear reactions**. It will become clear later that it is useful to take the energy instead of the relative speed as independent variable. The total kinetic energy, sum of the 2 nuclei's kinetic energies in the center of mass reference frame, often called the *kinetic energy of the relative particle* is given in the non-relativistic limit ( $v \ll c$ ) by :

$$E = (1/2) m_\mu v^2 . \quad (164)$$

For an ideal non-degenerated gas, the probability density of these kinetic energies is the Maxwell-Boltzmann's distribution :

$$f(E) = \frac{2}{\sqrt{\pi}} \frac{E^{1/2}}{(kT)^{3/2}} \exp\left(-\frac{E}{kT}\right) . \quad (165)$$

The  $\sigma v$  average is then given by :

$$\langle \sigma(v)v \rangle = \int_0^\infty \sigma(E)v(E)f(E)dE , \quad (166)$$

with  $v(E) = \sqrt{2E/m_\mu}$  in the non-relativistic limit.

Having defined  $r$ , we can now deduce from it the rate of energy generation by nuclear reactions  $\epsilon$ . For a reaction with rate  $r$  providing an energy per reaction  $Q$ , we find :

$$\begin{aligned} \epsilon &= Q r / \rho = Q \langle \sigma(v)v \rangle N_B N_C / \rho \\ &= \frac{Q}{M_B M_C} \rho X_B X_C \langle \sigma v \rangle , \end{aligned} \quad (167)$$

where  $X_B$  and  $X_C$  are the mass fractions of the nuclei,  $M_B$  and  $M_C$  their masses, and we have used the relation  $N_B = \rho X_B / M_B$ . Summing over all reactions (indexed by  $k$ ) gives the total energy generation rate :

$$\epsilon = \sum_k \epsilon_k . \quad (168)$$

Let's consider now the heart of the problem : the determination of the cross-sections. Different factors contribute to it.

### 6.3.1 Geometrical factor

The first condition for the occurrence of a nuclear reaction is the collision between two nuclei. In a simplified view where we see the nuclei as rigid spheres (like billiard balls), the cross-section associated to the collision phenomenon is  $\pi d^2$  where  $d$  is the sum of the two nuclear radii. We know also that in this classical view, the change of direction after collision depends on the impact parameter  $b$ , related to the angular momentum  $L$  and momentum  $p$  by  $L = bp$ . It is easy to see that the cross-section corresponding to the phenomenon “*colliding with an impact parameter between  $b$  and  $b + \delta b$* ” is

$$\sigma_{\delta b} = \pi((b + \delta b)^2 - b^2) = \pi\delta b(2b + \delta b), \quad (169)$$

which is the surface of the ring with radii between  $b$  and  $b + \delta b$ .

The quantum view of the problem is more complicate. In quantum physics, the square of the angular momentum of a particle obeys to the quantification condition  $L^2 = \ell(\ell + 1)\hbar^2$ , where the quantum number  $\ell$  is a natural. And we can reformulate the question as : what is the cross-section associated to the phenomenon “*Colliding with an angular momentum  $L = \sqrt{\ell(\ell + 1)}\hbar$* ”? The answer given by quantum physics is :

$$\sigma_{\ell} = (2\ell + 1)\lambda^2/4\pi, \quad (170)$$

where  $\lambda$  is the wavelength of the relative particle.

Most nuclear reactions correspond to frontal collisions, that is collisions with zero angular momentum ( $\ell = 0$ ). The cross-section associated to the “*frontal collision*” phenomenon is thus simply :

$$\sigma_0 = \frac{\lambda^2}{4\pi} = \frac{h^2}{4\pi p^2} = \frac{h^2}{8\pi m_{\mu} E} \propto E^{-1}, \quad (171)$$

where we used the de Broglie’s relation between the wavelength and momentum of a free particle. What we have to take in is the **geometrical factor** :  $E^{-1}$ .

### 6.3.2 Gamow factor

Colliding is of course not enough for the occurrence of a nuclear reaction ! The biggest obstacle is the Coulomb barrier. Nuclei are indeed positively charged particles and they must get very close ( $\approx 10^{-15}$  m) in order that the attraction coming from the strong interaction (finite scope) wins over the Coulomb repulsion (infinite scope).

It is useful to start by considering this problem in the frame of classical Newtonian physics. Consider two nuclei approaching each other with a zero angular momentum and a kinetic energy (of the relative particle) at infinity  $E$ . As in any problem where

the forces derive from a potential : the sum of the kinetic and potential energies is constant. Since, the strong interaction has a finite scope we can neglect it and we have :

$$\frac{1}{2} m_{\mu} v(r)^2 + \frac{Z_B Z_C e^2}{r} = E = cst. \quad (172)$$

The minimum rapprochement distance (such that  $v(r_{min}) = 0$ ) is thus such that :

$$\frac{Z_B Z_C e^2}{r_{min}} = E. \quad (173)$$

Moreover, the scope of the strong interaction and thus the required rapprochement distance for nuclear fusion is  $r_0 \approx 10^{-15}$  m. The required energy for crossing the Coulomb barrier is thus, in this classical reasoning :

$$E \geq E_{Cb} = \frac{Z_B Z_C e^2}{r_0} \simeq Z_B Z_C \text{ Mev} \quad (174)$$

We consider here thermo-nuclear reactions where the distribution of kinetic energy follows the Maxwell-Boltzmann distribution (equation 165). In average, it is  $\langle E \rangle = (3/2) kT \simeq 1$  kev. From equation 165, we deduce that the probability of having  $E \approx 1$  Mev is of the order of  $\exp(-1000)!!$  If the whole universe was a gas with temperatures lower than  $10^7$  K, not even one particle would have a so high kinetic energy. The crossing of the Coulomb barrier seems thus impossible. Since the ratio between the kinetic energy and the height of the Coulomb barrier is of the order of  $10^{-3}$ , one sees immediately that the minimum rapprochement distance is in average of the order of 1000 times the size of the nuclei.

Fortunately, the microscopic world doesn't follow the Newton laws. A key quantum effect offers a solution to nuclear fusion : quantum tunnelling.

### **Quantum tunnelling makes the crossing of the Coulomb barrier possible for some nuclei.**

I start with some reminder of what is quantum tunnelling. We consider the simple 1-dimension case of a free particle encountering a rectangular barrier. In the stationary case, the wave function is obtained by solving the (stationary) Schrödinger equation :

$$\frac{\hbar^2}{2m} \frac{d^2\psi}{dr^2} + (E - V)\psi = 0. \quad (175)$$

Even if the energy of the particle is lower than the height of the barrier,  $E < V$ , the wave function  $\psi$  is not zero below the barrier. For a free particle moving in the direction of increasing  $r$ , we have below the barrier :

$$\psi(r) = \exp(-kr) \quad \text{with} \quad k = (1/\hbar)\sqrt{2m(V - E)}. \quad (176)$$

The crossing probability is given by the ratio of  $|\psi|^2$  between the outbound and inbound sides :

$$P_{\text{cross}} = \exp(-2k\Delta r), \quad (177)$$

where  $\Delta r$  is the thickness of the barrier.

The problem of the fusion between two nuclei is more complicate than the tunnelling through a rectangular barrier because the potential varies now with the distance. Introducing the notation :

$$k(r) = (1/\hbar)\sqrt{2m_\mu(Z_B Z_C e^2/r - E)}, \quad (178)$$

the Schrödinger equation reads for  $r \leq r_{min}$  :

$$\frac{d^2\psi}{dr^2} = k(r)^2 \psi. \quad (179)$$

The problem is that there is no exact analytical solution of equation 179 in this case. However, in the limit case where the wavelength of the particle is much shorter than the size of the barrier, an approximate analytical solution exists, it is called the JWKB approximation. For a particle moving in the sense of decreasing  $r$ , this approximate solution is given by :

$$\psi(r) = \frac{1}{\sqrt{k(r)}} \exp\left(-\int_r^{r_{min}} k(r) dr\right). \quad (180)$$

Note that if  $k$  is constant, we recover eq. 176.

We can see when this approximation is justified by computing the second derivative of equation 180. One gets :

$$\begin{aligned} \frac{d^2\psi}{dr^2} &= \frac{d}{dr} \left( -\left(k^{1/2} + \frac{dk/dr}{2k^{3/2}}\right) \exp\left(-\int_r^{r_{min}} k(r) dr\right) \right) \\ &= \left( k^2 + \frac{d^2}{dr^2} \left( \frac{1}{\sqrt{k}} \right) \sqrt{k} \right) \frac{1}{\sqrt{k(r)}} \exp\left(-\int_r^{r_{min}} k(r) dr\right). \end{aligned} \quad (181)$$

Comparing it to the right hand side of eq. 179, one sees that this approximation is to neglect  $\frac{d^2}{dr^2} \left( \frac{1}{\sqrt{k}} \right) \sqrt{k}$  compared to  $k^2$ . This is justified if  $k(r)$  varies slowly in the interval  $\delta r = r_{min} - r_0$  and  $k(r) \gg 1/\delta r$ .

The barrier crossing probability is then approximately (without proof) :

$$\begin{aligned} P_G &\simeq \exp\left(-2 \int_{r_0}^{r_{min}} k(r) dr\right) \\ &\simeq \exp\left(-2\pi^2 r_{min}/\lambda\right) \\ &= \exp\left(-\left(Z_B Z_C e^2 \pi/\hbar\right) \sqrt{2m_\mu/E}\right) \\ &= \exp\left(-b E^{-1/2}\right). \end{aligned} \quad (182)$$

This is the **Gamow factor** where :

$$b = 31.29 Z_B Z_C A_\mu^{1/2} (keV)^{1/2} \quad \text{and} \quad A_\mu = \frac{A_B A_C}{A_B + A_C}. \quad (183)$$

This result is easily interpreted. The barrier crossing by quantum tunneling is less probable if :

- $Z_B Z_C$  and thus the Coulomb repulsion is larger,
- the kinetic energy at infinity  $E$  is smaller,
- the reduced mass is larger (factor  $m_\mu^{1/2}$  in equation 178).

### 6.3.3 Nuclear factor

Significant simplifications were introduced in the computation of the Gamow factor (the JWKB approximation). Moreover, the decrease of the Coulomb barrier due to free electrons passing between the two nuclei was not taken into. Last but not least, crossing the Coulomb barrier is not enough for nuclear fusion. Most of the time the produced nucleus is very unstable, and if a transition towards a stable state does not occur quickly, the two nuclei split again and the fusion does not occur. This leads to introduce an additional factor called the **nuclear factor**  $S(E)$ . This factor takes the strong interaction and weak interaction (when a  $\beta$  decay occurs) into account. The cross-section at energy  $E$  reads then :

$$\sigma(E) = \frac{S(E)P_G(E)}{E} = \frac{S(E)}{E} \exp(-b E^{-1/2}) \quad (184)$$

In general, this nuclear factor  $S(E)$  varies slowly with  $E$ , contrarily to the Gamow factor. More precisely, this is so for the non-resonant nuclear reactions. On the opposite, for resonant reactions (see Sect. 6.5),  $S(E)$  varies sharply around the resonant energy and some simplifications assumed in Sect. 6.4 will no longer be valid.

In practice, theoretical computations of  $S(E)$  are often too inaccurate. Experiments are needed to measure it. Target nuclei with given density  $N_C$  are bombarded by incident nuclei (density  $N_B$ ) with a fixed kinetic energy  $E$  and speed  $v$ . The number of nuclear reactions occurring during a given interval of time is measured, which gives  $r_v$ . Isolating the cross-section in equation 162 gives its measurement. And finally, the nuclear factor is given by  $S(E) = E P_G(E)^{-1} \sigma(E)$ . The main problem is that, contrarily to stars, we cannot perform such an experiment over billions of years!! A significant amount of reactions must occur during a short time interval. This is only the case for very high cross-sections and thus at very high energies. The measurement of  $S(E)$  is thus only possible at very high energies  $E$ , much higher than the kinetic energies in the core of stars. Hence, the experimental measurements must be extrapolated down to the stellar energies, which magnifies the errors.

## 6.4 The Gamow's peak

In the core of stars we talk about **thermo**-nuclear reactions, where the distribution of kinetic energies follows a distribution, usually the Maxwell-Boltzmann distribution (eq. 165). To obtain the  $\langle \sigma v \rangle$  in eq. 163, we have to average  $\sigma(E)v(E)$  by multiplying it by the probability density  $f(E)$  (eq. 165) and integrating over all energies (eq. 166). We have thus ( $v(E) = \sqrt{2E/m_\mu}$ ) :

$$\begin{aligned}
 \langle \sigma v \rangle &= \int_0^\infty \sigma(E)v(E)f(E)dE \\
 &= \int_0^\infty \frac{S(E)}{E} \exp(-b E^{-1/2}) \sqrt{\frac{2E}{m_\mu}} \frac{2}{\sqrt{\pi}} \frac{E^{1/2}}{(kT)^{3/2}} \exp\left(-\frac{E}{kT}\right) dE \\
 &= \left(\frac{8}{m_\mu\pi}\right)^{1/2} \frac{1}{(kT)^{3/2}} \int_0^\infty S(E) \exp\left(-\frac{E}{kT} - \frac{b}{\sqrt{E}}\right) dE. \quad (185)
 \end{aligned}$$

The function  $\exp(-f(E)) = \exp\left(-\frac{E}{kT} - \frac{b}{\sqrt{E}}\right)$  appearing in this integral takes non negligible values in a restricted range of energies only, this is the **Gamow Peak**. We consider here the non-resonant case where  $S(E)$  varies slowly compared to  $\exp(-f(E))$ . We can thus take  $S(E)$  out of the integral, as a good approximation. We see then that the majority of fusing nuclei have a kinetic energy around the Gamow's peak. This is easily understood. The Gamow's peak  $\exp(-f(E))$  is the product of the functions  $\exp(-E/kT)$  and  $\exp(-b/\sqrt{E})$ .

If  $E$  is too large, the factor  $\exp(-E/kT)$  is small. At the temperature  $T$ , the number of nuclei having an energy  $E \gg kT$  is negligible. These nuclei are thus too rare to contribute significantly to nuclear reactions. If  $E$  is too small, the factor  $\exp(-b/\sqrt{E})$  is small. At this energy, the length of the tunnel below the Coulomb barrier is too large and the probability of crossing it by quantum tunneling is negligible.

The Gamow's peak corresponds thus to a compromise, the energy must be accessible at the considered temperature and large enough to allow quantum tunneling below the Coulomb barrier.

In view of its importance, it is useful to characterize with more detail the Gamow's peak  $\exp(-f(E))$ . We determine first the location and height of the peak. The energy  $E_0$  where  $\exp(-f(E))$  has its maximum is found from  $f'(E_0) = 0$  :

$$E_0 = \left(\frac{bkT}{2}\right)^{2/3}. \quad (186)$$

This gives then :

$$\tau \equiv f(E_0) = 3E_0/(kT) = 3 \cdot 2^{-2/3} b^{2/3} (kT)^{-1/3}. \quad (187)$$

We approximate now the Gamow's peak by a Gaussian function and determine its standard deviation. A second order Taylor expansion of  $f(E)$  around  $E_0$  gives :

$$\begin{aligned}\exp(-f(E)) &\simeq \exp(-f(E_0) - f''(E_0)(E - E_0)^2/2) \\ &= \exp(-f(E_0)) \exp\left(-\left(\frac{E - E_0}{\Delta E/2}\right)^2\right),\end{aligned}\quad (188)$$

where the standard deviation of the Gaussian is :

$$\Delta E/2 = \sqrt{2/f''(E_0)} = 2\sqrt{E_0 kT/3} \propto b^{1/3} T^{5/6}. \quad (189)$$

What we are mainly interested on is  $\langle \sigma v \rangle$  and its dependence with respect to the temperature. Noting that  $\int_{-\infty}^{+\infty} b \exp(-(x/a)^2) dx = ab\sqrt{\pi}$ , one gets :

$$\begin{aligned}\langle \sigma v \rangle &\propto T^{-3/2} \Delta E e^{-f(E_0)} \propto T^{-3/2} T^{5/6} e^{-\tau} \\ &\propto \tau^2 e^{-\tau} \propto T^{-2/3} e^{-cst.T^{-1/3}}.\end{aligned}\quad (190)$$

This is the typical temperature dependence of non-resonant reactions. It is useful to quantify the main parameters associated to the Gamow's peak. We note  $T_7 \equiv T(K)/10^7$  and introduce the parameter :

$$W \equiv Z_B^2 Z_C^2 \frac{A_B A_C}{A_B + A_C}, \quad (191)$$

which is directly related to the height of the Coulomb barrier. One gets then :

$$\begin{aligned}\tau &= 19.721 W^{1/3} T_7^{-1/3} \\ E_0 &= 5.665 \text{ keV} \cdot W^{1/3} T_7^{2/3} \\ \Delta E &= 4.249 \text{ keV} \cdot W^{1/6} T_7^{5/6}\end{aligned}\quad (192)$$

Particularly important is the sensitivity of the nuclear reaction rate with respect to the temperature. It is quantified by the parameter  $\nu$  defined as : défini par :

$$\begin{aligned}\nu &\equiv \left. \frac{\partial \ln \langle \sigma v \rangle}{\partial \ln T} \right|_{\rho} = \frac{\tau}{3} - \frac{2}{3} \\ &\simeq 6.574 W^{1/3} T_7^{-1/3}.\end{aligned}\quad (193)$$

The energy generation rate  $\epsilon$  is proportional to  $\langle \sigma v \rangle$  (eq. 167). We have thus also :

$$\nu = \left. \frac{\partial \ln \epsilon}{\partial \ln T} \right|_{\rho}. \quad (194)$$

A first order Taylor expansion of  $\ln \epsilon$  around  $T_0$  directly gives :

$$\ln(\epsilon/\epsilon_0) = \ln \epsilon - \ln \epsilon_0 \simeq \nu (\ln T - \ln T_0) = \nu \ln(T/T_0).$$

The  $\epsilon - T$  relation is thus approximated by the following power law around  $T_0$  :

$$\epsilon = \epsilon_0 (T/T_0)^\nu \propto T^\nu. \quad (195)$$

From equation 193, one sees that  $\nu$  can be very high.

For **hydrogen fusion** ( $Z = 1$ ), one gets :

$$\nu \approx 6.$$

For the **fusion of heavy nuclei** :

$$\nu \approx 20 - 30 !!$$

The energy generation rates by nuclear reactions are thus always extremely sensitive to the temperature. This has numerous impacts on the evolution, the structure and the thermal stability of stars. One major example is the temperature control by nuclear reactions, which will be analysed in detail later. In a nutshell, in normal non-degenerated cases, nuclear reactions act like a very precise thermostat. A very small core temperature increase leads to a large increase of the energy generation rate. As a consequence, the stellar core expands and the temperature drops, coming back to its initial value.

## 6.5 Resonant reactions

Until now, we considered non-resonant reactions. We consider now the other case of resonant reactions. To understand them, it is first necessary to present the general problem of modeling the states of a nucleus in quantum physics. The wave function of a nucleus is written  $\psi(\vec{r}_1, \vec{r}_2, \dots, \vec{r}_A, t)$  and its squared modulus gives the probability of having the  $A$  nucleons located at  $\vec{r}_1, \vec{r}_2, \dots, \vec{r}_A$  in the center of mass frame. In principle, this wave function should be obtained by solving the Schrödinger equation of the system, which reads for stationary states :

$$-\frac{\hbar^2}{2m_u} \left( \sum_{n=1}^A \sum_{i=1}^3 \frac{\partial^2}{\partial x_{i,n}^2} \right) \psi + V(\vec{r}_1, \vec{r}_2, \dots, \vec{r}_A) \psi = E \psi, \quad (196)$$

where  $E$  is the energy of the nucleus,  $V(\vec{r}_1, \vec{r}_2, \dots, \vec{r}_A)$  is the potential energy and  $\vec{r}_i = (x_{1,i}, x_{2,i}, x_{3,i})$ . This partial differential equation whose unknown is the wave function defined in a domain of dimension  $3A$  is impossible to solve, even with present super-computers.

The **shell model** of a nucleus is motivated by this major difficulty. It consists in assuming that each nucleon is plunged into the mean constant potential generated by the others. Solving the Schrödinger equation associated with this mean potential is of course much simpler. There is a countable set of solution to this problem corresponding to the different possible states of the nucleon inside the nucleus. This is the same in atoms where the solution of the Schrödinger equation gives the possible states of the bound electrons. The major difference is that the electron states are weakly coupled in an atom while, on the opposite, the nucleon states are strongly coupled in a nucleus. In other words, the shell model is a crude approximation of a nucleus. A nucleus is built by filling the different possible states with protons and neutrons. Like for electrons filling different orbitals in an atom or molecule, the states of nucleons form different groups with similar energies. This explains the existence of particularly stable nuclei, when a nuclear orbital is filled. The simplest example corresponds to the filling of the fundamental lowest energy state. This gives a nucleus with 2 protons and 2 neutrons (2 for the two possible spins). Adding the lowest energy  $\ell = 1$  orbitals gives  $(2\ell + 1 = 3)$  times 2 (spins) additional states. This gives the oxygen nucleus with 8 protons and 8 neutrons. Continuing to fill orbitals defines so-called magic numbers (2, 8, ...) of protons and neutrons corresponding to very stable nuclei. Their high stability makes their fusion more difficult, leading to a significant increase of the required temperature compared to the previous phase of nuclear fusion.

Why is this important for nuclear fusion reactions? First, one sees that there is not one single possible state for a nucleus but a countable family of excited states (the lowest energy state is called the fundamental state). One can subdivide them into 2 families.

On one side, there are the energy levels below the value of the potential at infinity. These are the **stationary states**.

On the other side, there are the energy levels above the potential at infinity. These are the **quasi-stationary states**.

When a nucleus is in a quasi-stationary state, there is a non-zero probability that one part of it separates from the other, crossing the potential barrier. In return, the existence of quasi-stationary states leads to resonant reactions : when 2 nuclei collide with a kinetic energy  $E$  close to the resonance energy  $E_{res}$  of a quasi-stationary state and the good angular momentum, the fusion is much more probable. Such resonance effect is classical in eigenvalue problems. In quantum physics, it appears each time a bound state and a free state with same energy are possible for a particle. The

cross-section in the vicinity of a resonance has the shape of a Lorentzian profile :

$$\sigma(E) \propto \frac{1}{(E - E_{res})^2 + (\Gamma/2)^2}. \quad (197)$$

This is the equivalent of the natural broadening of spectral lines. It comes from the finite lifetime of the quasi-stationary state :  $\tau = \hbar/\Gamma$ . Over a broader interval of energy,  $\sigma(E)$  is the combination of a smooth component slowly increasing with  $E$  (because of the Gamow factor) and different Lorentzian peaks around each resonance, where the reactions are much more probable.

It is important to note that the computation of  $\langle \sigma v \rangle$  is very different for resonant reactions and the reasoning leading to the Gamow's peak no longer applies. The  $S(E)$  factor can no longer be taken out of the integral in equation 185. On the opposite, the derivative of  $S(E)$  is much larger than that of  $\exp\left(-\frac{E}{kT} - \frac{b}{\sqrt{E}}\right)$  around the resonance and it is this last factor that can be taken out of the integral. From eq. 185, we have approximately :

$$\begin{aligned} \langle \sigma v \rangle &\simeq \sqrt{\frac{8}{m_\mu \pi}} \frac{1}{(kT)^{3/2}} \exp\left(-\frac{E_{res}}{kT} - \frac{b}{\sqrt{E_{res}}}\right) \int_0^\infty S(E) dE \\ &\propto T^{-3/2} \exp\left(-\frac{E_{res}}{kT}\right). \end{aligned} \quad (198)$$

One sees that the dependence of  $\langle \sigma v \rangle$  (and thus  $\epsilon$ ) with respect to the temperature is totally different from the non-resonant case (where we had the factor  $\exp(-cst./T^{1/3})$ , see equations 187 and 190). The factor  $\nu = \partial \ln \langle \sigma v \rangle / \partial \ln T|_\rho$  is much larger in resonant reactions. For example, the fusion reaction synthesizing carbon is a resonant reaction (see Sect. 6.7, eq. 231), with a  $T$  dependence corresponding to  $\nu \approx 40$ . This means  $\epsilon \propto T^{40}$  in the vicinity of the temperature where this reaction happens ( $T \approx 10^8$  K)! Eq. 198 is easily interpreted. For resonant reactions, what only matters is having nuclei with the kinetic energy corresponding to the resonance. The reaction rate is thus proportional to the probability of having this energy at a given temperature, this explains the factor  $\exp(-E_{res}/kT)$  (from the Boltzmann distribution), which is extremely sensitive to the temperature.

A last specific aspect of resonant reactions is that they often occur with a non-zero angular momentum corresponding to the one of the quasi-stationary state ( $\ell \neq 0$ ). For an energy very close to the resonance, the cross-section can even saturate to the maximum value given by the experience of quantum diffusion with a given angular momentum :  $\sigma_\ell = (2\ell + 1)\lambda^2/4\pi$  (equation 170).

For  $\ell \neq 0$ , it is also useful to remember that the Schrödinger equation reads :

$$\frac{\hbar^2}{2m_\mu} \frac{d^2\psi}{dr^2} + \left( E - \frac{Z_B Z_C e^2}{r} - \frac{\ell(\ell + 1)\hbar^2}{2m_\mu r^2} \right) \psi = 0. \quad (199)$$

The crossing of the Coulomb barrier is thus modified by the “centrifugal term” :  $\ell(\ell + 1)\hbar^2/(2m_\mu r^2)$ .

## 6.6 Hydrogen fusion ( $T \approx 10^6 - 10^7$ K)

We consider now in more detail the nuclear reactions playing a major role in stellar evolution. As a star evolves, we will show that its core temperature increases (Virial theorem, see Sects. 8.1 and 10.3.1). As a consequence, its core goes through successive phases of nuclear fusion when the required temperature is reached. The first significant phase is hydrogen fusion into helium when the core temperature reaches values of  $10^6 - 10^7$  K. Different reactions are involved (see below), leading to the synthesis of helium 4 from 4 protons (and two annihilated electrons) :



The energy produced by this reaction is :

$$Q_{glob} = (4M_H + 2m_{e^-} - M_{He^4})c^2$$

where the  $M_i$  correspond to the nuclear masses and  $m_{e^-}$  is the electron rest mass. Neglecting the electron binding energies (compared to  $m_e c^2$ ), one gets :  $4M_H + 4m_{e^-} \simeq 4\mathcal{M}_H$  and  $M_{He^4} + 2m_{e^-} \simeq \mathcal{M}_{He^4}$ , where the  $\mathcal{M}_i$  correspond to the atomic masses. This gives :

$$Q_{glob} = (4\mathcal{M}_H - \mathcal{M}_{He^4})c^2 = 26.73 \text{ Mev}. \quad (201)$$

The main ingredient required for the modeling of the thermal structure of a star is the rate of energy production by nuclear reactions  $\epsilon_n$ . It is related to the nuclear reaction rate through eq. 167. However, we cannot apply directly this formula to 200 :

$$\epsilon_n \neq \frac{1}{4} \frac{Q_{glob}}{m_u^2} \rho X^2 \langle \sigma v \rangle_{pp}. \quad (202)$$

<sup>1</sup> The first reason is that different reactions with different reaction rates are hidden behind 200. The relations 167 apply individually to each reaction. We have to sum the  $\epsilon_k$  of each reaction  $k$  to get the total rate :  $\epsilon_n = \sum_k \epsilon_k$ . This total  $\epsilon_n$  appears to be different from the right hand side of eq. 202 when the individual reaction rates are different.

The second reason is that some intermediate reactions (mainly the  $\beta$  decays) lead to the production of neutrinos. The  $\epsilon_n$  in the equation of energy conservation (equation 87) corresponds to the **heat** provided to the gas by the nuclear reactions. However, the neutrinos nearly do not interact with stellar matter. They go out of the star taking with them their energy. If  $Q_k$  is the total energy produced by the reaction  $k$  and  $Q_{\nu,k}$  the energy of the emitted neutrino, the heat provided to the gas is  $Q_k - Q_{\nu,k}$ .

---

<sup>1</sup>The division by 4 in Eq. 202 comes from the fact that the incident nuclei (protons) are identical and two p-p reactions (Eq. 203) are required for the synthesis of one helium nucleus.

The power provided by unit mass to the gas by all nuclear reactions is thus :

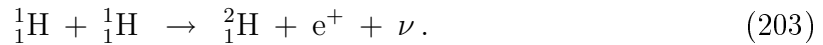
$$\epsilon_n = \sum_k \frac{Q_k - Q_{\nu,k}}{M_{1,k} M_{2,k}} \rho X_{1,k} X_{2,k} \langle \sigma v \rangle_k .$$

We examine now each reaction hidden behind 200. Depending on the temperature, there are mainly 2 groups of intermediate reactions. The first one is the so-called proton-proton chain and the second one is the carbon cycle.

### 6.6.1 The proton-proton chain

The reactions of the proton-proton chain (also called the p-p chain) are the dominating ones in the core of our Sun.

#### p-p reaction



This reaction is the most difficult (smallest cross-section) of the chain. Before Hans Bethe (1939) discovered it was possible, astrophysicists could not explain the energy production in the core of our Sun. Indeed, since the early times of nuclear physics, it was known that the nuclei  ${}^2_2\text{He}$  and  ${}^5_3\text{Li}$  were strongly unstable and could not stay in their fundamental state. The reactions involving  ${}^1_1\text{H}$  and  ${}^4_2\text{He}$ , the two main nuclei of the universe, such as  ${}^1_1\text{H} + {}^1_1\text{H} \rightarrow {}^2_2\text{He}$  and  ${}^1_1\text{H} + {}^4_2\text{He} \rightarrow {}^5_3\text{Li}$  are thus impossible channels for the synthesis of helium. In the reaction 203, the weak interaction reaction  $p \rightarrow n + \nu$  ( $\nu$  is a neutrino) occurs just during the crossing of the Coulomb barrier. This weak transition is of *Gamow-Teller* type where one of the nuclei changes its spin. Indeed, the 2 protons must arrive with opposite spins (Pauli exclusion principle) but the stable state of deuterium is with aligned spins. Such weak transition has a very small probability here because the initial and final wave functions are totally different : the initial one corresponds to a free state and the final one to a bound state. The cross-section of this reaction is thus the smallest of the p-p chain. Its kinetics is :

$$\frac{dH}{dt} = - \langle \sigma v \rangle_{pp} H^2 \quad (204)$$

where  $H$  is the number of protons per unit volume. Based on this equation, one defines its reaction time as  $\tau_H = (\langle \sigma v \rangle_{pp} H)^{-1}$ . In the core of our Sun, it is of the order of  $10^9$  years.

Note that the emitted positron directly annihilates with a free electron of the plasma :



Although it is the most difficult, the p-p reaction is the less productive from an energetical point of view. Summing the energies provided by the reactions 203 and 205 gives :

$$\begin{aligned} Q &= 2\Delta\mathcal{M}_H - \Delta\mathcal{M}_D - E_{neutrino} \\ &= 1.442 - 0.262 = 1.180 \text{ Mev} \end{aligned}$$

which is much smaller than the 26/2 Mev of the full chain.

### Deuterium fusion



This reaction is much easier because it only requires the crossing of the Coulomb barrier. Its typical reaction time (solar core) is very low :  $\tau_D = (\langle \sigma v \rangle_{pd} H)^{-1} \approx 1s$ . Consequently, the deuterium nuclei produced by the p-p reaction nearly instantaneously merge with a proton. An equilibrium between production and destruction of deuterium is thus established and we have :

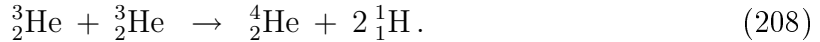
$$\begin{aligned} 0 &\simeq \frac{dD}{dt} = \langle \sigma v \rangle_{pp} \frac{H^2}{2} - \langle \sigma v \rangle_{pd} HD \\ \Rightarrow \left(\frac{D}{H}\right)_{eq} &= \frac{\langle \sigma v \rangle_{pp}}{2 \langle \sigma v \rangle_{pd}} = \frac{\tau_D}{2\tau_H} \approx 10^{-17}. \end{aligned} \quad (207)$$

This isotopic ratio is much smaller than the one observed in Earth's oceans :  $(D/H)_{Earth} \simeq 1.56 \times 10^{-4}$ . Therefore, it is clear that the deuterium of the universe (and in particular on Earth) does not find its origin in the core of stars. Big Bang nucleosynthesis is the main candidate. When the early universe became cool enough ( $kT \approx 100 \text{ keV}$ ), stable deuterium nuclei were synthesised. Before that, the mean kinetic energies of particles were greater than its binding energy, deuterium that was formed was immediately destroyed, a situation known as the deuterium bottleneck. This bottleneck explains the insignificant amount of carbon and heavier elements synthesised during the Big Bang. As we will see these heavier elements are synthesised in the core of stars. At twenty minutes after the Big Bang, the universe became too cool for any further nuclear fusion to occur and the Big Bang nucleosynthesis stopped. Big Bang nucleosynthesis explains the order of magnitudes of deuterium isotopic ratios in the present universe. In the solar system, comets have deuterium ratios similar to the Earth's ocean one, emphasizing the theory that Earth's surface water may be largely comet-derived.

From this point, there are 3 possible channels in the p-p chain.

### pp<sub>I</sub> chain

The pp<sub>I</sub> chain is the dominating channel at temperatures below  $1.5 \times 10^7$  K, as for example in the solar core. After the previous reactions, the next and last one is the fusion of 2  ${}^3_2\text{He}$  nuclei :



Although the Coulomb repulsion is larger than before (2 protons in each  ${}^3_2\text{He}$ ), this reaction is easier than the p-p reaction (203) because it does not require the simultaneous  $\beta$ -decay. In the solar core, its reaction time is  $\tau_{33} = (\langle \sigma v \rangle_{33} {}^3_2\text{He})^{-1} \approx 10^6$  years. The time variation of the  ${}^3_2\text{He}$  abundance is given by the difference between its production (206) and its destruction (208). As we can assume equilibrium for deuterium, one can use eq. 207, which gives :

$$\begin{aligned} \frac{d({}^3_2\text{He})}{dt} &= \langle \sigma v \rangle_{pd} HD - \langle \sigma v \rangle_{33} ({}^3_2\text{He})^2 \\ &= \langle \sigma v \rangle_{pp} \frac{H^2}{2} - \langle \sigma v \rangle_{33} ({}^3_2\text{He})^2. \end{aligned}$$

At equilibrium ( $d({}^3_2\text{He})/dt = 0$ ), this gives :

$$\left( \frac{{}^3_2\text{He}}{H} \right)_{eq} = \sqrt{\frac{\langle \sigma v \rangle_{pp}}{2 \langle \sigma v \rangle_{33}}}. \quad (209)$$

To see how the abundance of  ${}^3_2\text{He}$  varies from the core to the surface, I remind the equation 193 giving the dependence of the cross-section with respect to the temperature for a non-resonant reaction :  $\partial \ln \langle \sigma v \rangle / \partial \ln T \simeq 6.574 W^{1/3} T_7^{-1/3}$  where  $W = Z_B^2 Z_C^2 A_B A_C / (A_B + A_C)$ . With twice as many protons in  ${}^3_2\text{He}$ ,  $W$  is larger in reaction 208 than in 203. We have thus :

$$\frac{\partial \ln ({}^3_2\text{He}/H)_{eq}}{\partial \ln T} = \frac{1}{2} \left( \frac{\partial \ln \langle \sigma v \rangle_{pp}}{\partial \ln T} - \frac{\partial \ln \langle \sigma v \rangle_{33}}{\partial \ln T} \right) < 0. \quad (210)$$

One sees thus that the abundance of  ${}^3_2\text{He}$  must increase from the core to the surface. But of course this is only valid as long as the equilibrium (eq. 209) is established. This is not the case in the superficial layers of a star. Going down in hotter layers, the first reaction to occur is deuterium fusion (206). Hence, the  ${}^3_2\text{He}$  production increases with depth along with its abundance and it is not destroyed yet. It is only deeper that  ${}^3_2\text{He}$  fusion becomes possible, when there is enough available  ${}^3_2\text{He}$  (the reaction rate of 208 is proportional to  $({}^3_2\text{He})^2$ ). The result is a peaked profile of  $({}^3_2\text{He}/H)$  with a maximum around  $0.6 m/M$ .

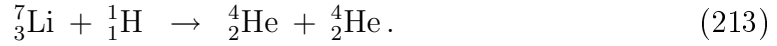
### pp<sub>II</sub> and pp<sub>III</sub> chains

At temperatures larger than  $2 \times 10^7$  K, an other reaction becomes more frequent than 208 :

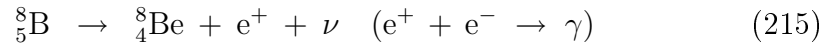


After this reaction, 2 channels are possible, constituting the pp<sub>II</sub> and pp<sub>III</sub> chains.

**pp<sub>II</sub> chain :**



**pp<sub>III</sub> chain :**



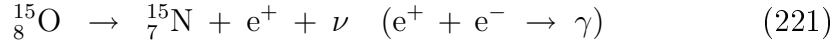
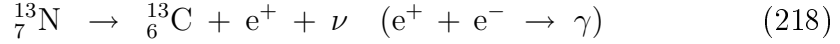
The pp<sub>II</sub> chain dominates at  $T \approx 2 - 3 \times 10^7$  K and the pp<sub>III</sub> chain dominates at  $T > 3 \times 10^7$  K.

Related to the solar neutrino problem (see later), it is useful to take a closer look to the reactions producing neutrinos : 203, 212 and 215. The neutrino energies differ significantly from one reaction to the other. In reactions 203 and 215, the energy is shared between the kinetic energy of the positron and the neutrino energy. There is a continuum of possible neutrino energies peaked around 0.263 MeV for the p-p reaction and around 7.2 MeV for the boron decay. The electron capture (212) occurs at specific energies corresponding to the two possible excited states of lithium. The neutrino energy has thus two possible values : 0.861 and 0.383 MeV.

Let's examine finally the dependence of  $\epsilon$  with respect to the temperature of the p-p chain. We have seen above (equation 193) that  $\nu = \partial \ln \epsilon / \partial \ln T \simeq 6.574 W^{1/3} T_7^{-1/3}$ , with  $W = Z_B^2 Z_C^2 A_B A_C / (A_B + A_a)$ . All reactions of the p-p chain involve light nuclei. At equilibrium, this gives  $\nu_{pp} \approx 5 - 6$  depending on the temperature. Out of equilibrium,  $\nu$  can be larger than that. In any case, this is much smaller than what we will find for the other reactions.

### 6.6.2 Carbon cycle

Although initially, stars are mainly constituted of hydrogen and helium, other heavier elements are also present. After H and He, the most abundant elements in the universe are oxygen and carbon. They can act as catalysts in the nucleosynthesis of helium from hydrogen, which constitutes the carbon or CNO cycle. Beyond  $T \approx 2 \times 10^7$  K and if there is enough initial carbon and oxygen (population I stars), this cycle becomes more efficient than the p-p chain. The main cycle of reactions is :

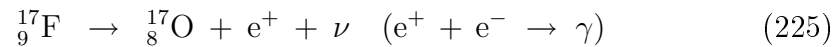
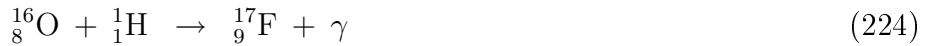


This is indeed a cycle since the carbon is restituted at the end. If all reactions occur at the same rate, the abundances of C, N, O isotopes remain constant, they are catalysts for the synthesis of helium from hydrogen.

Beyond this main cycle, there is also the following sub-cycle. Instead of 222, the following reaction rarely occurs (probability  $4 \times 10^{-4}$  compared to 222) :



Then come the following reactions :



From here, the main cycle is reached and the reactions 220, 221, ... can follow.

Two distinct regimes can settle during the life of a star. The first one is the **equilibrium regime** where the rates of reactions 217 to 222 are equal. In this case, the abundance of C, N, O isotopes remain constant, they are catalysts for the synthesis of helium from hydrogen. From an energetical point of view, 26 MeV are provided to the gas per produced helium nucleus. The sub-cycle 223, 224, 225, 226, plays a negligible role in this regime, because of the very low probability of 223.

The second possibility is the **out of equilibrium regime** typically occurring during the beginning of the life of a star. An important aspect of the CNO cycle is that the reaction 220 has a cross-section much smaller than the others. Initially, the stellar matter is mainly composed of  ${}^6_{12}\text{C}$  and  ${}^8_{16}\text{O}$  (after H and He). When the temperature reaches some  $10^6$  K, the reactions 217, 218 and 219 start to convert  ${}^6_{12}\text{C}$  into  ${}^7_{14}\text{N}$ . Slightly later, the reactions 224, 225 and 226 also convert  ${}^8_{16}\text{O}$  into  ${}^7_{14}\text{N}$ . Since the reaction 220 has a too small cross-section, it does not occur. The result is the conversion  ${}^6_{12}\text{C}$  and  ${}^8_{16}\text{O}$  into  ${}^7_{14}\text{N}$ . This out of equilibrium regime has a short duration compared to the equilibrium regime. Indeed, the quantity of available  ${}^6_{12}\text{C}$  and  ${}^8_{16}\text{O}$  is much smaller than hydrogen. When carbon and oxygen are exhausted, the production of energy drops. As a consequence, the core contracts and its temperature increases, which increases a lot the  $\langle \sigma v \rangle$  of 220. As a consequence, and because

the abundance of  ${}^7_7\text{N}$  has become much larger than before, the reaction rate of 220, given by  $r_{14} = \langle \sigma v \rangle_{14} ({}^{14}_7\text{N}) ({}^1_1\text{H})$ , becomes significant.  ${}^{12}_6\text{C}$  is produced again, the full cycle can occur and the star enters in the equilibrium regime.

It should be noted however that, in real cases, perfect equilibrium is not possible because of the presence of a convective core. During most of the main sequence phase (hydrogen burning phase), the averages of the rates of reactions 217 to 222 over the whole convective core are equal. But locally, they cannot be equal. The nuclear reactions mainly occur near the centre but not in the superficial layers of the convective core. Convective motions homogenize the chemical composition in the whole convective core. By continuously transporting fresh fuel in the core where it is consumed, they artificially maintain a local disequilibrium. Indeed, the dependences of the reaction rates with respect to the temperature vary from one reaction to the other. So local equilibrium is incompatible with homogeneity.

The origin of this convective core lies in the great sensitivity to the temperature of the rate of energy production through the CNO cycle. I remind that  $\nu = \partial \ln \epsilon / \partial \ln T$  increases with the height of the Coulomb barrier (eq. 193). With 6, 7 and 8 protons for C, N and O, we find thus particularly high values for the CNO cycle :  $\nu_{CNO} \approx 14 - 16$  depending on the temperature. There are two very important consequences to this very great sensitivity of  $\epsilon$  to  $T$ .

First, as  $\nu$  is very high and the temperature decreases from the center to the surface,  $\epsilon$  is significant only in a very small region near the center, with mass  $M_{nuc} \ll M_{tot}$ . We can write by integrating the equation of energy conservation at thermal equilibrium (82) :

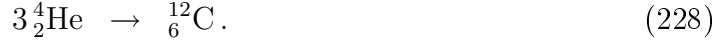
$$L(m) = \int_0^m \epsilon \, dm. \quad (227)$$

From the center until  $M_{nuc}$ ,  $dL/dm = \epsilon$  is large. Beyond this mass, the derivative is nearly 0 and  $L$  is constant. In the central layers,  $L(m)/m$  is thus very large. The radiative gradient (equation 59), which is proportional to  $L/m$  is thus very high and larger than the adiabatic gradient. These central regions are therefore convectively unstable according to the Schwarzschild criterion (60).

The second consequence of this very high sensitivity of  $\epsilon$  to  $T$  is the mechanism of temperature control by nuclear reactions. This mechanism plays a major role in stellar evolution, as we will see later.

## 6.7 Helium fusion ( $T \approx 10^8$ K)

At temperatures of the order of  $10^8$  K, the nucleosynthesis of carbon from 3 helium nuclei becomes possible, this is the **3  $\alpha$  reaction** :



The probability that 3  $\alpha$  particles collide simultaneously is zero. In practice, this fusion occurs in two steps.

First, 2 helium nuclei merge to form a  ${}^8_4\text{Be}$  nucleus in an excited state ( ${}^8_4\text{Be}^*$ ). The excited  ${}^8_4\text{Be}$  nucleus is very unstable and almost all the time splits again in two  $\alpha$  particles (the lifetime of  ${}^8_4\text{Be}^*$  is  $\approx 10^{-16}$  s!). A thermodynamic equilibrium is established with as much fusions and fissions :



In this situation of thermodynamic equilibrium, one gets :

$$\frac{({}^8_4\text{Be}^*)}{({}^4_2\text{He})^2} \propto T^{-3/2} \exp(-E_{2\alpha}/kT) \approx 1.87 \times 10^{-33} f_{2\alpha} T_8^{-3/2} \times 10^{-4.64/T_8}, \quad (230)$$

where  $T_8 = T(\text{K})/10^8$ ,  $E_{2\alpha} = 92$  keV is the difference of energy  $E({}^8_4\text{Be}^*) - 2E({}^4_2\text{He})$ ,  $f_{2\alpha}$  is the electron screening factor<sup>2</sup> and abundances are in number/cm<sup>3</sup>. At  $T_8 = 1$  and a typical density  $\rho = 10^5$  g/cm<sup>3</sup>, one gets one  ${}^8_4\text{Be}^*$  nucleus for  $10^9$   ${}^4_2\text{He}$  nuclei (one part per billion).

Although the abundance of  ${}^8_4\text{Be}^*$  is very small, it is large enough to make the next step possible : the fusion of  ${}^8_4\text{Be}^*$  with an helium nucleus to form a carbon nucleus :



The fusion reactions 229 and 231 are resonant reactions<sup>3</sup>. Although 229 is endothermic, 231 produces more energy and thus 228 is exothermic. The reaction rate 228 is equal to the one of 231 and follows the law of a resonant reaction (eq. 198) :

$$r_{3\alpha} \propto ({}^8_4\text{Be}^*)({}^4_2\text{He}) T^{-3/2} \exp(-E_{\alpha\text{Be}}/kT). \quad (232)$$

The heat provided by the fusion of 3 helium nuclei into a carbon nucleus is :

$$Q_{3\alpha} = (3M_\alpha - M_C)c^2 = 7.275 \text{ MeV}. \quad (233)$$

<sup>2</sup>Electrons go between the nuclei and decrease the Coulomb repulsion.

<sup>3</sup>The discovery of the resonance state of  ${}^{12}_6\text{C}$  required for reaction 231 was not trivial (Hoyle 1954, Cook et al. 1957). It was taken as an argument to support the *anthropic principle* according to which the constants of physics must have very specific values to make the existence of humans possible...

This is much less than the 26 MeV of hydrogen fusion. Because of that and the larger luminosity during this phase of helium fusion, its duration is much shorter than the hydrogen fusion phase. The rate of energy production is obtained by combining 230, 232 and 233. This gives in cgs units ( $Y$  is the usual notation for the helium mass fraction) :

$$\epsilon_{3\alpha} = 5.09 \times 10^{11} f_{3\alpha} \rho^2 Y^3 T_8^{-3} \exp(-44.027/T_8). \quad (234)$$

One sees in this equation an extreme sensitivity to the temperature. At  $T_8 = 1$ , one gets  $\nu = \partial \ln \epsilon / \partial \ln T \approx 40!!$  The core fusion of helium leads thus to the presence of a convective core, like the CNO cycle.

### $\alpha$ captures

The reactions 229 and 231 are not the only ones during this phase. As the abundance of helium decreases and that of carbon increases, the following reaction starts to be possible and progressively takes precedence over 228 :



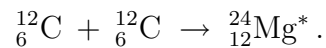
Finally, when enough oxygen is synthesized, it can also capture an  $\alpha$  particle :



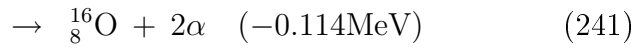
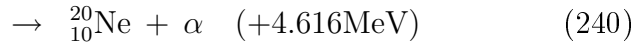
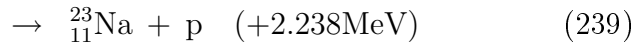
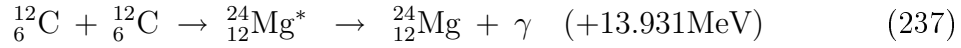
**Carbon and oxygen are synthesized in comparable proportions from helium during this phase**, plus a very small amount of neon synthesis.

## 6.8 Carbon fusion ( $T \approx 6 - 8 \times 10^8$ K)

At temperatures of more than half a billion degrees, the kinetic energies of carbon nuclei are sufficient to make possible their fusion :



At these high temperatures, the Gamow's peak is larger (law in  $T^{5/6}$  in equation 192). As a result, there are a large number of quasi-stationary magnesium levels in the corresponding energy range. Although the reaction of carbon fusion into magnesium is resonant, the nuclear factor  $S(E)$  varies thus slowly in the interval of the Gamow's peak. Therefore, the temperature dependence of this reaction is similar to that of a non-resonant reaction with a  $\exp(-cT^{-1/3})$  law (eq. 190). The formed magnesium nucleus is in an unstable excited state that rapidly disintegrates through one of the following channels :



Of these different channels, the most likely are the reactions 239 and 240.

At such high temperatures, the produced protons, neutrons and  $\alpha$  particles are immediately recaptured by other nuclei (see the reaction grid in the powerpoint slides). Among others, there are the  $\alpha$  captures :



Let's also quote the following interesting series of reactions :



We already met the first two of these reactions in the CNO cycle. The third is only possible at these high temperatures and leads, together with 238, to the production of free neutrons. This is important because neutrons without charge have no Coulomb barrier to cross. They are therefore easily captured to form heavier nuclei. We will come back to this later in the course (see s process).

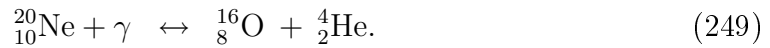
In terms of energy, the balance of all these reactions is complex ; on average, approximately 13 MeV are released per pair of merging carbon nuclei. The temperature dependence of the energy production rate follows approximately a law  $\epsilon_{CC} \propto \exp(-84.165/T_9^{1/3})$ , as in non-resonant reactions (see above) ( $T_9 = T(\text{K})/10^9$ ).

**In terms of nucleosynthesis, the result is complex, the main final products of all these reactions are, in decreasing order of abundance :  ${}^{16}_8\text{O}$ ,  ${}^{20}_{10}\text{Ne}$ ,  ${}^{24}_{12}\text{Mg}$  and  ${}^{28}_{14}\text{Si}$ .**

## 6.9 Neon photo-disintegration ( $T \approx 1.2 - 1.5 \times 10^9$ K)

At  $T = 1.2 \times 10^9$  K,  $kT = 0.1$  MeV. At such a temperature, a not completely negligible number of photons corresponding to the tail of the Planck distribution has the energy required to enable the neon photo-disintegration reaction :  ${}^{20}_{10}\text{Ne} + \gamma \rightarrow {}^{16}_8\text{O} + {}^4_2\text{He}$ . On the other hand, the temperature and therefore the energy of the photons is not yet sufficient to allow the photo-disintegration of the other more stable previously synthesized nuclei (O, Mg, ...).

The energy required for this endothermic reaction is  $Q = 4.73$  MeV. This fission is done in 2 stages. A photon of energy  $h\nu = 5.63$  MeV is first captured to bring the neon nucleus to an excited level. Then this unstable nucleus splits spontaneously into nuclei of oxygen and helium, with release of the energy difference (5.63-4.73 MeV) in the form of kinetic energy. Of course, the fusion of helium and oxygen into neon is also possible at these temperatures :



The thermodynamic equilibrium between the direct and inverse reactions leads to an abundance ratio obeying a Saha-like equation (see eq. 151) :

$$\frac{({}^4_2\text{He}) ({}^{16}_8\text{O})}{({}^{20}_{10}\text{Ne})} \propto T^{3/2} \exp(-Q/kT), \quad (250)$$

with  $Q = 4.73$  MeV,  $Q/(kT) = 54.89/T_9$ ,  $T_9 = T(K)/10^9$ . If there was only that, once this equilibrium reached with as many direct and inverse reactions, the energy production would be zero. This is not so because, from time to time, one of the helium nuclei produced by the neon photo-disintegration can be captured by a nucleus heavier than oxygen :



After the equilibrium reactions 249, reaction 251 has the highest rate. Combining the neon photo-disintegration and 251, we get :



Although the photo-disintegration reaction is endothermic, the energy released by 251 is larger than the 4.73 MeV. **The energy balance of 253 and more generally this phase is exothermic.** The heat released per gram of consumed neon is approximately one quarter of that of the carbon fusion phase. 253 dictates the evolution of the chemical composition during this phase, which gives :

$$\frac{d(O)}{dt} = \frac{d(Mg)}{dt} = -\frac{1}{2} \frac{d(Ne)}{dt} = \langle \sigma v \rangle_{\alpha Ne} (Ne) (He). \quad (254)$$

Substituting in this equation the abundance of helium given by the equilibrium relation 250, we get the energy production rate  $\epsilon_{Ne}$  :

$$\epsilon_{Ne} \approx 8.54 \times 10^{26} T_9^{12} \frac{Y_{Ne}^2}{Y_O} \exp(-54.89/T_9), \quad (255)$$

where  $Y_{Ne}$  and  $Y_O$  are the mass fractions of neon and oxygen. **In terms of nucleosynthesis, this phase is thus characterized by a decrease in the neon abundance, an increase in the abundance of oxygen (which was already before the most abundant element), a significant production of magnesium and to a lesser extent of silicon.**

## 6.10 Oxygen fusion ( $T \approx 2 \times 10^9$ K)

The oxygen nucleus is particularly stable because of its doubly magical nature :  $Z = N = 8$ . Consequently, it is necessary to wait for very high temperatures of the order of 2 billion degrees for the fusion reaction of oxygen nuclei to become possible :



For the same reasons as for carbon fusion, the dependence on temperature of this reaction is similar to that of a non-resonant reaction with a law in  $\exp(-cT^{-1/3})$ .

The produced sulfur nucleus is in a unstable excited state which decays rapidly through one of the following channels :



Of these different channels, the most likely are the reactions 258 and 259.

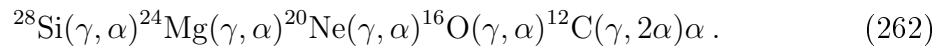
At such high temperatures, the produced deuterium is immediately photodisintegrated. As for the emitted protons, neutrons and  $\alpha$  particles, they are immediately recaptured by other nuclei (see the reaction grid in the powerpoint slides). In addition, a growing number of photodisintegration reactions becomes possible, balancing the inverse fusion reactions (for example  ${}^{29}_{14}\text{Si} + \gamma \leftrightarrow {}^{28}_{14}\text{Si} + \text{n}$ ,  ${}^{30}_{15}\text{P} + \gamma \leftrightarrow {}^{29}_{14}\text{Si} + \text{p}$ ).

In terms of energy, the balance of all these reactions is complex ; on average, approximately 16 MeV are released per pair of merging oxygen nuclei.

**In terms of nucleosynthesis, the balance is complex, the main end products of all the involved reactions is about 90% of silicon and sulfur, followed by argon, calcium, Ti and Cr.**

### 6.11 “Silicon burning” ( $T \approx 3.3 \times 10^9$ K)

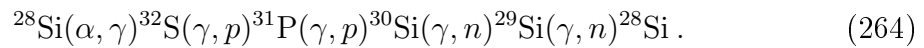
At temperatures of the order of 3 billion degrees, a considerable number nuclear reactions becomes possible (see reaction grid in the powerpoint slide). Among these, photodisintegrations of silicon and other heavy nuclei and recaptures of the light nuclei become very numerous. As the main element at the beginning of this phase is silicon, we refer to this phase as “silicon burning” ; however, the corresponding fusion reaction does not occur. Photo-disintegration reactions starting from silicon lead mainly to the production of free helium nuclei according to the chain :



These released helium nuclei are recaptured, allowing the synthesis of increasingly heavy nuclei from silicon :



Two groups of near-equilibrium reaction are established. The first, around silicon, goes up to  ${}^{48}\text{Ti}$ , with for example the following reactions :



The second group goes from  ${}^{52}\text{Cr}$  to  ${}^{56}\text{Fe}$ . At the interface between these 2 groups in near-equilibrium,  $\alpha$  captures are favored, which results in the destruction of silicon in favor of elements of the Fe group.

**In terms of nucleosynthesis, the balance is complex, the main end products of all the involved reactions are, in decreasing order of abundance : iron, nickel, Cr and Ti.**

## 6.12 Nuclear statistical equilibrium ( $T \approx 5 - 7 \times 10^9 \text{ K}$ )

We have seen that the network of nuclear reactions has become considerably more complex as the temperature rises. Beyond a threshold,  $kT$  becomes non-negligible compared to the energies involved in most reactions. Therefore, all fusion reactions and photodisintegrations become possible. A statistical equilibrium is established between all direct and inverse reactions. The powerful tools of statistical physics allow us to describe the statistical distribution of different nuclei by simple functions depending essentially on the temperature, we are talking about **nuclear statistical equilibrium**. We have already met above with the photodisintegration of neon the equivalent of the Saha equation governing this thermodynamic equilibrium (eq. 250). So, now considering a neutron capture-release reaction :



we have by noting  $N$  the abundances :

$$\frac{N_Z^{A-1} N_n}{N_Z^A} \propto T^{3/2} \exp(-Q_{A,Z,n}/kT), \quad (266)$$

with

$$Q_{A,Z,n} = (M_n + M_Z^{A-1} - M_Z^A)c^2. \quad (267)$$

Similarly, we can write :

$$\frac{N_Z^{A-2} N_n}{N_Z^{A-1}} \propto T^{3/2} \exp(-Q_{A-1,Z,n}/kT). \quad (268)$$

Proceeding step by step until separating the complete nucleus into each of its components, then multiplying the corresponding equations (eqs. 266, 268, ...), we finally get :

$$N_Z^A \propto N_p^Z N_n^{A-Z} T^{-3(A-1)/2} \exp(-\Delta\mathcal{M}_{A,Z}/kT), \quad (269)$$

where  $-\Delta\mathcal{M}_{A,Z}$  is the binding energy of the nucleus  ${}^A_Z\text{X}$ . Eq. 269 gives the abundance of each of the nuclei. In practice, the numbers of free protons and neutrons  $N_p$  and  $N_n$  are not imposed; the total number of nucleons is imposed (free or in a nucleus). Under this constraint, it can be shown that at a not too high temperature ( $kT < -\Delta\mathcal{M}_{A,Z}$ ),  $N_Z^A$  takes a maximum value for nuclei having the largest binding energy per nucleon :  $f_{A_Z} \equiv -\Delta\mathcal{M}_{A,Z}/A$ . If this nuclear reaction phase goes slowly enough, the  $\beta$  decays have time to bring the nuclei to the stability valley of nuclei. In this case, the most abundant element (maximum of  $f_{A_Z}$ ) is  ${}^{56}_{26}\text{Fe}$ . On the other hand, if it happens extremely quickly (type Ia supernovae),  $\beta$  decays do not have time to take place, the ratio between total number of protons and neutrons (free or not) remains unchanged and very close to 1, and the most abundant element is  ${}^{56}_{28}\text{Ni}$ .

As we will see, when the “iron core” reaches the Chandrasekhar’s limiting mass, it starts to collapse and the temperature increases very quickly, the equilibrium

governed by eq. 269 moves in the direction of photodisintegrations, and therefore an increase abundance of light particles (helium, protons, neutrons) at the expense of heavy nuclei. The energy balance then becomes endothermic, which as we shall see accelerates the core collapse triggering a type II supernova explosion.

## 7 Polytropic gaseous spheres

In the previous chapters, we have studied the different physical phenomena that must be modeled to describe the internal structure of stars. In this chapter, we consider simplified models of stars called polytropes. Their simplicity will allow us to present some fundamental features of stars such as the Chandrasekhar's limiting mass.

A polytrope is a fluid where the pressure and density are related by a power law of the following form :

$$P = K\rho^\gamma = K\rho^{1+1/n}, \quad (270)$$

in which  $n$  is called the polytropic index.

### 7.1 Lane-Emden equation

We want to model a sphere in hydrostatic equilibrium obeying to the polytropic relation 270. From the equation of hydrostatic equilibrium, we have :

$$-\frac{1}{\rho} \frac{dP}{dr} = \frac{Gm}{r^2} = \frac{d\phi}{dr}, \quad (271)$$

where  $\phi$  is the gravitational potential. This potential is obtained by solving the Poisson equation :  $\nabla^2\phi = 4\pi G\rho$ . Under our hypothesis of spherical symmetry, it reads :

$$\frac{1}{r^2} \frac{d}{dr} \left( r^2 \frac{d\phi}{dr} \right) = 4\pi G \rho. \quad (272)$$

Combining equations 270, 271 and 272, we will obtain a very simple 2nd order differential equation describing the internal structure of a polytrope. We start by developing the left hand side of equation 271 and using equation 270. We have :

$$\begin{aligned} \frac{d\phi}{dr} &= -\frac{1}{\rho} \frac{dP}{dr} = -K \gamma \rho^{\gamma-2} \frac{d\rho}{dr} \\ &= -K \frac{\gamma}{\gamma-1} \frac{d\rho^{\gamma-1}}{dr} \end{aligned} \quad (273)$$

We define the surface of the polytrope by the condition  $P(R) = \rho(R) = 0$ . As we are always free to add a constant to a potential, we choose this constant such that the gravitational potential is zero at the surface :  $\phi(R) = 0$ . We integrate now the 2 members of equation 273.  $\phi(R) = 0$  fixes the integration constant and we get :

$$\phi(r) = -K \frac{\gamma}{\gamma - 1} \rho(r)^{\gamma-1} = -K(n+1)\rho(r)^{1/n}, \quad (274)$$

or :

$$\rho(r) = \left[ \frac{-\phi(r)}{K(n+1)} \right]^n. \quad (275)$$

Substituting the relation in the Poisson equation, we finally get :

$$\frac{1}{r^2} \frac{d}{dr} \left( r^2 \frac{d\phi}{dr} \right) = 4\pi G \rho = 4\pi G \left[ \frac{-\phi}{K(n+1)} \right]^n \quad (276)$$

With the following change of variables, we can simplify this equation.

$$z = Ar, \quad w = \frac{\phi}{\phi_c} = \left( \frac{\rho}{\rho_c} \right)^{1/n} \quad (277)$$

is the new dependent variable, with  $\phi_c$  and  $\rho_c$  the central values of  $\phi$  and  $\rho$  :

$$A^2 = \frac{4\pi G}{(n+1)^n K^n} (-\phi_c)^{n-1} = \frac{4\pi G}{(n+1)K} \rho_c^{\frac{n-1}{n}}. \quad (278)$$

After some algebra, it is easily seen that these new variables change eq. 276 into :

$$\frac{1}{z^2} \frac{d}{dz} \left( z^2 \frac{dw}{dz} \right) + w^n = 0. \quad (279)$$

This differential equation is called the **Lane-Emden equation**. At the core :

$$w(0) = 1, \quad dw/dz(0) = 0.$$

We have thus to solve a Cauchy problem. This is easily done numerically. The numerical integration is stopped at the point  $z_n$  where  $w$  is zero, which defined the surface of the polytrope.

The advantage of this dimensionless formulation of the problem is that the Lane-Emden equation is very simple and only depends on the polytropic index  $n$ . Once this equation is solved for a given  $n$ , the solution can be used for all polytropic sphere with this index.

## 7.2 Some polytropes

For 3 values of  $n$  only, the Lane-Emden equation has an analytical solution :

$$\begin{aligned} n &= 0 \text{ } (\rho \text{ } cst.) : w(z) = 1 - z^2/6 \\ n &= 1 \text{ } (\gamma = 2) : w(z) = \sin z/z \\ n &= 5 \text{ } (\gamma = 6/5) : w(z) = (1 + z^2/3)^{-1/2} \end{aligned}$$

$n = 0$  corresponds to spheres with constant density. For  $n = 5$ ,  $w$  tends asymptotically to 0 as  $z$  tends towards infinity. The surface as defined above is thus at infinity.  $n = 5$  is a critical value : for  $n < 5$ , the solutions have a finite radius and for  $n \geq 5$  the radius.

We now consider different values of  $n$  useful for stellar physics applications.

### **n=0**

As said before, this corresponds to a sphere of constant density. The solution is a parabola. The constant density is equal to the mean density :

$$\rho = \frac{3M}{4\pi R^3}. \quad (280)$$

The mass of each sphere is simply :

$$m(r) = \frac{4\pi}{3} r^3 \rho = M \frac{r^3}{R^3} \quad (281)$$

Using these relations, we get for the pressure :

$$\begin{aligned} P(r) &= \int_r^R \frac{Gm\rho}{r'^2} dr' \\ &= \frac{3GM^2}{8\pi R^6} (R^2 - r^2). \end{aligned}$$

We assume now we have an ideal gas, the temperature profile is then also parabolic :

$$T(r) = \frac{P}{\rho} \frac{\mu m_u}{k} = \frac{GM}{R^3} \frac{\mu m_u}{2k} (R^2 - r^2). \quad (282)$$

In an ideal gas with constant density, we also have :

$$\frac{d \ln T}{d \ln P} = 1. \quad (283)$$

We have seen previously that convective instability occurs if  $\nabla \equiv d \ln T / d \ln P > \partial \ln T / \partial \ln P|_s \equiv \nabla_{ad}$ . In an ideal gas,  $\nabla_{ad} = 2/5$ .

**A constant density sphere is thus extremely unstable with respect to**

**convection.** Indeed, in deep stellar layers where the heat capacity is huge, we have seen before that values of  $\nabla$  very slightly larger than  $\nabla_{ad}$  enable an efficient transport of energy by convection. What would happen to a constant density star? The huge amount of heat lost by the core due to convection would lead to its quick contraction (see the Virial theorem, Sect. 8.1). The density would thus quickly increase in the core, generating a density gradient :  $d \ln \rho / d \ln P > 0$ . Hence,  $\nabla \simeq 1 - \ln \rho / d \ln P > 0$  would decrease until it becomes close to  $\nabla_{ad}$ . **The very strong convective instability of constant density models explains thus why the density is decreasing from the center to the surface of stars.**

**n=1 ( $\gamma=2$ )**

We have seen that we have the analytical solution  $w(z) = \sin z/z$  in this case. This function has an inflection point at the surface. For  $n < 1$ ,  $d^2w/dz^2 < 0$  from the center to the surface. For  $n > 1$ , the function  $w(z)$  has an inflection point below the surface. We will also see later that  $n = 1$  is a limit case for the mass-radius relation : for  $n < 1$ , the radius increases with the mass, for  $n > 1$  the radius decreases with the mass.

**n=3/2 ( $\gamma=5/3$ )**

This case is very important because we can associate to it 2 physical situations often encountered in stars.

The first one corresponds to a **completely degenerated non-relativistic gas**. We have seen in chapter 4.5 (eq. 136) that in this limit case, the pressure is completely dominated by degenerated electrons and is given by :

$$P = K \rho^{5/3} \quad (284)$$

with

$$K = \left( \frac{3h^3}{8\pi} \right)^{2/3} \frac{1}{5m_e(m_u\mu_e)^{5/3}}. \quad (285)$$

Note that  $K$  depends only on fundamental physical constants and the molecular weight per electron ( $\mu_e$ ).

The second one corresponds to an efficient convective zone. We have seen previously that, except near the surface, convection is very efficient in stars because of the very high enthalpy and temperature ( $h \approx c_p T$ ) in stellar interiors. As a consequence, the stratification of convective layers is quasi-isentropic (adiabatic). Consider an ideal completely ionized gas without radiation pressure. In this case, we have in a convective zone :

$$\frac{d \ln P}{d \ln \rho} \simeq \Gamma_1 \simeq \frac{5}{3} \quad (286)$$

Integrating this relation, we find again  $P = K\rho^{5/3}$ . Note however that now  $K$  is no longer fixed by the fundamental constants. It is not constant in a set of fully convective models with different masses. Hence, fully convective models do not obey a mass-radius relation (see Sect. 7.3).

### **n=3 ( $\gamma=4/3$ )**

This case is also very important. It corresponds to the limiting case of a **completely degenerated extremely relativistic gas**. We have seen in eq. 138 that, in this case, the pressure is given by :

$$P = K\rho^{4/3} \quad (287)$$

with

$$K = 2\pi c (3h^3)^{1/3} \left( \frac{1}{8\pi m_u \mu_e} \right)^{4/3} = \frac{1.2435 \times 10^{15}}{\mu_e^{4/3}} \text{ (cgs)} \quad (288)$$

We will see later the special properties of completely degenerated extremely relativistic spheres.

### **n=5 ( $\gamma=6/5$ )**

We have seen that this case, of which the analytical solution is given at the beginning of this subsection, corresponds to the limit between polytropes of finite and infinite radii.

### **n= $\infty$ ( $\gamma=1$ )**

This corresponds to an isothermal sphere. Indeed, in an ideal isothermal gas,  $P = kT/(\mu m_u)\rho \propto \rho$ , which corresponds to  $n \rightarrow \infty$  in Eq. 270. The ‘‘Lane-Emden equation’’ is here obtained through another change of variable ( $w^\infty$  has no meaning). Eq. 273, which is still valid, reads with  $\gamma = 1$  :  $d\phi/dr = -K d \ln \rho/dr$ . Integrating it and assuming for simplicity that the potential is zero at the center gives :

$$\frac{\rho}{\rho_c} = e^{-\phi/K}. \quad (289)$$

As we did before for finite polytropic indices, we substitute this equation in the Poisson equation. We now introduce the following change of variable :

$$w = \phi/K, \quad z = Ar, \quad A^2 = 4\pi G\rho_c/K. \quad (290)$$

With this change of variable, the equivalent of the Lane-Emden equation for the isothermal sphere reads :

$$\frac{1}{z^2} \frac{d}{dz} \left( z^2 \frac{dw}{dz} \right) = e^{-w}. \quad (291)$$

The boundary conditions are here different :  $w(0) = 0$  (not 1) and  $dw/dz(0) = 0$ . As for the other polytropes with  $n \geq 5$ , the isothermal sphere has an infinite radius. The solution is here regular at the center by construction.

It is useful to notice that a simpler singular solution is often used in stellar dynamics and extragalactic astrophysics. With our notation, it reads :  $w(z) = 2 \ln(z) - \ln(2)$ . The corresponding density profile reads :

$$\rho(r) = \frac{K}{2\pi G} \frac{1}{r^2} = \frac{kT}{2\pi\mu m_u G} \frac{1}{r^2} \propto \frac{1}{r^2}. \quad (292)$$

It can be shown that the asymptotic behaviors ( $r \rightarrow \infty$ ) of the regular and singular isothermal spheres coincide. In particular,  $m(r)$  behaves asymptotically as  $m(r) \propto r$  and thus  $\lim_{r \rightarrow \infty} m(r) = \infty$ .

### 7.3 Mass-radius relation

We have established at the very beginning equation. 13 giving the mass of a sphere of radius  $r$  :

$$m(r) = \int_0^r 4\pi r^2 \rho dr \quad (293)$$

With the change of variables 277, we have  $\rho(r) = \rho_c w(z)^n$  and  $r^2 dr = (1/A)^3 z^2 dz$ , so that

$$m(r) = 4\pi \frac{1}{A^3} \rho_c \int_0^z w^n z^2 dz = 4\pi \frac{r^3}{z^3} \rho_c \int_0^z w^n z^2 dz \quad (294)$$

We use now the Lane-Emden equation 279, which gives :

$$m(r) = -4\pi \frac{r^3}{z^3} \rho_c \int_0^z \frac{d}{dz} \left( z^2 \frac{dw}{dz} \right) dz = -4\pi r^3 \rho_c \frac{1}{z} \frac{dw}{dz}. \quad (295)$$

Integrating over the whole sphere, we have thus in particular :

$$M = -4\pi R^3 \rho_c \frac{1}{z_n} \frac{dw}{dz}(z_n). \quad (296)$$

For the total radius, we have from eq. 277 :

$$R = \frac{z_n}{A} = z_n \left[ \frac{(n+1)K}{4\pi G} \right]^{1/2} \rho_c^{\frac{1-n}{2n}} \quad (297)$$

Substituting this relation into eq. 296, we find thus :

$$M = -4\pi \left[ \frac{(n+1)K}{4\pi G} \right]^{3/2} z_n^2 \frac{dw}{dz}(z_n) \rho_c^{\frac{3-n}{2n}} \quad (298)$$

These 2 last equations relate the total mass and radius to  $\rho_c$ .  $\rho_c$  can thus be eliminated, which gives :

$$R \propto \rho_c^{\frac{1-n}{2n}} \propto M^{\frac{1-n}{3-n}},$$

more precisely :

$$R = z_n^{\frac{1+n}{3-n}} \left[ \frac{(n+1)K}{4\pi G} \right]^{\frac{n}{3-n}} \left[ -4\pi \frac{dw}{dz}(z_n) \right]^{\frac{n-1}{3-n}} M^{\frac{1-n}{3-n}}. \quad (299)$$

This relation is fundamental, this is the **mass-radius relation of polytropic spheres**. Note that the proportionality constant in eq. 299 depends on the polytropic index  $n$  and the constant  $K$ . This equation relates thus the masses and radii of a set of polytropes with **same  $n$  and  $K$** . This is the case for non-relativistic completely degenerated gaseous spheres. They obey thus to a mass-radius relation  $R \propto M^{-1/3}$ . On the contrary, although completely convective spheres are also approximated by  $n = 3/2$  polytropes, they do not obey a mass-radius relation because  $K$  is not constant for them.

Depending on the values of  $n$ , there are two possibilities for the mass-radius relation. If  $n < 1$ , the exponent of  $M$  in 299 is positive ; the radius of the polytrope increases thus as the mass increases. On the contrary, if  $1 < n < 3$ , the exponent of  $M$  is negative and the radius of the polytrope decreases as the mass increases. A special analysis will be dedicated to the limiting case  $n = 3$ . This trend can be understood through the following reasoning. Consider an initial polytropic model with given mass  $M$  and radius  $R$ . I try to build now a second model by multiplying the mass of each layer by a given factor  $q > 1$ , keeping the same radius. I note with a " ' " the new structure. The different functions of  $r$  are thus transformed as follows :

$$m(r) \rightarrow m'(r) = q m(r) \quad (300)$$

As the volume is kept constant :

$$\rho(r) \rightarrow \rho'(r) = q \rho(r) \quad (301)$$

For the pressure, using the polytropic relation (eq. 270), we have :

$$P(r) \rightarrow P'(r) = K(\rho')^{1+1/n} = q^{1+1/n} P(r). \quad (302)$$

The weight of the gas column is given by  $weight(r) = \int_r^R (Gm\rho)/r^2 dr$ , we have thus :

$$Weight(r) \rightarrow Weight'(r) = \int_r^R (Gm'(r)\rho'(r))/r^2 dr = q^2 Weight(r). \quad (303)$$

We see thus that, **if  $n < 1$  (and  $q > 1$ )**,  $P'(r) > Weight'(r)$ . The pressure increased more than the weight of the gas column. The resultant of the forces is thus towards the exterior and **the star must expand** until the hydrostatic equilibrium is established. On the opposite, **if  $n > 1$** , the weight increased more than the pressure ( $P'(r) < Weight'(r)$ ). The weight wins over the pressure, the resultant of the force is towards the center and **the star must contract**.

## 7.4 Chandrasekhar's limiting mass

We study now in more detail the case of an  $n = 3$  polytrope corresponding to a relativistic completely degenerated gas. With  $3 - n = 0$  on the denominator of the exponent, we see that it is not possible to use equation 299. We must come back to equation 298, which gives for  $n = 3$  :

$$\begin{aligned} M_{Ch} &= -4\pi \left[ \frac{K}{\pi G} \right]^{3/2} z_3^2 \frac{dw}{dz}(z_3) \\ &= \left( \frac{2}{\mu_e} \right)^2 1.459 M_\odot. \end{aligned} \quad (304)$$

This result is fundamental, it shows that in any set of  $n = 3$  polytropic spheres with same constant  $K$ , the total mass is constant and given by eq. 304. For relativistic completely degenerated gaseous spheres, this mass is called the **Chandrasekhar's limiting mass**<sup>4</sup>. In advanced stages of stellar evolution, the very dense stellar core can reach relativistic complete degeneracy. In advanced stages of stellar evolution, there is no longer hydrogen in the core and  $\mu_e \simeq 2$  (see eq. 144). The Chandrasekhar's limiting mass is then  $M_{Ch} \simeq 1.459 M_\odot$ .

Before interpreting this limiting mass, we consider the radii of  $n = 3$  polytropes. Equation 297 relates the radius and central density of polytropes. We start with an  $n = 3$  polytrope in hydrostatic equilibrium having the Chandrasekhar's mass  $M_{Ch}$  and an initial radius  $R$ . We expand (or contract) now this model by multiplying the radii of all spheres inside the star by the same factor  $x$  (keeping their masses constant). As before, I note with a " ' " the new structure. We have thus :

$$r(m) \rightarrow r'(m) = x r(m). \quad (305)$$

The mass is kept constant and the volume is multiplied by  $x^3$ , so that :

$$\rho(m) \rightarrow \rho'(m) = \rho(m)/x^3. \quad (306)$$

For the pressure, using the polytropic relation  $P = K\rho^{4/3}$ , we have :

$$P(m) \rightarrow P'(m) = K\rho'(m)^{4/3} = K\rho(m)^{4/3}/x^4 = P(m)/x^4. \quad (307)$$

The weight of the gas column above the sphere of mass  $m$  is  $Weight(m) = \int_m^M Gm dm/(4\pi r^4)$ , so that :

$$Weight(m) \rightarrow Weight'(m) = \int_m^M Gm dm/(4\pi r'^4) = (m)/x^4. \quad (308)$$

---

<sup>4</sup>Subrahmanyan Chandrasekhar (Lahore 1910 - Chicago 1995) was one of the greatest astrophysicist of his time. He was awarded the 1983 Nobel Prize for Physics for "...theoretical studies of the physical processes of importance to the structure and evolution of the stars".

The initial model was in hydrostatic equilibrium with  $P(m) = P_{\text{oids}}(m) \forall m$ . Expanding or contracting the star, equations 307 and 308 show that the pressure and weight are divided by the same factor  $x^4$ , remaining equal. The polytropic relation  $P = K\rho^{4/3}$  ensures thus that the hydrostatic equilibrium is automatically maintained as the star contracts or expands. The radius of the star is thus free.

We can come back now to the mass. Why is the mass fixed to a unique possible value?? In order to understand that, imagine the following. We start again from a polytrope  $n = 3$  having the Chandrasekhar's mass and being in hydrostatic equilibrium. We add next a spherical shell of matter around it, without changing the inner part. Adding this shell increases the weight of the gas column in the inner part. It is now larger than the pressure, so that the star starts to contract. Suppose as a simplification that the contraction is homologous (the initial radii of the spheres are multiplied by the same factor  $x(t)$  at each time of the contraction). The above derivations remain then valid. In particular, at each time of the contraction, the pressure and weight are divided by the same factor  $x(t)^4$ . We started from a disequilibrium of the forces (weight  $>$  pressure). It is thus maintained and the collapse continues as long as the physical conditions justifying  $n = 3$  (relativistic complete degeneracy) remain valid. You can do the same reasoning by removing a superficial shell from the star. In this case, the weight became smaller than the pressure and the star expands as long as relativistic degeneracy is maintained.

## 7.5 White dwarfs

At the end of the evolution of low to intermediate mass stars, their envelope is expelled. What remains is a compact star mainly composed of carbon and oxygen without nuclear reactions. It is called a **white dwarf**. Because of the high densities, the electron gas is degenerated in white dwarfs. We have seen that non-relativistic completely degenerated gaseous spheres are  $n = 3/2$  polytropes obeying to a mass-radius relation :

$$R \propto M^{-1/3}. \quad (309)$$

The trend of this relation remains valid in white dwarfs, they also obey to a mass-radius relation : the larger their masses, the smaller their radii. Because of the absence of nuclear reactions, white dwarfs are slowly cooling. We can assume that the mass of an isolated white dwarf remains constant during its evolution, its radius remains thus also constant because of the mass-radius relation. Its luminosity and effective temperature decrease slowly with  $L \propto T_{\text{eff}}^4$  (equation 10 with constant  $R$ ).

We now consider a set of white dwarfs with increasing masses below  $M_{Ch}$ . This typically corresponds to a white dwarf slowly accreting matter from a companion (a red supergiant for example). As the mass of the white dwarf increases, its radius decreases (eq. 309) and thus the density increases. When  $\rho$  reaches values of about 2 tons/cm<sup>3</sup> (see eq. 145), the electron gas becomes relativistic. This occurs when

the mass approaches the Chandrasekhar's limiting mass  $M_{Ch}$ . Because the electrons saturate to the speed of light, the star encounters more and more difficulties to sustain its weight and the radius decreases quickly :  $R \rightarrow 0$  and  $dR/dM \rightarrow -\infty$  as  $M \rightarrow M_{Ch}$  ( $n \rightarrow 3$ ). What follows is extremely violent (as always when the Chandrasekhar's limiting mass is reached!). Due to the huge densities, carbon burning starts near the core. As we will see later, nuclear burning cannot be controlled in a degenerated gas. Within a few seconds, carbon and oxygen are transformed into nickel, with a huge production of energy. This energy is larger than the binding energy of the star ( $\int_0^M Gm dm/r$ ) and the star explodes as a huge thermonuclear bomb. This phenomenon is called a **type Ia Supernova**.

## 7.6 Potential energy of a polytrope

The gravitational potential energy of a sphere in hydrostatic equilibrium is

$$E_G = - \int_0^M \frac{Gm}{r} dm. \quad (310)$$

$-E_G$  is its binding energy, the work required to separate each mass element of the star to an infinite distance from each other. For a polytrope of index  $n < 5$ , mass  $M$  and radius  $R$ , it can be shown that this relation simplifies to :

$$E_g = - \frac{3}{5-n} \frac{GM^2}{R}. \quad (311)$$

This relation does not apply to infinite radius polytropic spheres ( $n \geq 5$ ). As we will see later, it is useful to determine the potential energy of a truncated isothermal sphere. First, it is easy to see that the potential energy of the truncated *singular* isothermal sphere of mass  $M$  and radius  $R$  is :

$$E_g = - \frac{GM^2}{R}. \quad (312)$$

The potential energy of the truncated *regular* isothermal sphere of mass  $M$  and radius  $R$  is :

$$E_g = -q(z_s) \frac{GM^2}{R}, \quad (313)$$

where  $\lim_{z \rightarrow \infty} q(z) = 1$  and  $z_s = AR = (4\pi G \rho_c \mu m_u / (kT))^{1/2} R$ .

# Stellar Evolution

In this second part, we analyse in detail how stars evolve as a function of time. The Virial theorem as well as homologous relations will be very useful. We begin by establishing them.

## 8 Theorems and useful relations

### 8.1 Virial theorem

Consider a gaseous sphere in hydrostatic equilibrium. We start from the equation of hydrostatic equilibrium  $dP/dm = -Gm/(4\pi r^4)$ , we multiply both sides by  $4\pi r^3$  and integrate over the mass. Integrating by parts the left hand side and using  $dm/dr = 4\pi r^2\rho$  gives :

$$\begin{aligned}\int_0^m 4\pi r^3 \frac{dP}{dm} dm &= 4\pi r^3 P(m) - \int_0^m 12\pi r^2 \frac{dr}{dm} P dm \\ &= 4\pi r^3 P(m) - 3 \int_0^m \frac{P}{\rho} dm \\ &= - \int_0^m \frac{Gm}{r} dm.\end{aligned}\tag{314}$$

Extending the integration domain over the whole star and assuming that the surface pressure is negligible gives :

$$3 \int_0^M \frac{P}{\rho} dm = \int_0^M \frac{Gm}{r} dm.\tag{315}$$

For a monoatomic non-relativistic ideal gas, we have :

$$\frac{P}{\rho} = \frac{2}{3} u.\tag{316}$$

This relation is easily deduced from the pressure integral established in the first part (sect. 4.3, eq. 120). As long as  $v \ll c$ , the kinetic energy of a particle with momentum  $p$  and speed  $v$  is  $E = vp/2$ . The pressure integral reads thus :

$$P = \frac{2}{3} \int_0^\infty E n(E) dE = \frac{2}{3} u_v = \frac{2}{3} \rho u,\tag{317}$$

where  $n(E)$  is the density of particles per unit volume and energy and  $u_v$  is the internal energy per unit volume. Note that the possible degeneracy of the gas does not affect the validity of eq. 316. On the opposite, if the radiation pressure is non negligible compared to the gas pressure, eq. 316 is no longer valid (the energy of a

photon is  $E = h\nu = cp$ , not  $cp/2!$ ). We find thus for a sphere of monoatomic, ideal, non-relativistic gas in hydrostatic equilibrium :

$$E_G = -2 E_i , \quad (318)$$

where  $E_G = -\int_0^M Gm dm/r$  is the gravitational potential energy of the whole star and  $E_i = \int_0^M u dm$  is its total internal energy (the sum of the kinetic energies of all particles of the star). Suppose now that a star has contracted, releasing the potential energy  $-\Delta E_g$ . Eq. 318 gives :  $\Delta E_i = -(1/2)\Delta E_G$ . In other words :

**During the contraction of a star maintaining the hydrostatic equilibrium, half of the released potential energy is converted into an increase of the internal energy.**

## 8.2 Homologous relations

Although approximate, homologous relations are a good tool for the understanding of the main tendencies in stellar evolution. Stellar models are called “homologous” under the following condition. For each model and each local physical quantity (noted  $y$ ), we can write

$$y(r) = yy(x) f_y(M, R) , \quad (319)$$

where  $x = r/R$  and  $yy(x)$  remains the same function from a model to another one. In other words, the profile from the center to the surface of a given physical quantity is the same from a model to another one, except for a multiplicative factor. Under this condition of homology, the functions  $f_y(M, R)$  can be obtained. We start with the function  $m(r)$ . We have simply :

$$m(r) = mm(x)M. \quad (320)$$

From the relation  $\rho = (dm/dr)/(4\pi r^2)$  and using eq. (320), we simply find :

$$\rho(r) = \frac{1}{4\pi x^2} \frac{dmm}{dx} M/R^3 = \rho\rho(x) \frac{M}{R^3}. \quad (321)$$

For the pressure, from the integrated equation of hydrostatic equilibrium and using equations (320) and (321), we get :

$$P(r) = \int_r^R \frac{Gm\rho}{r^2} dr = \int_x^1 \frac{Gmm(x)\rho\rho(x)}{x^2} dx M^2/R^4 = PP(x) \frac{M^2}{R^4}. \quad (322)$$

To get the temperature, we assume here that the gas is ideal, non-degenerated and without radiation. We also assume the homologous relation for the mean molecular weight :  $\mu(r) = \mu\mu(x)\mu$ . However,  $\mu\mu(x)$  is usually very different for two models at

different evolution stages, so that the dependence with respect to  $\mu$  in homologous relations is only indicative. We find then :

$$T(r) = \frac{m_u}{k} \frac{\mu(r)P(r)}{\rho(r)} = TT(x) \frac{\mu M}{R}, \quad (323)$$

Finally, we want to know the luminosity in a radiative zone. I remind the equation of radiation transport in stellar interiors (eq. 39) :

$$L = -\frac{16\pi r^2 ac T^3}{3\kappa\rho} \frac{dT}{dr}. \quad (324)$$

The main factors in eq. 324 are deduced from the above equations. The only one requiring a closer look is the temperature gradient :

$$\frac{dT}{dr}(r) = \frac{dT}{dx}(x) \frac{\mu M}{R^2}. \quad (325)$$

We have thus :

$$L(r) = -\frac{16\pi ac}{3\kappa_0} \frac{x^2 TT(x)^3}{\rho\rho(x)} \frac{dT}{dx}(x) (\mu^4/\kappa) M^3 \propto (\mu^4/\kappa) M^3. \quad (326)$$

We assume now a power law for the opacity :  $\kappa = \kappa_0 \rho^b T^a$ . This gives :

$$L(r) = LL(x) \mu^{4-a} M^{3-a-b} R^{a+3b} = LL(x) \mu^{7.5} M^{5.5} R^{-0.5}, \quad (327)$$

where we used a Kramers law ( $a = -3.5$ ,  $b = 1$ ) for the last equality. We note the rapid growth of the luminosity with the mass, this is the **mass-luminosity relation**. We will come back to it several times in the next chapters. As we said above, the dependence with respect to  $\mu$  in homologous relations is only indicative. It explains why the luminosity of a star increases as it evolves during the main sequence phase.

## 9 Proto-stellar phase : gravitational collapse

The disk of our galaxy and other spiral galaxies is mainly composed of large gaseous regions and stars. Its chemical evolution is due to the exchanges between these two components. On the one hand, parts of interstellar clouds can collapse, leading to stellar formation. On the other hand, stars enrich the interstellar medium with heavy elements synthesized in their core during advanced stages of evolution through winds and when some of them explode as a supernova. I begin with a reminder of the 3 types interstellar clouds.

## 9.1 Interstellar clouds

### Molecular clouds

As indicated by their name, they are mainly composed of hydrogen molecules ( $H_2$ ). Their temperatures typically are around 10-15 K, which is not much larger than the cosmological background (3 K); they are the coldest clouds. The number densities are of the order of  $10^{10}$  molecules /  $m^3$ . The hydrogen atoms of a cold and denser gas combine to form molecules. Molecular and atomic clouds are thus closely linked : due to local contractions and cooling, parts of atomic clouds can become molecular clouds. To complete their identity card, their masses are of the order of  $10^4$ - $10^5 M_\odot$  and their sizes are in the range 1-50 pc typically. **Stars form from these molecular clouds.** Their study is thus essential for understanding the process of stellar formation. As a consequence of their very low temperatures, their thermal radiation flux is negligible (Stefan law) and in the radio domain (Wien law). Moreover,  $H_2$  does not have observable lines in this domain, which is an obstacle to their direct characterization. To map them ; we can mainly use the radio emission at  $\lambda=2.6$  cm of the  $CO$  molecule. Some molecular clouds are however observable in the visible thanks to their illumination by massive very luminous stars formed from them (see e.g. the wonderful images of the aquila nebula, ...). Isolated parts of molecular clouds, the **Bok globules** can also be detected thanks to the occultation of the stars behind them.

### Atomic clouds : HI regions

As indicated by their name, they are mainly composed of atomic hydrogen. They are slightly hotter and less dense than the molecular clouds :  $T \approx 30 - 80$  K,  $10^7 - 10^9$  particles /  $m^3$ . They are the main contributors in mass to the interstellar medium. However, they are particularly difficult to detect : too cold for thermal radiation and not dense enough for occultation. The **hyperfine line at 21 cm** corresponding to the spin change of the electron at the fundamental level of an hydrogen atom constitutes the main observational source to characterize and map them.

### Ionized clouds : HII regions

As indicated by their name, they are mainly composed of ionized hydrogen, in other words free protons and electrons, constituting what is called a **plasma**. As in all plasmas, their temperatures are very high, of the order of 8000 K. On the opposite, their densities are extremely low :  $10^2 - 10^6$  particles /  $m^3$ ,  $\approx 10^{-25}$  times the air ! These regions are the product of the interaction between the interstellar medium and the energetic radiation from nearby massive and very luminous O-B stars. This radiation heats the gas up to high temperature, ionizes the atoms and/or bring their electrons to higher bound levels. As the electrons come back to the lower levels, photons are emitted, producing emission lines in the visible.

## 9.2 Gravitational instability, isothermal collapse and fragmentation

Clouds in the sky don't collapse because their auto-gravity, the gravitational attraction between each part, is completely negligible because of their very small masses. Any attempt to destabilize them produces a pressure gradient opposed to the collapse. On the opposite, molecular clouds and Bok globules are extremely large. Because of their very high masses and auto-gravity, they are in a precarious equilibrium. This can be quantified through a well-known criterion called the Jeans criterion.

### 9.2.1 Jeans criterion

We have seen that the main difference between a cloud in our sky and another in our galaxy is the size and the mass. The Jeans criterion gives the order of magnitude of the limiting sizes and masses beyond which a cloud is unstable due to its too high auto-gravity.

#### Size criterion :

A cloud with a size  $R$  significantly larger than the Jeans size  $R_J$  is gravitationally unstable, with

$$R_J = \left( \frac{27}{16q_2\pi G \langle \rho \rangle} \right)^{1/2} v_s \approx \tau_{ff} v_s \quad (328)$$

$\langle \rho \rangle$  is its mean density,  $v_s^2 = \partial P / \partial \rho|_T \simeq P / \rho = kT / (\mu m_u)$  is the square of the isothermal sound speed,  $\tau_{ff} = \sqrt{\pi / (G \langle \rho \rangle)}$  is the free-fall time-scale, of the order of the dynamical time-scale and  $q_2 \simeq 1$  is a parameter (see below).

#### Mass criterion :

A molecular cloud with a mass  $M$  significantly larger than the Jeans mass  $M_J$  is gravitationally unstable, with

$$M_J = \frac{27}{16} \left( \frac{3}{\pi q_2^3} \right)^{1/2} \left( \frac{k}{\mu m_u G} \right)^{3/2} T^{3/2} \langle \rho \rangle^{-1/2} . \quad (329)$$

The typical initial condition of a molecular cloud gives  $M_J \approx 400 M_\odot$ .

Different ways to establish this criterion have been proposed in the literature, the results differ by a factor of the order of unity. I only present here the most realistic proof. We approximate the cloud by an isothermal sphere in hydrostatic equilibrium. The surface pressure is always strictly larger than zero (remind that the pressure of an isothermal sphere tends towards 0 at an infinite radius, see Sect.7). The Virial theorem (eq. 314) gives the value of this pressure :

$$P_S = \left[ 3 \int_0^M \frac{P}{\rho} dm - \int_0^M \frac{Gm}{r} dm \right] / (4\pi R^3)$$

$$= \frac{c_v T M}{2\pi R^3} - q \frac{GM^2}{4\pi R^4}, \quad (330)$$

where we assumed that the gas is ideal with a constant temperature. We have shown previously (eq. 312) that  $q = 1$  for the truncated singular isothermal sphere. In the regular case,  $q$  is a function of  $z_s$  (see end of Sect. 7.6).

Consider now a contraction of the sphere (produced by increasing slightly the external pressure). Assuming that the hydrostatic equilibrium is maintained, eq. 330 remains valid. We assume that the mass and temperature are fixed during this contraction. Eq. 330 explicitly shows how the surface pressure changes as  $R$  decreases. It is easily seen that the function  $P_S(R)$  has a local maximum at

$$R_{max} = \frac{4q_2}{9} \frac{\mu m_u}{k} \frac{GM}{T}, \quad (331)$$

where  $q_2 = 1$  for the singular case and  $q_2 = q(1 - (1/4)\partial \ln q / \partial \ln R|_{M,T})$  for the regular case. Let the radius  $R$  be larger than  $R_J$ . Replacing  $\langle \rho \rangle$  by  $3M/(4\pi R^3)$  in the definition of  $R_J$  (eq. 328) and isolating  $R$  in the inequality  $R > R_J$  gives  $R < R_{max}$ . Eq. 330 tells us that  $dP_S/dR > 0$  at this  $R$ . The contraction leads thus to a decrease of the surface pressure. As we initially increased the external pressure  $P_{ext}$ , we get  $P_{ext} > P_S$  and the star contracts even more. This corresponds to an unstable equilibrium. We find directly through the same reasoning that the equilibrium is stable for  $R < R_J$ . Finally, the mass criterion 329 is simply obtained by taking the power 3 of the radius criterion and multiplying by the mean density.

The main assumption for the establishment of the Jeans criterion was to consider an isothermal contraction of an isothermal cloud. It is important to justify now this hypothesis. The gravitational collapse is a dynamical process where the equilibrium of the forces is broken. The time-scale of this process is thus the dynamic time introduced in the first chapter (eq. 24) :

$$\tau_{dyn} = \sqrt{R^3/GM} \approx 1/\sqrt{G\rho}. \quad (332)$$

With the typical initial density of a molecular cloud, the time-scale of the gravitational collapse is  $1/\sqrt{G\rho} \approx 10^6$  years. We will introduce in Sect. 10.1.2, eq. 341 the Helmholtz-Kelvin time-scale  $\tau_{HK}$  associated to processes driven by a *thermal* disequilibrium. For the collapsing sphere with radius  $R_J$  and mass  $M_J$ ,  $\tau_{HK} \approx GM_J^2/(R_J L)$ . Taking  $L = 4\pi R_J^2 \sigma T^4$  and the typical initial mean density and temperature of the molecular cloud, we get  $\tau_{HK} \approx 100$  years, which is much smaller than the dynamic time. This means that the cloud has all the required time to maintain thermal equilibrium with its environment during its initial collapse. We conclude that the temperature is approximately constant during a first phase of the collapse. With a constant temperature and an increasing density, eq. 329 tells us that the Jeans mass decreases during the collapse. This explains the **cloud fragmentation** during the isothermal phase of the collapse.

As a summary, during a first phase, a part of the molecular cloud of  $10^2 - 10^3$  solar masses collapses, keeping a more or less constant temperature. During this phase, it fragments into several pieces : the future stars.

### 9.3 Adiabatic collapse

During the collapse,  $\tau_{dyn} \approx 1/\sqrt{G\rho}$  drops quickly as a consequence of the density increase. On the opposite, we find from equations 328, 329 and the Stefan law :

$$\tau_{HK} \propto T^{-5/2} \rho^{1/2}. \quad (333)$$

The thermal time-scale increases thus as long as the temperature remains constant. At some point, both become of the same order of magnitude. Hence, the collapse can no longer be isothermal. When the thermal time-scale is significantly larger than the dynamic one, the radiated energy is significantly lower than the released potential energy. The cloud enters in a phase of **adiabatic collapse**. Therefore, its temperature increases and the Jeans mass no longer decreases (Eq. 333). **Fragmentation stops**. Equalizing equations 332 and 333, we find  $\rho = k_1 T^{5/2}$ . Using equation 329 and replacing the constants by their numerical values, we find for the mass at the end of the isothermal fragmentation process :

$$M > M_J \approx 0.018 T^{1/4} M_\odot. \quad (334)$$

With  $T \approx 10$  K, this gives for the smallest fragments :  $M \approx 0.03 M_\odot$ . Smaller mass objects like planets are thus not formed by this process.

For a diatomic gas (5 degrees of freedom), adiabatic increases of temperature and pressure are related by  $P/P_0 = (\rho/\rho_0)^\gamma = (\rho/\rho_0)^{7/5}$ ,  $T/T_0 = (\rho/\rho_0)^{\gamma-1} = (\rho/\rho_0)^{2/5}$ . The increase of the pressure finally goes over the weight of the gas column and a sharp braking follows. In the central regions where the collapse speed is subsonic, **the hydrostatic equilibrium** is quickly established. On the opposite, the collapse is supersonic in the external layers. The sharp braking leads thus to the formation of a **first shock wave** at the sonic point where the sound and collapse speed are equal.

When the core temperature reaches values of the order of  $T \approx 2000$  K, **the hydrogen molecules dissociate** and, at  $T \approx 3000$  K, **hydrogen atoms are ionized**. These two reactions are endothermic. A significant part of the released potential energy is pumped by these reactions. As a consequence, the temperature and pressure increase less. More quantitatively, the adiabatic exponent  $\Gamma_1 \equiv \partial \ln P / \partial \ln \rho|_s$  goes below the critical value of 4/3. We will see in Sect. ?? that this characterizes dynamic instability : the pressure increases less than the weight of the gas column and a **second collapse of the core starts**. Once all the hydrogen is ionized in the core, the reactions stop and  $\Gamma_1$  goes back up to 5/3 (monoatomic gas, 3 degrees

of freedom). Therefore, the second collapse stops in the core and a **second shock wave** forms at the interface between the fully ionized core and the partially ionized layers above it.

It is good to notice that the density contrast between the core in hydrostatic equilibrium and the external layers of the collapsing envelope is huge. The dynamic time in the core is thus much shorter than in the envelope. Hence, as the core reaches this stage, the external envelope has not contracted significantly yet and is still on the isothermal collapse phase, evolving over a much longer time-scale.

## 9.4 Accretion disk

All bodies have some angular momentum. In molecular clouds, the specific (per unit mass) angular momentum is huge :  $j \approx 10^{21-22} \text{ cm}^{-2}\text{s}^{-1}$ . The centrifugal force is also significant compared to gravity. As a consequence, an accretion disk forms where the resultant of both forces is zero, which is only possible on the equatorial plane. Matter spirals from the accretion disks and falls on the proto-star. It is eaten by the star around the poles where gravity overcomes the centrifugal force. Since the provision of angular momentum from matter arriving at the poles is low, the specific angular momentum of the proto-star goes down and reaches values much smaller than those of the initial molecular cloud. As an example, in a **T Tauri star** (typical star in this phase), the specific angular momentum is of the order of  $j \approx 10^{16-17} \text{ cm}^{-2}\text{s}^{-1}$ ,  $10^5$  smaller than its initial value! It is said that **the accretion disk ensures the evacuation of angular momentum**. The loss of angular momentum is however a complex process. During binaries formations (around half of the stars form a binary system), tidal effects lead to a significant transfer of angular momentum from rotational to orbital motion. Moreover, the magnetic field, which is always present, acts against shear. It prevents thus the establishment of a too strong rotation frequency contrast between the star and its accretion disk, amplifying strongly the evacuation of angular momentum. It is said that **the magnetic fields couples the proto-star with its accretion disk**. The accretion disk appears during the phase of adiabatic collapse and can remain partly during the beginning of the Pre-Main Sequence phase we are going to describe now.

## 10 Pre-Main Sequence (PMS) : Contraction in hydrostatic equilibrium

The establishment of hydrostatic equilibrium marks the transition to a new phase in stellar evolution : the Pre-Main Sequence (PMS) phase. The hydrostatic equilibrium does not stop stellar contraction. It continues during the PMS phase, but much more slowly. As we will see, the driver of this contraction is no longer the forces imbalance, but thermal imbalance. At first, the core in hydrostatic equilibrium is completely hidden by the molecular cloud from which it formed. By definition, the effective temperature of an object is  $T_{eff} = (F/\sigma)^{1/4}$ , where  $F$  is the flux emitted by this object from its photosphere, that is its visible surface. The effective temperature is thus initially very low, of the order of the temperature of the surrounding cloud. Next, the surrounding gas dissipates, revealing the hotter star in hydrostatic equilibrium.

To facilitate the understanding of this phase, it is appropriate to consider first a star evolving with a constant mass. Next, we will discuss how the accretion of matter affects its evolution.

### 10.1 PMS evolution with constant mass

#### 10.1.1 The Hayashi tracks

Constant mass models predict that the star in hydrostatic equilibrium is initially entirely convective. This comes from the high opacity of stellar matter at low temperatures. This naturally leads to the definition of the Hayashi track. Consider the set of **fully convective stellar models with a given mass** (and chemical composition). Each of these models has a given location, a point, in the HR diagram. The whole set of models forms a curve in the HR diagram called the **Hayashi track of mass  $M$** . I now simplify the problem to get a simple mathematical view of the Hayashi track. Because convection is very efficient in almost the whole star, I assume that the entropy is constant from the centre to the surface of the star (in reality, this approximation is not justified near the surface where convection is less efficient).

The equations to solve to build such simple model are simply the equation of mass conservation (equation 90), the equation of hydrostatic equilibrium (eq. 92) and the equation associated to our hypothesis of constant entropy :

$$\frac{dT}{dm} = -\nabla_{ad} \frac{Gm}{4\pi r^4} \frac{T}{P}. \quad (335)$$

The equation of state relates  $\rho$  and  $\nabla_{ad}$  to the temperature and pressure. This gives a system of 3 differential equations with three unknowns :  $r$ ,  $P$  and  $T$ <sup>5</sup>. 3 boundary

---

<sup>5</sup>This problem is simplified even more if we assume that the gas is ideal, giving a polytropic sphere of index  $n = 3/2$  (see Sect. 7.2).

conditions are thus needed. At the centre, we have of course  $r(0) = 0$ . Defining the photosphere as the layer where the local temperature is equal to the effective temperature and  $R = r(M)$  its radius, we get :

$$T(M) = (L/(4\pi R^2\sigma))^{1/4}. \quad (336)$$

The last boundary condition is obtained by imposing a continuous match with atmosphere models (see Sect. 3.9 for more detail). Note that equation 336 introduced a new variable in the problem : the luminosity  $L$ . For each  $L$ , the mathematical problem has a distinct solution. Letting  $L$  vary, we get the Hayashi track of mass  $M$  in the HR diagram.

It is important to notice that we did not assume thermal equilibrium in our definition. The fully convective stars constituting the Hayashi tracks are usually **not in thermal equilibrium**. This is completely different from the main-sequence. As we will see, the latter characterizes models with different masses in thermal equilibrium.

The Hayashi tracks of different masses are close quasi-vertical curves occupying the cold (right) side of the HR diagram. They separate two distinct regions of the HR diagram : an allowed zone on the hot (left) side and a forbidden zone on the cold (right) side. This is easily seen by considering the above mathematical problem, but for another fixed value of  $\nabla = d \ln T / d \ln P$  different from  $\nabla_{ad}$ . For an ideal gas, the solution is a polytrope of index  $n = 1/\nabla - 1$ . It can be shown that these models occupy a line quasi-parallel to the Hayashi track of same mass, located on its hot (left) side for  $\nabla < \nabla_{ad}$  and on the cold (right) side for  $\nabla > \nabla_{ad}$ . Since convection is very efficient, stellar models with  $\nabla$  significantly larger than  $\nabla_{ad}$  in a significant part of the star are unrealistic. With such temperature gradient, the transport of energy by convection would be by far too large and incompatible with the boundary condition eq. 336. On the opposite, we know that  $\nabla < \nabla_{ad}$  in radiative zones. Models on the hot (left) side of the Hayashi track are thus fully acceptable, corresponding to fully or partly radiative stars.

### 10.1.2 Descent along the Hayashi track of a fully convective star

During this phase of evolution, the star is in hydrostatic equilibrium but not yet in thermal equilibrium. More precisely, some nuclear reaction such as deuterium and lithium burning (eqs. 206 and 213) can already occur in low mass stars, but the power generated by them is smaller than the luminosity :  $\int_M \epsilon dm < L$ . The thermal imbalance is the driver of stellar evolution at this stage, which is easily quantified by the Virial theorem. We have shown in Sect. 8.1 that  $E_i = -(1/2)E_G$ . Derivating this relation gives simply :

$$dE_i/dt = -(1/2)dE_G/dt. \quad (337)$$

Moreover, the conservation of energy law applied to the full star gives :

$$dE_{tot}/dt = \int_M \epsilon dm - L. \quad (338)$$

With  $E_{tot} = E_i + E_G$ , these two equations give :

$$L - \int_M \epsilon dm = dE_i/dt = -(1/2)dE_G/dt. \quad (339)$$

As said above,  $L - \int_M \epsilon dm > 0$  during this phase. We have thus  $dE_G/dt < 0$  : **the star contracts as a consequence of the thermal imbalance** and  $dE_i/dt > 0$  : **its internal energy increases**. If there are no nuclear reactions ( $\epsilon = 0$ ), equation 339 tells us what are the shares of the cake :

**Half of the released potential energy is converted into internal energy and the other half is radiated by the star.**

As long as it is entirely convective, **the star must thus go down along the Hayashi track** corresponding to its mass.

The time-scale of this phase of thermal imbalance is easily evaluated :

$$\tau \approx \frac{\Delta E_G}{dE_G/dt} \approx \frac{GM^2}{RL}, \quad (340)$$

where we used  $-\Delta E_G \approx GM^2/R$  for the order of magnitude of the released potential energy and, from eq. 339,  $-dE_G/dt \approx L$ . This is the **Helmholtz-Kelvin time** :

$$\tau_{HK} \equiv \frac{GM^2}{RL}. \quad (341)$$

The present Helmholtz-Kelvin time of our Sun is  $\tau_{HK} \simeq 3.1 \times 10^7$  years. As long as the electron gas is non-degenerated<sup>6</sup>, the increase of the internal energy leads to an increase of the temperature (for an ideal gas,  $u = c_v T$ ). We gave in Sect. 5, eqs. 153 and 154, the approximate kramers laws for the opacity. Their dependence in  $T^{-3.5}$  shows that the opacity decreases in the core of the star during this phase. We established in Sect. 3.6, eq. 60 the Schwarzschild criterion for convective instability :  $\nabla_{rad} > \nabla_{ad}$ , with  $\nabla_{rad} \propto \kappa$  (eq. 59). As the opacity decreases, it finally goes below the adiabatic gradient and **the core of the star becomes radiative**. This marks the end of the descent along the Hayashi track.

---

<sup>6</sup>We come back later on the key question of degeneracy

### 10.1.3 Evolution along the Henyey track of a partly radiative star

We have seen that partly radiative stars with a mean temperature gradient below the adiabatic one are located on the hot (left) side of the Hayashi track. As a significant part of the core becomes radiative, the stellar evolution track turns thus towards the hot (left) side of the HR diagram. During this turn, the luminosity reaches a minimum and next increases. This minimum luminosity significantly increases with the mass of the star. To interpret this, I simplify the problem by assuming that the stars at the minimum are homologous. The mass-luminosity relation 327 tells us how the luminosities compare in the radiative core. Extending the homology to the convective envelope, the luminosity ratio between the surface and the core is constant and the relation 327 also applies for the surface luminosity. We can eliminate the radius by using  $L = 4\pi R^2 \sigma T_{eff}^4$ , which gives :

$$L_{min} \propto M^{5.5} R^{-0.5} \propto M^{5.5} L^{-1/4} T_{eff}. \quad (342)$$

The effective temperatures of stars on their Hayashi tracks are close, which finally gives :

$$L_{min} \propto M^{4.4}.$$

We see the great sensitivity of  $L_{min}$  with respect to the mass.

When the core becomes radiative, the contraction is accelerated in the core and the opposite in the envelope. The thermal imbalance at the origin of the contraction explains that. The equation of energy conservation gives at this stage  $Tds/dt = \epsilon - dL/dm < 0$ .

- 1) As long as the star is entirely convective, the entropy profile is quasi-constant from the center to the near surface layers (see Sect. 3.6.9) and decreases as a function of time.
- 2) When the core becomes radiative, a positive entropy gradient  $ds/dr > 0$  appears there (Sect. 3.6.9). At the same time, the entropy plateau does not decrease significantly. By continuity, this means a quick decrease of the core entropy and thus an acceleration of the core contraction. In other words, the drop in core opacity increases the evacuation of energy by radiation, which strengthens the thermal imbalance in the core and accelerates its contraction. While the core contracts quickly, the envelope doesn't move significantly and the total radius stops to decrease. As for the luminosity, it reincreases slightly because of the more efficient evacuation of energy from the core.

After the turn in the HR diagram, the evolution track is characterized by a more or less constant luminosity and increasing effective temperature, this part of the evolution track is often called the Henyey track.

## 10.2 Evolution with mass accretion : the birthline

In our study of the pre-main sequence phase, we neglected until now accretion. However, it does not stop sharply when the cloud dissipates and the proto-star appears. Because of the absence of precise observational constraints, the mass accretion is usually modeled by a constant rate  $dM/dt$ . We define the **birthline** as the track in the HR diagram followed by a star in hydrostatic equilibrium accreting mass at a constant rate. Different accretion rates give different birthlines. On the contrary, the birthline is quasi-insensitive to the initial mass. The birthline is characterized by increasing effective temperature and luminosity. The radius evolution is affected by deuterium burning, as will be discussed later. The modeling of the evolution of a star with given final mass is a two step process. During step 1, a constant accretion rate is adopted and the star moves along the birthline corresponding to this rate until it reaches the desired mass. Next, the modeling is carried on with constant mass and its track is as we discussed in the previous sections. Let's assume a typical accretion rate of  $10^{-5}M_{\odot}/\text{year}$  for a population I star. If the mass at the end of the accretion phase is below  $\approx 2.5M_{\odot}$ , the star is entirely convective at this time. In the HR diagram, it is thus at the intersection between the birthline and the Hayashi track corresponding to its mass and next go down along it. On the contrary, for  $2.5M_{\odot} < M < 6M_{\odot}$ , the star already has a radiative core when the accretion stops and next follows its path along the Henyey track corresponding to its mass. For more massive stars, nuclear burning starts and a convective core appears while the star is still accreting matter.

## 10.3 First nuclear reactions

### 10.3.1 Nuclear reactions : yes or no ?

As we have seen, the main challenge for nuclear reactions is the crossing of the Coulomb barrier. This crossing is only possible if the nuclei have high enough kinetic energies, in other words if the temperature is high enough. For efficient hydrogen burning through the p-p chain, temperatures of about  $10 - 15 \cdot 10^6$  K are required. This naturally leads us to study the evolution of the core temperature during the pre-main sequence phase. The Virial theorem showed us that the thermal imbalance before the starting of nuclear reactions leads to a contraction of the star. And this contraction leads to an increase of the internal energy. This leads us to a key question of this section : does this increase of internal energy always leads to an increase of the temperature ? For an ideal non-degenerated gas,  $u = c_v T$  and the answer is yes. But is thus always the case out of this ideal case ? To answer this question, we consider a homologous infinitesimal contraction of a gaseous sphere. Eqs. 321 and 322 give,

with a constant mass :

$$\frac{d\rho}{\rho} = -3 \frac{dR}{R}, \quad (343)$$

$$\frac{dP}{P} = -4 \frac{dR}{R} = \frac{4}{3} \frac{d\rho}{\rho}. \quad (344)$$

The thermodynamic quantities obey to an equation of state. For a given chemical composition, it allows us to express  $\rho$  as a function of  $P$  and  $T$ . Differentiating this function gives :

$$\frac{d\rho}{\rho} = \alpha \frac{dP}{P} - \delta \frac{dT}{T} \quad (345)$$

$$\Rightarrow \frac{dT}{T} = \frac{\alpha}{\delta} \frac{dP}{P} - \frac{1}{\delta} \frac{d\rho}{\rho}, \quad (346)$$

where we have introduced the notations  $\alpha \equiv \partial \ln \rho / \partial \ln P$  and  $\delta \equiv -\partial \ln \rho / \partial \ln T$ . Eliminating  $dP/P$  with eq. 344, we finally get :

$$\frac{dT}{T} = \frac{4\alpha - 3}{3\delta} \frac{d\rho}{\rho}. \quad (347)$$

This equation answers to our question : since the density must necessarily increase, the temperature increases if  $\alpha > 3/4$  and decreases if  $\alpha < 3/4$ .

A first important limiting case is an ideal non-degenerated gas, for which we have  $\alpha = \delta = 1$  ( $\rho \propto P/T$ ) and thus  $dT/T = (1/3)d\rho/\rho$ . As we already found, the temperature must increase in this case.

On the opposite, for a completely degenerated non-relativistic gas, differentiating the polytropic relation  $P = K\rho^{5/3}$  gives  $\alpha = 3/5$ ,  $\delta = 0$  and thus  $dT/T \rightarrow -\infty d\rho/\rho$ . A small contraction leads thus to a very large drop of the temperature, even though the internal energy increases! This surprising result is important and deserves examination. In a degenerated electron gas, all "boxes" of low energy are occupied by electrons. Yet, the contraction decreases the number of cases in the phase space. The electrons deprived of place must go to another free one at much higher energy. This energetical cost is very high, larger than the increase of total internal energy due to the contraction. Where can this energy be found? The reservoir of internal energy can be splitted in 2 main contributions : the kinetic energy of the electrons and of the ions. Moreover, there is no obstacle to a decrease of the ions kinetic energy because they are non-degenerated. We see thus the solution found by nature : the missing energy for the electrons is drawn from the ions' thermal reservoir. The contraction of a sphere of degenerated electrons leads thus to a decrease of the ions' kinetic energy. Since the ions are non-degenerated, the mean kinetic energy of an ion is  $3/2 kT$ . The temperature must thus decrease. With the increase of the electrons' kinetic energy and the drop of the ions' kinetic energy, equipartition of energy (as it is in usual

gases) is thus completely broken, the mean kinetic energy of an electron becomes more and more larger than  $3/2 kT$ .

We follow now the core conditions in a diagram  $\log \rho - \log T$  for stars with different masses (see the powerpoint slides). Based on the degeneracy criterion ??, we can separate this diagram in 2 regions : one at high temperature and relatively low density where the gas is non-degenerated and the other at relatively low temperature and very high density where the electron gas is degenerated. During the beginning of the pre-main sequence phase, the electron gas is always non-degenerated due to the low densities. At fixed core density, the core temperature increases with the mass of the star. This is clearly seen by combining the homologous relations 321 and 323 :

$$T_c = TT(0) \frac{M}{R} = TT(0) \frac{M^{1/3}}{R} M^{2/3} \quad (348)$$

$$= TT(0) \left( \frac{\rho_c}{\rho \rho(0)} \right)^{1/3} M^{2/3}. \quad (349)$$

More simply, at fixed density, the weight of the gas column and thus the temperature increases with the mass.

We follow now the track of a star in the  $\log \rho - \log T$  diagram. We start from the left (low density) with a high temperature much above the degeneracy limit. The temperature increases as the stellar core contracts ( $dT/T = (1/3)d\rho/\rho$ ) and can reach the value required for nuclear reactions. On the opposite, for a low mass star, the degeneracy limit is early crossed. Therefore, the core temperature reaches a maximum and next drops for the reasons explained above. The nuclear reactions requiring a temperature above this limit can never start. The critical reaction at the current evolution stage is the fusion of 2 protons to form a deuterium nucleus. It requires temperatures of about  $10^7$  K.

A rigorous modelling of stellar evolution during the pre-main sequence phase shows that *if the mass of the proto-star is lower than  $0.08 M_\odot$ , the degeneracy prevents the temperature from reaching the temperature required for the onset of the p-p reaction. Such stars are called **brown dwarfs**.*

### 10.3.2 Cooling of brown and white dwarfs

What happens to them ? After the burning of minority elements like deuterium and lithium if the required temperatures can be reached ( $T \approx 1-2 \times 10^6$  K for deuterium,  $T \approx 2.5 \times 10^6$  K for lithium), the electron degeneracy appears and the temperature drops, making any new nuclear reaction impossible. Homologous relations help to clarify the shares of the energetical cake during this cooling. We assume that the ion gas is ideal and the electron gas is completely degenerated and non-relativistic in what follows. We first estimate the increase of the degenerated electrons' kinetic

energy due to an infinitesimal contraction. Noting  $E_e$  this energy, we deduce from eqs. 316 and 136 :

$$E_e = \frac{3}{2} \int_0^M \frac{P_e}{\rho} dm = \frac{3}{2} K_1 \int_0^M \rho^{2/3} dm$$

For a homologous contraction, this gives :

$$\frac{dE_e}{E_e} = \frac{2}{3} \frac{d\rho}{\rho}.$$

Under the same hypothesis, we have for the potential energy  $E_g = -\int_0^M Gm dm/r$  :

$$\frac{dE_g}{E_g} = -\frac{dr}{r} = \frac{1}{3} \frac{d\rho}{\rho},$$

and thus by combining these 2 equations :

$$\frac{dE_e}{E_e} = 2 \frac{dE_g}{E_g}.$$

Assuming moreover that the electrons' kinetic energy is much larger than the ions' one ( $E_e \gg E_i$ ) and using the Virial theorem,  $E_g = -2(E_i + E_e)$ , we get :

$$dE_e = -\frac{E_e}{E_i + E_e} dE_g \simeq -dE_g.$$

This last result tells us that, during the contraction, **the whole released potential energy is transferred to the electrons**. Therefore, by energy conservation, **the whole radiated energy is taken from the ions** :  $L = -dE_i/dt$ . This illustrates the decoupling between ions and electrons when the electron gas becomes highly degenerated.

### 10.3.3 Structural effects of the onset of nuclear reactions

The onset of nuclear reactions modifies the energetical balance by providing heat in the core of the star. How does the star react to this change ?

#### Gravothermal specific heat

First, we examine how the temperature reacts to this heat input. The first principle of thermodynamics gives :

$$dq = Tds = du + Pdv = c_v dT + (\partial u / \partial \rho|_T - P/\rho^2) d\rho. \quad (350)$$

Introducing the notation  $\Gamma_3 - 1 = \partial \ln T / \partial \ln \rho|_s$ , we find thus for the differential of the equation of state  $T = T(\rho, s)$  :

$$\frac{dT}{T} = \frac{ds}{c_v} + (\Gamma_3 - 1) \frac{d\rho}{\rho}. \quad (351)$$

We get thus :

$$dq = c_v dT - c_v T (\Gamma_3 - 1) d\rho/\rho. \quad (352)$$

Once again, we approximate the stellar reaction to the heat input by a homologous contraction or expansion. Since the Helmholtz-Kelvin time is much larger than the dynamical time, we can assume that the hydrostatic equilibrium is maintained : the driver of the structural changes is the thermal imbalance, not the dynamical imbalance. With these 2 hypotheses, we can now use the eq. 347, which gives :

$$\begin{aligned} dq &= c_v dT - c_v T (\Gamma_3 - 1) d\rho/\rho \\ &= c_v T \left( \frac{4\alpha - 3}{3\delta} - (\Gamma_3 - 1) \right) \frac{d\rho}{\rho} \\ &= c_v \left( 1 - \frac{3\delta(\Gamma_3 - 1)}{4\alpha - 3} \right) dT = c^* dT, \end{aligned} \quad (353)$$

where  $c^*$  is called “the gravothermal specific heat”. We examine now the two already encountered limiting cases of an usual monoatomic ideal gas and a completely degenerated gas.

### Ideal non-degenerated gas

For an ideal gas,  $\alpha = \delta = 1$  and  $\Gamma_3 - 1 = 2/3$ . Eq. 353 gives thus :

$$dq = -c_v dT, \quad (354)$$

an unexpected result, **providing heat to the star leads to a decrease of its temperature!** How can we understand that ? When heat is provided to a gas at rest it always expands (if it can). The weight of the gas column is huge inside the star, the resulting expansion work is thus very large, larger than the provided heat. Since the provided heat is not sufficient for the work, the missing energy is taken from the internal energy réservoir, which leads to a decrease of the temperature. More quantitatively, for an ideal gas and a homologous expansion maintaining the hydrostatic equilibrium, the expansion work is twice the provided heat :  $Pdv = 2dq$ . From  $dq = du + Pdv$ , we get thus also  $du = -dq$ . A very similar result can be found without the use of the homologous approximation.  $dQ/dt = \int_M \epsilon dm - L$  is the net input of heat per unit time to the whole star (power provided by nuclear reactions minus radiated power). The Virial theorem (eq. 339), tells us that  $dE_G/dt = 2dQ/dt$  and  $dE_i/dt = -dQ/dt$ .

### Degenerated gas

Consider now the limiting case of a completely degenerated electrons gas. We have now  $\delta = 0$  and thus

$$dq = c_v dT. \quad (355)$$

This is the usual result for heat provided at constant volume. Why is the volume of a degenerated gas “frozen” ? Let’s try to compress a sphere in which the pressure of

degenerated electrons dominates. The number of available “boxes” in the phase space decreases. Since all states of small energy and momentum are already occupied, the electrons having lost their box, must occupy new boxes of much larger momentum. Hence, the electron pressure (the flux of momentum) increases a lot, more than the weight of the gas column. The resultant of the forces is thus towards the exterior and the star come back to its initial volume. Let’s try now to expand the sphere, the number of available “boxes” in the phase space increases. Electrons from the highest energy levels directly come to occupy these free places waiting for them. Hence, the electron pressure decreases a lot, more than the weight of the gas column. The weight wins and the star come back to its initial volume. We show this more rigorously in Sect. ?? (just replace  $\Gamma_1$  by  $5/3$  in this proof). You should keep in mind that **the volume of a sphere where electron degeneracy pressure dominates is frozen**. Any input of heat is thus at constant volume, with an increase of the temperature. This very different reaction of the star depending on degeneracy leads to the fact that the onset of nuclear reactions in the core of a star is unstable in degenerated medium and stable in non-degenerated medium, as detailed in Sect. ??.

### Structural readjustment

How does the structure of a star react in practice when the nuclear reactions start in its non-degenerated core? I start with the core. Before the onset of nuclear reactions, we know from the Virial theorem that the star globally contracts because of the thermal imbalance, so that the internal energy and thus the temperature increase (see Sect. 10.1.2. When the temperature reaches the required value, some nuclear reactions start. At some point, the power provided by nuclear reactions overwhelms the luminosity ( $\int_M \epsilon dm > L$ ). Due to this heat input, the core contraction stops and it starts to expand. First, the temperature temporarily continues to increase. But the part of the star in expansion increases and the corresponding work soon overwhelms the heat input. The missing energy is then taken from the internal energy reservoir and the core temperature decreases, as we found with homology. Hence, the nuclear reaction rates drop and the power provided by them goes back below the luminosity ( $\int_M \epsilon dm < L$ ). Due to this heat loss, the core expansion stops and it comes back to contraction. Consequently, the core temperature increases and thermal equilibrium is finally established :  $\int_M \epsilon dm = L$ . As illustrated in the powerpoint slides, this structural readjustment of the core takes the form of a loop in a core density-temperature diagram.

Interpreting the evolution of the stellar envelope when the nuclear reactions start is more complicate.

The structural readjustment of the central regions requires a significant amount of energy to produce the work and is characterized by a decrease of the mean temperature gradient. As a consequence, **the luminosity drops when the nuclear reactions start**. This counterintuitive result is found with all numerical simulations of this evolution stage. From  $L = 4\pi R^2 \sigma T_{eff}^4$ , we easily understand that this

luminosity drop stops the effective temperature increase and leads to a contraction of the envelope ( $R$  decreases). As we will see, **mirror effects** are always associated to nuclear reactions : when the core expands, the envelope contracts ; when the core contracts, the envelope expands.

### Starting of the CNO cycle

Above 1.5 solar masses (for a solar chemical composition), the CNO cycle is the dominating channel for the fusion of hydrogen into helium. We have seen in Sect. 6.6.2 that there are two regimes of this cycle : in the out of equilibrium regime the rates of the nuclear reactions are different ; in the equilibrium regime they are equal and carbon, nitrogen, ...act as catalysors for the fusion of hydrogen into helium. More precisely, the two fusion reactions from carbon to nitrogen (217 and 219) and to a lower extent those from oxygen (224 and 226) have a relatively high cross-section. On the opposite, the nitrogen-proton fusion reaction (220) has a much lower cross-section. Note also that after hydrogen and helium, oxygen ( $\approx 0.7$  % of the visible mass in our galaxy) and carbon ( $\approx 0.3$  % of the mass) are the most abundant elements of the universe. The first reactions providing a significant amount of heat are thus those transforming carbon and oxygen into nitrogen. As explained above, this heat input leads to the core expansion, envelope contraction and a drop of the luminosity. Moreover, the cross-sections of these reactions are extremely sensitive to the temperature ( $\epsilon \propto \langle \sigma v \rangle \propto T^{15}$  typically). These reaction act thus only in a small sphere in the stellar core (above it the temperatures are too low).  $\nabla_{rad} \propto L/m$  gets soon higher than the adiabatic gradient there, and according to the Schwarzschild criterion (eq. 60), **the core of the star becomes convective**. However, the amount of carbon and oxygen is hundred times smaller than hydrogen and they are soon fully transformed into nitrogen. The heat input from these reactions stops thus, the core becomes radiative again and contracts. From the Virial theorem, the internal energy and thus the temperature restart to increase, as well as the luminosity thanks to the important release of potential energy in the core. When the central temperature reaches values of about  $20 \times 10^6$  K,  ${}^1_7\text{N}$  fusion (220) starts and the CNO cycle enters in its equilibrium regime. The star readjust a second time its internal structure, which is observationally characterised by a small **2nd luminosity drop**. Finally, thermal equilibrium is established ( $\int_M \epsilon dm = L$ ) and the main-sequence phase starts.

## 11 The main-sequence phase

After the structural readjustment following the onset of nuclear reactions, a stable thermal equilibrium is established : globally the power provided by nuclear fusion reactions of hydrogen into helium is equal to the power radiated by the star ( $\int_M \epsilon dm = L$ ) and locally the equation of energy conservation reads  $dL/dm = \epsilon$ .

This is the main sequence phase. Since the star is in both hydrostatic and thermal equilibrium, there are no time derivatives in the structure equations (see Sect. 3.8). **The temporal evolution of the star has another origin : the modification of its internal chemical composition due to the nuclear reactions.** A new time-scale is associated to this evolution phase in thermal equilibrium : **the nuclear time.** We obtain it by dividing the total heat provided by nuclear reactions during the whole main sequence phase by the luminosity. We assume that approximately one tenth of the total hydrogen mass is transformed into helium during this phase (nuclear reactions only occur in the core), this gives :

$$\tau_{nuc} = (Q_{pp}/4)N_{av}(M/10)/L, \quad (356)$$

where  $Q_{pp} \simeq 25MeV$  is the heat provided per produced helium nucleus and  $N_{av}$  is the Avogadro number. Inserting in this formula the solar mass and luminosity, one gets a nuclear time scale of the order of 10 billions years, which is indeed the order of magnitude of the life-time of the Sun on the main sequence, as predicted by rigorous solar evolution computation. This time is much higher than the Helmholtz-Kelvin time (for the present Sun,  $\tau_{HK} \simeq 3.1 \times 10^7$  years), the star has thus all the required time to maintain thermal equilibrium during this phase.

When a star enters in this main-sequence phase, it has a given location in the HR diagram. Relating all these points for models of different masses defines a curve in the HR diagram called the **Zero Age Main Sequence**. The evolution track of the star has an angular point with a local minimum of luminosity at the ZAMS. This helps to locate it by eyes.

## 11.1 Mass-Luminosity relation, ages and stellar populations

Based on homologous transformations, we established in Sect. 8.2 a mass-luminosity relation (eq. 326) telling us that the luminosity of stars steeply increases with their mass. Indeed, a mass-luminosity relation shows up from rigorous stellar models, as long as they are mainly radiative. However, it does not have the form of a power law  $L \propto M^\alpha$  with a constant  $\alpha$  because stars are not homologous. Moreover, the luminosity does not only depend on the mass, it also depends on the chemical composition of the star. Since  $d \ln L / d \ln M \approx 3 - 4 > 1$ , we see from the nuclear time definition (eq. 356) that the duration of the main-sequence phase steeply decreases with the mass. These tendencies are quantified (order of magnitudes) in Table 11.1.

The steep decrease of the main-sequence duration with the mass has numerous consequences in astrophysics. In our galaxy, the less massive stars have a life-time much larger than the universe's age. Therefore, some of its present stars formed very early in the history of our galaxy. The first-ever generation of stars of our galaxy, composed of hydrogen and helium only constitute the so-called **population III**.

---

$M/M_{\odot}$	0.5	1	2	10	80
$L/L_{\odot}$	0.04	0.7	15	6000	$10^6$
$\alpha$	3	4.3	4	3	2
MS duration (years)	$50 \times 10^9$	$10 \times 10^9$	$10^9$	$20 \times 10^6$	$3 \times 10^6$
$R/R_{\odot}$	0.45	0.9	1.6	4	12
$M_{cc}/M$	0	0	0.2	0.4	0.8
$\bar{\rho}$ (g/cm <sup>3</sup> )	8	2.1	0.65	0.25	0.055
$\rho_c$ (g/cm <sup>3</sup> )	75	80	60	8	1.8
$T_c$ (10 <sup>6</sup> K)	9	14	21	32	41

---

TAB. 1 – Characteristics of stars with different masses on the ZAMS : masses, luminosities,  $\alpha = d \ln L / d \ln M$ , duration of the main-sequence phase, radii, mass fractions of the convective core, mean densities ( $\bar{\rho}$ ), central densities ( $\rho_c$ ) and central temperatures.

We haven't observed a representative of this population yet. We think that most of them were very massive and thus have already exploded as a supernova. Next, come the **population II stars** populating the halo and bulge of our galaxy. These stars were formed before the galactic disk 11-13 billions years ago. They have low masses, which allowed them to survive until now. They also have low metallicities. To be more precise, the metallicity is defined in astrophysics by :

$$[Fe/H] \equiv \log_{10} \left( \frac{n_{Fe}}{n_H} \right)_{\text{star}} - \log_{10} \left( \frac{n_{Fe}}{n_H} \right)_{\text{sun}}, \quad (357)$$

where  $n_i$  is the number density of the element  $i$ . The metallicities of population II stars are in the interval  $-5 \leq [Fe/H] \leq -1$ , in other words they are between 10 and 100 000 times less “metallic” than the Sun. The galactic disk (90 % of the stars of our galaxy) is composed of **population I stars** with metallicities of the same order of magnitude of our Sun. All masses up to  $\approx 100M_{\odot}$  are found in pop II stars. Hence, all possible ages are also found, up to around 9 billions years for the less massive.

As shown in Table 11.1, the most massive stars (O-B spectral types) have life-times of only several millions years ; they are thus much less numerous in our galaxy. However, from an observational point of view, instruments (e.g. photometers) are designed for a given range of apparent magnitude. Since massive stars are much more luminous, we can see them very far away and they constitute a significant part of the bright stars of the firmament (e.g. : *Spica*). Because of their very high luminosity, they significantly contribute to the total luminosity of spiral galaxies. Stars form in spiral arms, which can be seen as density waves (kinds of traffic jam zones). The life-time

of massive stars are much shorter than the orbital periods around the galactic center ( $\approx 220 \times 10^6$  years for the Sun); they have thus not quitted the spiral arms yet when they explode as supernovae. This explains the bluish appearance of spiral arms in images of spiral galaxies, it comes from the very bright O-B stars only present there.

Let's come back to the mass-luminosity relation and its physical interpretation. We can approximately find the behavior of  $\alpha = d \ln L / d \ln M$  as a function of the mass (Tab. 11.1) through homologous reasoning. Around the mass of the Sun, increasing the mass increases the temperature, thus decreases the opacity (see the Kramers laws eqs. 153 and 154) and thus increases even more the luminosity (eq. 324). Hence,  $\alpha > 3$  in this mass domain. For more massive stars, the temperature is larger and electron scattering dominates as opacity source. Since it doesn't depend on  $T$  but only on  $X$  ( $\kappa_{es} \simeq 0.02(1 + X)m^2/kg$ ), we find from eq. 327 :  $\alpha \simeq 3$ . For even more massive stars, the radiation pressure becomes significant compared to the gas pressure. Let's consider the extreme case where the radiation pressure dominates. Eq. 323 obtained from the ideal gas equation of state is thus not valid. We have  $P \simeq (1/3)aT^4$ , and thus using eq. 322 :

$$T^4 = TT(x)^4 M^2/R^4 \quad \text{and} \quad T^3 dT/dr = TT(x)^3 dTT/dx M^2/R^5.$$

Since  $r^2/\rho = x^2/\rho\rho(x) R^5/M$ , we get from eq. 324,

$$L(r) = LL(x)M, \tag{358}$$

thus  $\alpha \simeq 1$  for hypothetical hyper-massive stars where the radiation pressure dominates everywhere. Radiation pressure explains thus why  $\alpha$  decreases when we enter in the domain of very massive stars.

It is important to notice that the mass-luminosity relation was obtained assuming a purely radiative transport of energy. Hence, it doesn't apply to stars having a large convective envelope. The Hayashi track associated to fully convective models with same mass but very different luminosities clearly illustrates this. Note also that nuclear reactions don't play any role in the establishment of the mass-luminosity relation, they don't impact it. **Stars radiate as they do because they have internal temperature gradients and opacities enabling it, whatever the origin of energy** (nuclear reactions or potential energy release). The radiated energy is taken from where it is available. If there are nuclear reactions, they provide this energy and the star evolves over the nuclear time-scale. Imagine now that this source of energy is suddenly cutted off. The gradient of temperature would not be instantaneously modified and the star would continue to radiate. It would enter in a global contraction phase, half of the released potential energy being radiated and the other half converted into internal energy, it would evolve over the Helmholtz-Kelvin time-scale.

Let's try now to physically interpret the mass-luminosity relation. Consider first an increase of the stellar mass at constant radius. The relations 322 and 323 tell us that this implies an increase of the weight of the gas column and thus the temperature. We

directly see from eq. 324 that this temperature increase leads to a significant increase of the luminosity (massive stars are hotter and thus more luminous). Consider now an increase of the radius at constant mass. The radius increase leads to a significant decrease of the density (eq. 321) and a decrease of the temperature (eq. 323). Both effects compensate in eq. 324, so that the luminosity doesn't change. Finally, it should be noted that the luminosity doesn't depend on the mass only. It also depends on the internal chemical composition. First, increasing the mean molecular weight (as nuclear fusion reactions do) increases the temperature (eq. 323) and thus the luminosity (eq. 326). Second, increasing the metallicity increases the opacity and thus decreases the luminosity. We come back to this later.

## 11.2 Internal physical characteristics of stars along the ZAMS

We have examined in detail the mass-luminosity relation in the previous section. We show in Table 11.1 how other quantities vary with the mass along the ZAMS. The radius of main-sequence stars reasonably increases with the mass. At low masses, stars have a convective envelope and a radiative core. For example, at  $0.5 M_{\odot}$ , the convective envelope encompasses 20% of the mass. For the Sun, this convective envelope corresponds to 2% of the mass. The location of its bottom is precisely and accurately known by helioseismology, it is at a radius of 0.713 solar radii. Above 1.2 solar masses, main-sequence stars have a convective core. The mass fraction of this convective core is given in Table 11.1. As discussed at the end of section 6.6.2, this convective core originates from the highly temperature sensitive CNO cycle, dominating the pp chain from intermediate to high mass stars. We can also see that the mean density decreases as the mass increases. After a plateau at small masses, the same tendency is found for the core density. Finally, the core temperature slowly increases with the mass.

We now interpret these results by an approximate reasoning based on homologous transformations. At this stage, we have to consider the impact of nuclear reactions. Main-sequence stars are at thermal equilibrium, the power produced by nuclear reactions is equal to their luminosity :

$$L = \int_0^M \epsilon dm. \quad (359)$$

We approximate the dependence of  $\epsilon$  with respect to the temperature by a power law :

$$\epsilon \propto \rho T^{\nu}.$$

Using the homologous relations 321 and 323, we find :

$$\epsilon = \epsilon(x) \frac{\mu^{\nu} M^{\nu+1}}{R^{\nu+3}}.$$

Combining this result with eq. 359, we find :

$$L(r) = LL_2(x) \frac{\mu^\nu M^{\nu+2}}{R^{\nu+3}}. \quad (360)$$

This relation corresponds to the power produced by nuclear reactions. At thermal equilibrium, it must be equal to the radiated power. With a constant opacity in 326, it is given by :

$$L(r) = LL(x) \mu^4 M^3, \quad (361)$$

Equalizing 360 and 361, noting that the  $LL(x)$  and  $LL_2(x)$  functions must be multiple and isolating the radius, we find :

$$R \propto M^{\frac{\nu-1}{\nu+3}} \mu^{\frac{\nu-4}{\nu+3}}. \quad (362)$$

We can now substitute the relation 362 in equations 321 and 323, which gives :

$$\rho(r) = \rho\rho(x) M^{1-3\frac{\nu-1}{\nu+3}} \mu^{-3\frac{\nu-4}{\nu+3}}, \quad (363)$$

$$T(r) = TT(x) M^{1-\frac{\nu-1}{\nu+3}} \mu^{1-\frac{\nu-4}{\nu+3}}. \quad (364)$$

Since  $\nu \gg 1$  ( $\approx 13 - 15$  for the CNO cycle), we find in agreement with rigorous models that the radius of main sequence stars increases with their mass, their density decreases with their mass and their core temperature slightly increases with their mass. This last result is important and warrants a physical interpretation. Suppose that the temperature would increase significantly with the mass, the production of energy by nuclear reactions would considerably increase (very high  $\nu$ ), more than the energy evacuation by radiation, we would clearly go out of thermal equilibrium. This net heat input would lead to an expansion of the gas and, as a consequence, a decrease of the temperature. This is the important **control of the temperature by nuclear reactions** in stellar interiors. Note that the decrease of the core density as the mass increases (see Table 11.1) also contributes to the maintaining of the thermal equilibrium by facilitating the evacuation of energy by radiation ( $\rho$  is on the denominator in eq. 324) and decreasing the power produced by nuclear reaction (proportional to  $\rho^2$ ).

These results also enable to understand the location of the main-sequence in the HR diagram. The logarithm of  $L = 4\pi R^2 \sigma T_{\text{eff}}^4$  reads :  $\log L = 2 \log R + 4 \log T_{\text{eff}} + c_1$ . For a fixed  $\mu$ , the logarithms of equations 361 and 362 read  $\log L = 3 \log M + c_2$  and  $\log R = (\nu - 1)/(\nu + 3) \log M + c_3$ . This defines a system of 3 linear equations with 4 unknowns :  $\log L$ ,  $\log T_{\text{eff}}$ ,  $\log M$  and  $\log R$ . Solving it allows us to express  $\log L$  as a linear function of  $\log T_{\text{eff}}$  :

$$\log L = \frac{12}{3 - 2\frac{\nu-1}{\nu+3}} \log T_{\text{eff}} + c_4. \quad (365)$$

This approximate development explains why the main-sequence is more or less a straight line in the HR diagram.

### 11.3 Evolution of the internal structure

The evolution of the internal structure of a star during the main-sequence is dictated by the progressive modification of its chemical composition, mainly due to nuclear reactions. Helium is progressively synthesized from hydrogen, which leads to an increase of the mean molecular weight in the core. This increase of  $\mu$  modifies the relation between the density, the temperature and the pressure in the equation of state. Therefore, the thermodynamic quantities must change, which leads to a modification of the whole stellar structure.

Interpreting the modification of this structure is not easy because a homologous reasoning is not valid here. Indeed, the mean molecular weight change due to nuclear reactions only occurs near the centre (if the core is radiative) or in the whole convective core if there is one.

If on the contrary,  $\mu$  was multiplied by a same factor everywhere in the star, a homologous reasoning would be more justified. Considering this simpler case can help us to understand what happens in reality. In this case, the dependence with respect to  $\mu$  of the different physical quantities would be given by equations 361, 362, 363 and 364. Eqs. 362 and 364 tell us that the radius and temperature should increase with  $\mu$ . However, since  $\nu$  is very high, eq. 364 tells us that the temperature increase is strongly inhibited by nuclear reactions. This is another example of the **temperature control by nuclear reactions** : as  $T$  is proportional to  $\mu/R$ ,  $R$  must increase to compensate for the  $\mu$  increase and avoid a significant increase of the temperature.

But this is for homology, what happens in reality ? What remains is the temperature control by nuclear reactions. However,  $\mu$  only increases in the center. This leads us to consider what happens locally in the core. Consider the equation of state of an ideal gas and isolate  $\mu$  :

$$\mu = \frac{k\rho T}{Pm_u}. \quad (366)$$

Since the temperature is controlled by nuclear reactions, it cannot increase significantly. From this equation, it seems natural that the density should locally increase where  $\mu$  increases. But this cannot be the case in the envelope where  $\mu$  remains constant. Indeed, if the whole star would contract, eq. 323 tells us that the temperature would significantly increase, which is not permitted by nuclear reactions. So, the only possible channel for the star is a contraction of the core and a simultaneous significant expansion of the envelope. To understand this, I split the weight of the gas column (and thus the pressure) at the stellar centre into two terms corresponding to the core and the envelope :

$$P_c = \int_0^M \frac{Gm}{4\pi r^4} dm = \int_0^{m_1} \frac{Gm}{4\pi r^4} dm + \int_{m_1}^M \frac{Gm}{4\pi r^4} dm .ref M - L3 \quad (367)$$

As we have seen, the core must contract ( $r$  decreases) because of the local  $\mu$  increase. This leads to a significant increase of the first term ( $r^4$  on the denominator). The envelope cannot do the same, because this would lead to a very large increase of the core pressure and thus a significant increase of the temperature ( $T$  and  $P$  are closely related through the equation of state). On the contrary, if it expands, the second term decreases and compensates for the increase of the first one. This inhibits the increases of the core pressures and temperatures. As conclusion, the consequence of the  $\mu$  increase in the core and the control of the temperature by nuclear reactions is a contraction of the core and an expansion of the envelope.

## 11.4 Global characteristics' evolution and HR track

We have seen in the previous section that the envelope must expand during the main-sequence. This is valid for all masses. However, the radius increase is much larger in massive stars than in low mass stars. E.g. ... Although the evolution of the internal structure is not homologous at all, some tendencies found with homology remain valid. The  $\mu$  increase leads to a slight increase of the core temperature. Moreover, the radius increase due to the temperature control by nuclear reactions leads to a significant decrease of the envelope density. As a consequence, the luminosity (proportional to  $T^3/\rho$ , see eq. 324) increases as the star evolves. We will see later that this luminosity increase is strongly inhibited by mass loss in very massive stars. The evolution of the effective temperature comes from  $L = 4\pi R^2 \sigma T_{\text{eff}}^4$ . In intermediate to high mass stars,  $R^2$  increases more quickly than  $L$  and the effective temperature decreases as the star evolves. In low mass stars,  $T_{\text{eff}}$  increases. In our Sun,  $T_{\text{eff}}$  slightly increased first, has reached a maximum now, and will decrease in the future.